AD-A071 260 PURDUE UNIV LAFAYETTE IND RAY W HERRICK LABS F/G 20/4
AN EXPERIMENTAL STUDY OF THE FLAPPING MOTION OF A TURBULENT PLA--ETC(U)
AUG 76 J G CERVANTES DE GORTARI N00014-75-C-1048
UNCLASSIFIED HL-78-40 NL

1 OF 2
AD A071260

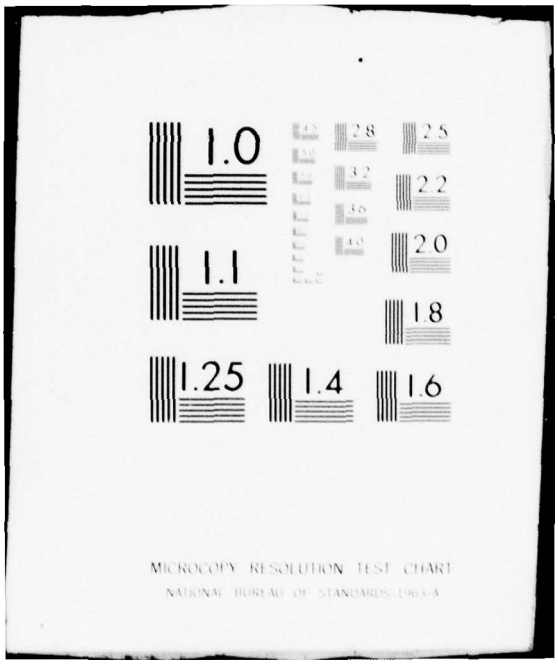
1.0
1.1
1.25
1.4
1.6
2.8
3.2
3.6
4.0
2.5
2.2
2.0
1.8
MICROCOPY RESOLUTION TEST CHART
NATIONAL BUREAU OF STANDARDS 1963-A

RAY W. HERRICK LABORATORIES

A Graduate Research Facility

PURDUE UNIVERSITY

Lafayette, Indiana 47907

DATA SHEET

PHOTOGRAPH THIS SHEET

LEVEL III

INVENTORY 1

AD A071260

DDC ACCESSION NUMBER

HL 78-40

DOCUMENT IDENTIFICATION

DISTRIBUTION STATEMENT A
Approved for public release;
Distribution Unlimited

DISTRIBUTION STATEMENT

Accession For
NTIS GRA&I
DDC TAB
Unannounced
Justification
By
Distribution/
Availability Codes
Dist | Avail and/or special
A

DISTRIBUTION STAMP

DDC
RECEIVED
JUL 17 1979
D

DATE ACCESSIONED

DDC FILE COPY

79 07 05 094

DATE RECEIVED IN DDC

PHOTOGRAPH THIS COPY

Research Contract ONR No. N00014-75-C-1048

National Science Foundation Research Grant NSF ENG 74-20780

AN EXPERIMENTAL STUDY OF THE FLAPPING MOTION OF A TURBULENT PLANE JET

Sponsored in part by

NATIONAL SCIENCE FOUNDATION,
OFFICE OF NAVAL RESEARCH
AND CONACYT

HL 78-40

Submitted by:

J. G. Cervantes de Gortari, Graduate Research Assistant
Victor W. Goldschmidt, Principal Investigator

Approved by:

Raymond Cohen, Director
Ray W. Herrick Laboratories

August 1978

AN EXPERIMENTAL STUDY OF THE FLAPPING MOTION OF A TURBULENT PLANE JET

A Thesis

Submitted to the Faculty

of

Purdue University

by

Jaime Gonzalo Cervantes de Gortari

In Partial Fulfillment of the

Requirements for the Degree

of

Doctor of Philosophy

August 1978

Note: This report is part of a dissertation submitted by Mr. Jaime Cervantes, in partial fulfillment of the requirements for the degree of Doctor of Philosophy.

Professor V. W. Goldschmidt assisted in this work as thesis advisor and major professor.

The first author acknowledges financial support received from the Consejo Nacional de Ciencia y Tecnologia, of Mexico. The research reported had phases sponsored by the Office of Naval Research and others by the National Science Foundation.

TABLE OF CONTENTS

LIST OF TABLES

LIST OF FIGURES

Page

Page

Appendix Figure

NOMENCLATURE

A	constant used for hot-wire cooling law, eq. (5.14)
$A(\xi)$	Amplitude function, eq. (C.6)
B	constant used for hot-wire cooling law, eq. (5.14)
b	jet half-width, Figure 2.1
C_1	geometric virtual origin, eq. (A.1)
C_2	kinematic virtual origin, eq. (A.2)
d	nozzle slot width, cm
$\bar{E}$	d.c. voltage, volts
$E\{\ \}$	mean (expected) value
e, e_1, e_2	a.c. voltage, volts
f	frequency of flapping, cycles/sec
f_1	frequency of flapping, Figure 5.5, cycles/sec
f_2	frequency of flapping, Figure 5.5, cycles/sec
h	mixing layer thickness, cm
k_1, k_2	empirical constants
K_1	widening rate
K_2	centerline mean velocity decay
m	lag number
l	sampling interval
$p(x_1, x_2)$	joint probability density function
Q	linear stability theory eigenfunction, eq. (C.6)
$\bar{q}$	time-averaged quantity

q'	organized wave component
q''	random component
r	separation distance, cm
$R_x(\tau)$	autocorrelation of random process $\{x(t)\}$, eq. (2.5), volts^2
$R_{xy}(\tau)$	crosscorrelation of random processes $\{x(t)\}$ and $\{y(t)\}$, eq. (2.7), volts^2
$R(r,\tau)$	space-time correlation, eq. (2.16), volts^2
$\underline{R}(\tau)$	normalized crosscorrelation function, eq. (2.17)
Re	Reynolds number
$R_v(\tau)$	autocorrelation of the v-component velocity at the centerline, eq. (B.1), volts^2
$\hat{R}_{xy}(\tau)$	estimate of crosscorrelation
R_w	hot-wire operating resistance, ohms
R_f	hot-wire cold resistance, ohms
t	time, seconds
T	averaging time, seconds
u	x-component fluctuating velocity, cm/sec
$\overline{u}$	time-average of the x-component velocity, cm/sec
u'	periodic wave part of the x-component velocity, cm/sec
u''	random part of the x-component velocity, cm/sec
U	local mean velocity, cm/sec
U_c	convective velocity, cm/sec
U_{cf}	flapping motion convective velocity, cm/sec
U_m	centerline mean velocity, cm/sec
U_o	nozzle exit mean velocity, cm/sec
v	y-component fluctuating velocity, cm/sec
x	longitudinal coordinate, cm

$\{x(t)\}$	random process
x_1, x_2	random variables
y	lateral coordinate, cm
$\{y(t)\}$	random process
β	local dimensionless frequency
η	similarity variable
ξ	similarity variable
τ	time delay, seconds or milliseconds

ABSTRACT

Cervantes de Gortari, Jaime Gonzalo. Ph.D., Purdue University, August 1976. AN EXPERIMENTAL STUDY OF THE FLAPPING MOTION OF A TURBULENT PLANE JET. Major Professor: Victor W. Goldschmidt.

Measurements were conducted in order to characterize the flapping motion of a turbulent plane jet. The flapping is defined as the (apparently natural) lateral pseudo-oscillatory motion (in the average) of the flow field of the jet. The technique employed in these measurements was to compute crosscorrelation functions between the velocity fluctuations (one delayed in time) in the longitudinal direction, at two points on opposite sides of the jet. Standard hot-wire anemometry and on-line digital processing instrumentation were used. Four types of measurements were performed: (a) with the probes symmetrically positioned with respect to the centerline of the jet; (b) with the probes asymmetrically set with respect to the centerline; (c) with the probes at points of different longitudinal coordinate; (d) with an x-wire at the centerline of the jet where the autocorrelation of the lateral component of the velocity was measured.

The existence of flapping was indicated by a distinctive negative value at zero time delay and a quasi-periodic nature at the measured crosscorrelation functions.

These were obtained at longitudinal stations ranging from 10 to 100 times the slot width. The frequency characterizing the flapping motion showed approximate self-preservation (when scaled by the half-width and the mean velocity at the centerline of the jet) for stations with longitudinal coordinate larger than 30 times the slot width. It was found that $fb/U_m \simeq 0.11$. The flapping frequency did not show dependence on the lateral coordinate. The amplitude of flapping was estimated to about 20% of the jet half-width. The flapping behavior seems to travel in the downstream direction with a velocity smaller than the convective velocity of the turbulent structure. The frequency of flapping showed Reynolds number independence in the range $7900 \leq Re \leq 15100$, where Re is based on the nozzle exit characteristics.

CHAPTER 1

INTRODUCTION

The subject of turbulent shear flows has received considerable attention in recent years. Sufficient motivation for studying this kind of flow will result if one recalls engineering applications like mixing processes, diffusers, jet engines, fluid amplifiers or the more recent attempts to control environmental pollution, to mention but a few.

The understanding of turbulence in general and turbulent shear flows in particular, is, however, far from complete. The main reason for this is the lack of a general mathematical theory of turbulence. The advances in this field have proceeded to a large extent on an experimental basis. By this means, empirical models are constructed which may be used in a descriptive way or as a criterion for design. Experimental results also contribute to the general body of data against which any mathematical theory may be verified.

Among the various aspects of turbulent shear flows not sufficiently investigated up to date is the phenomenon of flapping of a turbulent plane jet. The flapping is defined as the lateral oscillatory-like motion (in the

average) of the flow field of the jet. Effectively, a plane jet issueing from a rectangular slot attains a turbulent state after some distance downstream from the nozzle exit. This turbulent flow is characterized by random fluctuations in the velocity field and the usual statistical parameters like mean velocity, intensity of turbulence, energy spectra and length scales can be defined and measured. However, hidden in the randomness of the longitudinal velocity fluctuations appears to exist a low-frequency, almost periodic component. The longitudinal velocities detected at two points, each one at opposite sides of the jet centerline, are such that their corresponding low-frequency components are in counterphase with respect to each other (in the average). In other words, when the velocity at one point increases, the velocity at the opposite point generally decreases. The overall result is that the flow field moves in a lateral oscillatory fashion, as depicted in Figure 1.1.

The objective of this investigation was to perform experiments aiming to detect and quantify the phenomenon of flapping of a turbulent plane jet. The technique employed in this investigation was to compute statistical crosscorrelations between longitudinal components of the velocities (one delayed in time) at two points, each one on opposite sides of the jet. The existence of flapping would be indicated by a distinctive negative value at zero time delay and a

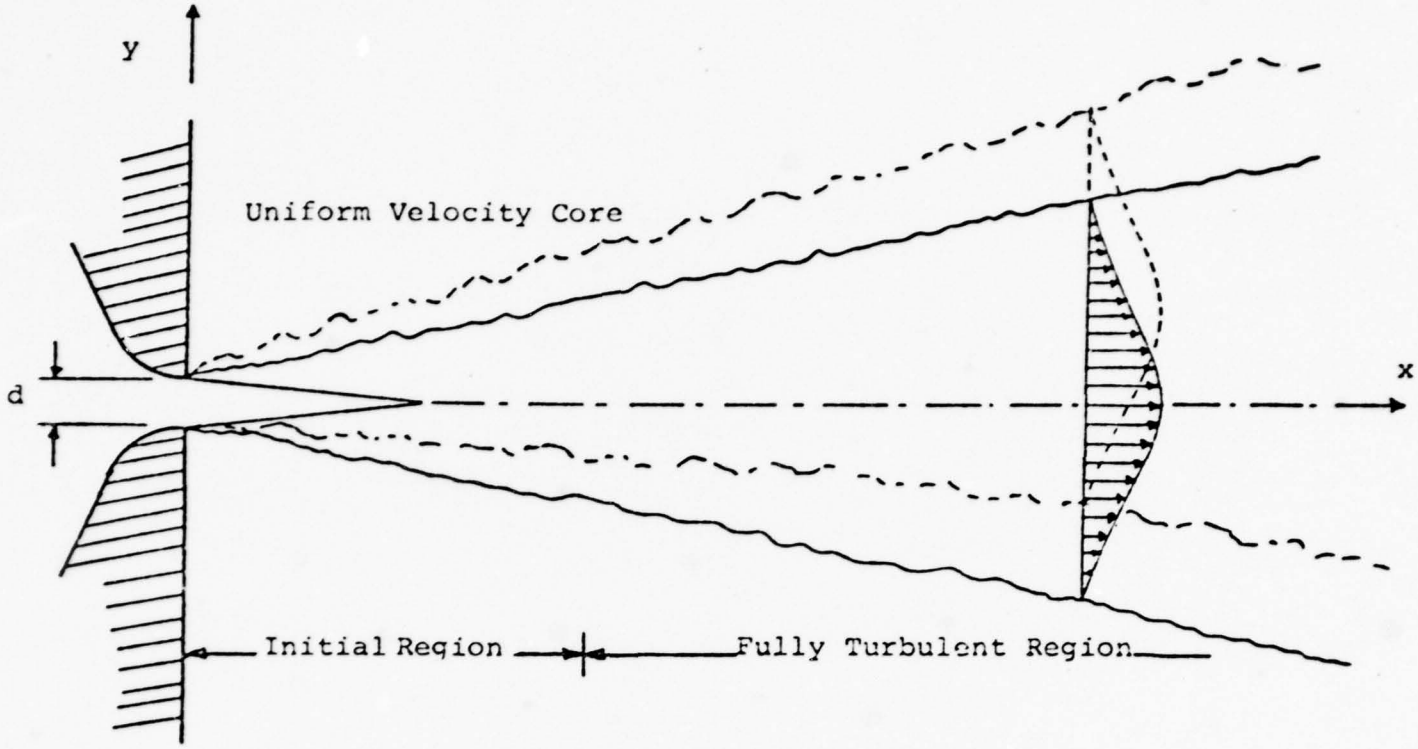

Figure 1.1 Flapping of a Turbulent Plane Jet

quasi-periodic nature of the measured crosscorrelation functions. Standard hot-wire anemometry and on line digital processing instrumentation were used in the four types of performed measurements: (a) with two normal hot-wires symmetrically positioned with respect to the centerline of the jet; (b) with the probes asymmetrically set with respect to the centerline; (c) with the probes at points of different longitudinal coordinate; (d) with an x-wire at the centerline of the jet where the autocorrelation of the lateral component of the velocity was measured. Longitudinal stations ranging from 10 to 100 times the slot width were investigated.

These experiments were planned to satisfy the following specific objectives. First, to clearly establish the existence of the flapping motion as opposed to a puffing effect, i.e., longitudinal oscillations of the flow field (this effect would be originated by artificial instabilities somewhere upstream of the nozzle exit and would be characterized by periodic crosscorrelation functions with positive values at zero time delay). Second, to look for any dependence of the flapping frequency on the longitudinal and lateral coordinates. Third, to study the traveling characteristics of the flapping behavior in the downstream direction. Finally, to show the possibility of Reynolds number independence and self-preservation of the flapping motion.

In what follows, after a review of the general characteristics of turbulent plane jets and relevant correlation techniques, a summary of the available literature related to this investigation is presented. Thereafter a detailed description is given of the experimental procedures and employed instrumentation. The last three chapters refer to the experimentally obtained results and some concluding remarks are offered. Suggestions for further work, in the light of this investigation, are also given.

It is hoped that characterizing the flapping behavior of turbulent plane jets may contribute to a better insight of the structural properties of turbulence, particularly in the context of the new trends in turbulence research, where a more deterministic point of view is employed.

CHAPTER 2

REVIEW OF CHARACTERISTICS OF PLANE JETS AND CORRELATION TECHNIQUES

2.1 General Characteristics of a Plane Turbulent Jet.

A plane turbulent jet belongs to the class of flows known as free turbulent shear flows. Typically, a plane jet is formed when a fluid with sufficiently large velocity, is discharged through a slot-shaped orifice into a volume of quiescent fluid. Initially, a wedge-shaped core is produced close to the nozzle with a uniform velocity and low turbulence level, bounded by two mixing layers with high turbulence intensity, which gradually diffuse momentum from the core to the surroundings (see Figure 2.1).

As the development continues, the two mixing layers merge together after a distance of about six times the slot width and the mean velocity at the centerline starts to decay. After this transitional region a fully turbulent region is established, where the mean velocity profiles take a shape close to a gaussian or normal function and the static pressure is constant.

In the fully turbulent region, the jet attains Reynolds number similarity, i.e., the mean flow structure is independent of viscosity and the transverse distributions

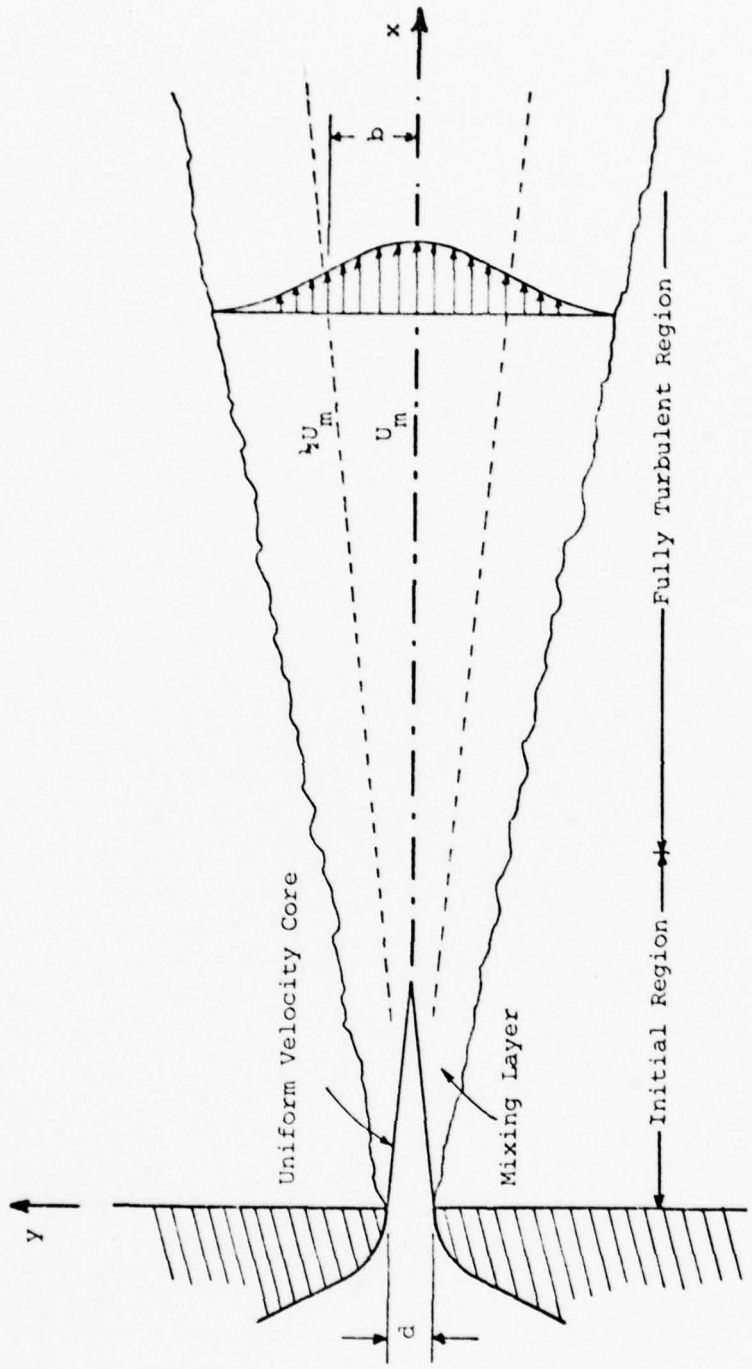

Figure 2.1 Schematic Top View of a Plane Turbulent Jet

of mean velocity and other mean quantities (although changing in the downstream direction) become self-preserving if they are expressed non-dimensionally through prop scales. For instance, the mean velocity profile becomes an universal function if (a) the mean velocity itself is divided by the jet centerline mean velocity and (b) the corresponding transverse y coordinate by the jet half-width b. The latter is defined as the lateral distance where the mean velocity is exactly one-half of the centerline value (see Figure 2.1).

The basic equations of motion can be simplified for this kind of flow by making use of one experimental observation: the flow is confined to a region of space elongated in the direction of the general motion and narrow in the transverse direction. In effect, through an order of magnitude analysis (Townsend [1956]), the incompressible mean flow equations can be reduced to:

momentum in the mean flow direction:

$$U \frac{\partial U}{\partial x} + V \frac{\partial U}{\partial y} + \frac{\partial (\overline{uv})}{\partial y} = 0 \qquad (2.1)$$

continuity:

$$\frac{\partial U}{\partial x} + \frac{\partial V}{\partial y} = 0 \qquad (2.2)$$

Similarity solutions of equations (2.1) and (2.2) were first obtained by Tollmien [1926], as referred by Schlichting [1968], after using Prandtl's mixing length hypothesis. Goertler [1942] and Reichardt [1951] also

reported solutions which better agreed with measured mean velocity profiles. These are:

Goertler's solution: $$\frac{U}{U_m} = 1 - \tanh^2 \eta \qquad (2.3)$$

Reichardt's solution: $$\frac{U}{U_m} = \exp\left[-(0.8326\ \frac{Y}{b})^2\right] \qquad (2.4)$$

where $\eta = 7.67\ \frac{Y}{x}$, b is the half-width of the jet (Figure 2.1) and U_m is the mean velocity at the centerline. Equation (2.4) is plotted in Appendix A together with measurements of U taken in the present jet.

Further details about self-preservation, basic equations and various other aspects of turbulent jets are available in the literature (Townsend [1956], Abramovich [1963], Schlichting [1968]).

2.2 Correlation Techniques

Correlation analysis is a well accepted statistical technique. Its usage in sciences like agriculture, biology and economic statistics, (although somewhat restricted through the concept of correlation coefficient), is extensively used in comparing series of measurements of any kind. It is perhaps in the theory and applications of communications and random processes where its broadest utilization may be found. (see for instance Lange [1966], Lathi [1968], Bendat and Piersol [1971], Jenkins and Watts [1968]).

Correlation techniques have been also widely used in experimental turbulent flow studies since Taylor [1935]

first suggested them. Indeed, one of the methods used to get some insight into the structural and transport characteristics of this kind of flows is to measure correlations between various fluctuating quantities like velocity, pressure, temperature, etc. at different points and times.

The correlation function gives the general relationship between two random variables. In a mathematical sense it is defined as follows.

Consider a random process $\{x(t)\}$ as described by its ensemble and a probability measure over the ensemble. Further, consider two random variables x_1 and x_2 contained in the process and their joint probability-density function $p(x_1,x_2)$. These random variables $x_1 = x(t_1)$ and $x_2 = x(t_2)$ are defined by the amplitudes of the *sample functions* forming the ensemble, at instants t_1 and t_2, respectively. The correlation between the two random variables x_1 and x_2, or better, the autocorrelation of the random process $\{x(t)\}$ is defined as the ensemble average:

$$R_x(\tau) = \int_{-\infty}^{\infty} \int_{-\infty}^{\infty} x_1 x_2 p(x_1,x_2) dx_1 dx_2 \qquad (2.5)$$

where τ is the difference between t_1 and t_2.

If the random process is ergodic, the complete statistical properties of the process may be described through the properties of any one of the sample functions. In other words, averaging over the whole ensemble is equal to

time-averaging over a single sample function. The autocorrelation function then becomes:

$$R_x(\tau) = \lim_{T\to\infty} \frac{1}{T} \int_{-T/2}^{T/2} x(t)x(t+\tau)dt \tag{2.6}$$

where $x(t)$ is the amplitude at any instant t for a single sample function.

The above concepts may be extended to the case of two jointly ergodic random processes $\{x(t)\}$ and $\{y(t)\}$. The crosscorrelation between the two processes may be defined in terms of the time-average:

$$R_{xy}(\tau) = \lim_{T\to\infty} \int_{-T/2}^{T/2} x(t)\ y(t+\tau)dt \tag{2.7}$$

where now $x(t)$ and $y(t)$ represent any samples of the processes $\{x(t)\}$ and $\{y(t)\}$, respectively.

The main properties of correlation functions are summarized in the following relationships:

$$R_x(\tau) = R_x(-\tau) \tag{2.8}$$

$$R_x(0) = \overline{x^2} \tag{2.9}$$

$$R_x(\tau) = R_x(\tau+nT), \text{ for } x(t) = x(t+nT) \tag{2.10}$$

$$R_x(0) \geq |R_x(\tau)| \tag{2.11}$$

$$R_{xy}(\tau) = R_{yx}(-\tau) \tag{2.12}$$

$$|R_{xy}(\tau)| \leq [R_x(0)R_y(0)]^{\frac{1}{2}} \tag{2.13}$$

In utilizing the defined correlation functions in the field of turbulence, it is convenient to consider the sample functions x(t) and y(t) as any two quantities of interest. For instance, assume that the velocity fluctuations at two points separated by a distance r are considered: u(x) and u(x+r), respectively, where x is a space coordinate; then the autocorrelation of u(x) is written as:

$$R(\tau) = \overline{u(x,t)u(x,t+\tau)} \tag{2.14}$$

where the overbar denotes time-averaging. The space-correlation between u(x) and u(x+r) is defined as:

$$R(r) = \overline{u(x,t)u(r+r,t)} \tag{2.15}$$

Furthermore, if both space and time are taken into account, the space-time correlation function may be defined:

$$R(r,\tau) = \overline{u(x,t)u(x+r,t+\tau)} \tag{2.16}$$

Note that the above defined space-time correlation becomes an autocorrelation when the separation distance is zero, and becomes a space-correlation for null time delay τ (stationarity and homogeneity are assumed).

Normalized (dimensionless) correlation functions are obtained after dividing them by the root-mean-square values

of the corresponding fluctuations (in this work a normalized correlation function will be indicated by an underlined $\underline{R}$). A review on correlation functions, including measurements in various flow situations, is given by Favre [1965].

Correlation techniques have become a powerful tool in studying turbulent flow properties. They can give an indication of the changing pattern, both in space and time, of a given flow. They can provide a means of testing theoretical predictions, as in some instances of isotropic turbulence (Hinze [1959]). The use of correlation functions in characterizing the size and shape of turbulent eddies, and estimating appropriate scales for the corresponding flow, is generalized. The study of convective velocities (the velocity at which the turbulent structure moves) and the validity of Taylor's hypothesis (that turbulence remains as a frozen structure moving at U) has been carried out through the measurement of correlation functions for different flow configurations (Favre et al. [1958], Fisher and Davies [1963]) as noted by Ott [1972].

Finally, the mean properties of the large-scale orderly structures in the mixing region of round jets, have been investigated using correlation techniques (Lau et al. [1972], Fuchs [1972], Ko and Davies [1975]).

The use of correlation techniques in this investigation is circumscribed by the following normalized cross-correlation function:

$$\underline{R}(\tau) = \frac{\overline{u(y,t)\,u(-y,t+\tau)}}{\sqrt{\overline{u^2(y)}}\,\sqrt{\overline{u^2(-y)}}} \qquad (2.17)$$

that is, a time correlation function between axial velocity fluctuations at opposite sides of the jet. A positive value of $\underline{R}$ for zero time delay between signals ($\tau=0$), would indicate that both velocity fluctuations change in the same direction (in the average), whereas a negative value would indicate that when one fluctuation increases, the other one generally decreases.

The same correlation function was employed by Wygnanski and Gutmark [1971] in trying to relate the motion of the boundaries of a plane jet. They used, however, intermittency signals consisting of constant positive or negative voltages representing turbulent or potential flow, respectively, in place of the velocity fluctuations in equation (2.17). Their conclusion (they found a zero correlation) was that the boundaries of the jet flow moved independently of each other.

On the other hand, Goldschmidt and Bradshaw [1973] performed preliminary experiments following equation (2.17) exactly and found that for large averaging times, negative correlation values at zero time delay are persistent.

The experiments reported in this work are a natural extension of the latter preliminary investigation.

CHAPTER 3

LITERATURE REVIEW

In this chapter a review of the literature most closely related to this investigation is presented. The flapping motion of a turbulent plane jet, a naturally occurring phenomenon, has not been previously reported. Indeed, a carefully conducted search in the literature did not show, except for the preliminary experiments of Goldschmidt and Bradshaw [1973], any reference to this aspect of plane jets. It seems therefore, that we are faced with an unknown effect not sufficiently investigated up to now.

With this in mind, a review of the literature was done along three directions. One of them, as summarized in the first section of this chapter, really refers to a documentation of turbulent plane jets. As will be noted, experimental investigation on plane jets has been conducted to a large extent and the measurement of several statistical quantities has been successfully accomplished.

The other two areas of the explored literature are the recent work on coherent structures and the study of disturbed plane jets. They are relatively new lines of approach in studying turbulent shear flows and are presented

here for the purpose of providing a background to the problem.

In the appendix a review of the wave-guide modeling of turbulent shear flows is also presented.

3.1 Plane Turbulent Jets

The documentation of plane turbulent jets has been quite extensive. In what follows, only some of the salient publications are retraced.

Classical publications include Townsend [1965] and Abramovich [1963]. They emphasize the statistical description of the flow variables, the similarity and self-preservation characteristics and the role of phenomenological theories for various turbulent shear flows.

Van der Hegge Zijnen [1958], after having reviewed earlier theories and experiments, estimated turbulent shear stresses and the momentum exchange coefficient and mixing length in a plane jet.

More recent experimental results were reported by Heskestad [1965], Bradbury [1965] and Mih and Hoopes [1972]. The measurements by Heskestad included distributions of mean velocity, turbulent intensities, Reynolds stresses and intermittency and flatness factors for the streamwise velocity component. An energy balance for a location in the self-preserving region, was also done. Bradbury did similar measurements including some spectral data and compared them

with previously reported results, particularly the ones by Townsend [1956] for a plane wake. He also reported on the eddy structure and the applicability of available phenomenological theories. Mih and Hoopes performed similar experiments in a water jet. They used an electromagnetic induction method to detect the fluctuating velocities. Their measurements included energy spectra and length micro- and macro-scales.

Energy spectra measurements in a plane jet have been also reported by Bashir and Uberoi [1974] and by Young [1973]. The latter also determined micro- and macro-scale distributions.

The measurement of static pressure fluctuations has been of interest for a long time in turbulence studies. Recent attempts to deal with this aspect of shear flows are reported by Siddon [1969], Spencer [1970] and Planchon [1974].

Very recently, Gutmark and Wygnanski [1976] published their measurements in a plane jet. They included mean velocity profiles, turbulent intensities, third and fourth order moment quantities, intermittency factor and two-point correlations. Extensive use of conditional sampling techniques was done. The resulted data obtained exclusively within the turbulent zone of the jet were compared with conventionally averaged measurements.

Table 3.1 summarizes the measurements reviewed in this section. As noted, the quantities that have been

Table 3.1 Measurements performed in Turbulent Plane Jets.*

INVESTIGATOR	Re	MEASURED QUANTITIES
Van der Hegge Ziejnen [1958]	1.33×10^4	Turbulent shear stresses, momentum exchange coefficient, mixing length.
Heskestad [1965]	3.4×10^4	Mean velocity, turbulent intensities, Reynolds stresses, intermittency factors, flatness factor.
Bradbury [1965]	3×10^4	Same as Heskestad [1965], energy spectra.
Mih and Hoopes [1972]	1.77×10^4 3.14×10^4	Mean velocity, turbulent intensities, Reynolds stresses, autocorrelation functions, energy spectra, length micro- and macro-scales.
Bashir and Uberoi [1975]	2.57×10^3	Mean velocity and temperature profiles, turbulent temperature and velocity intensities, velocity and temperature spectra.
Young [1973]	1×10^4	Convective velocities, energy spectra, micro- and macro-scales.
Gutmark and Wygnanski [1976]	3×10^4	Mean velocity, turbulent intensities, turbulent shear stresses, space-correlations, micro-scales, flatness factors.

*Other works not specifically referred to here are listed in the General References.

measured in a turbulent plane jet are: mean velocity profiles, turbulent intensities, turbulent shear stresses, intermittency factors, energy spectra, length micro- and macro-scales and some high-order statistical moments. A possible closure theory of turbulence requires nevertheless, more experimental information; particularly in respect to the structural characteristics of the turbulence in shear flows. The study of the flapping of a plane jet might contribute to this.

3.2 Organized Structures in Free Turbulent Shear Flows

A new line of work in understanding turbulent shear flows has emerged in the last ten or so years. It consists of studying the large scale coherent structures that seem to exist. The development of digital data processing techniques and the utilization of more sophisticated experimental methods, among other things, have contributed to the growth of this new trend in turbulence research. The interest in these large scale structures has been highly motivated by the aerodynamic noise problem. Indeed, a large amount of the available literature refers to research conducted in the near-field of a circular jet and its relation to noise production. Since the pioneering works by Townsend [1956], Grant [1958] and Corrsin and Kistler [1954], there is an increasing evidence that the large scale structures greatly contribute to the transport of momentum, mass and heat in shear flows.

Among the flow visualization experiments which show how these ordered structures might look, are the now classic works by Brown and Roshko [1971] and Roshko [1975]. They took shadowgraph pictures of a turbulent mixing layer between two different gases moving at high speed. Coherent vortex-like structures appeared in their pictures, with size and space between them increasing with distance downstream of the origin. The merging of neighboring eddies accounted for the increase of eddy size and thus the spreading of the mixing layer, although this coalescing process occurred quite irregularly.

Winant and Browand [1974] reported similar experiments conducted in a channel where two streams of water at different velocity were brought together. Although the Reynolds number range was considerably lower than the one used by Brown and Roshko, again the coalescing mechanism shown by dye injection seemed to control the growth of the mixing layer. They studied the properties of these structures by performing ensemble averages through conditional sampling, over a large number of structures. They found a characteristic Strouhal number fh/U of 0.2, associated with the passage of the structures (f is the frequency of the lowest peak in the longitudinal velocity spectrum, h is the mixing layer thickness and U is the mean value of the two streams velocities). They further proposed a model for the shear layer growth based on the merging process.

In conducting a statistical study of the pressure and velocity fluctuations in a mixing layer, Spencer and Jones [1971] using modern signal processing techniques, noted the existence of peaks in the one-dimensional energy spectra of velocity fluctuations. They found these at the irrotational outer regions of the shear layer. As suggested by Winant and Browand [1974], these peaks may be related to the passage of the paired structures, with a Strouhal number fh/U of 0.19.

Yule et al. [1974] and Bruun and Yule [1974], as described by Davies [1975], investigated the coherent structures in the first ten diameters of round jets. Visualization techniques showed interaction and coalescence of large ring vortex-like eddies with stronger three dimensional characteristics than the previously reported mixing layers. Measurements of turbulent energy, shear stresses and cross-correlations associated with those structures, were done.

The phenomenon of vortex coalescence in various shear flows have been reported previously in the literature. Outstanding publications are the ones by Rockwell and Niccolls [1972] for a planar jet and Becker and Massaro [1968] for a circular jet. Rockwell and Niccolls reported visualization experiments using the hydrogen bubble technique, in studying the breakdown process of a plane jet with exit Reynolds numbers ranging from 2,000 to 10,000. Two types of vortex growth and coalescence were found: symmetrical

and asymmetrical with respect to the jet centerline. The Strouhal number corresponding to the formation of the vortices was estimated to follow the relationship $St = 0.012\sqrt{Re}$, where both the Strouhal number St and the Reynolds number Re are based on the nozzle exit characteristics.

Becker and Massaro [1968] performed experiments with a circular jet at moderate Reynolds numbers. Using light scatter and photography by sheet illumination techniques, they were able to study the vortex evolution and coalescence in the instability region of the circular jet, excited by a pure tone. Based on the frequency which gave maximum excitation and which was identical to the measured vortex-shedding frequency, the Strouhal number was also found to follow the relationship $St = 0.012\sqrt{Re}$.

On dealing with the scalar mixing mechanism in shear flows, Fiedler [1974], described experiments conducted in two-dimensional shear layers between still ambient air and a heated stream of air. Measurements of the characteristics of mean and fluctuating temperatures, suggested a predominant bulk convection mechanism for the temperature which was explained by the presence of large-scale coherent structures. The measurements were performed using conventional averaging and by averaging separately over the turbulent and non-turbulent parts of the flow.

It was pointed out before that considerable motivation in studying the mixing region of turbulent jets has

been in its connection with the noise generation problem. The literature in this topic is rather extensive and only some of the outstanding reports will be referred to here. Bradshaw et al. [1963] conducted a detailed investigation in a circular jet with an exit Mach number of 0.3. They found that the flow in the noise-producing region is dominated by a group of large eddies; these eddies in turn, appeared to be the source of the pressure fluctuations near the nozzle. They even commented on the possibility of artificial augmentation of the large eddies in order to increase the mixing rate and thus allow the reduction of noise.

Mollo-Christensen and coworkers, as referred to by Mollo-Christensen [1967], have performed experiments in a higher speed but still subsonic circular jet. Pressure crosscorrelation measurements suggested an ordered structure underneath the mixing layer.

In a series of publications (see for instance Ko and Davies [1971], Lau et al. [1972], Fuchs [1972]), researchers at the University of Southampton have reported on studies in regions adjacent to the mixing layer of a circular jet. By measuring correlations between pressure and velocity fluctuations in both the potential core and the entrainment region, Lau et al. [1972] inferred events occurring in the adjacent mixing layer. In fact, they postulated a model for the structure of this region, consisting of a train of discrete vortices, evenly spaced and traveling with a velocity

of approximately 60% the nozzle exit velocity and a characteristic dimensionless frequency $fd/U_o = 0.66$.

As an extension of the above mentioned investigation, Fuchs [1972] completed a survey of full-band and narrow-band pressure space-correlations obtaining a strong coherence both laterally in a cross-section and longitudinally up to eight diameters from the nozzle exit.

Wooldridge et al. [1972] reported spectral and correlation measurements of the axial velocity component in the initial and transitional regions of a round jet at various subsonic regimes. Their results agreed with those obtained by Ko and Davies [1971].

More recently, Lau and Fisher [1975] conducted a probability analysis of the time intervals between succesive downward spikes in the longitudinal velocity fluctuations in the region close to the potential core of the mixing layer. The highest probability corresponded to the vortex passing frequency found in their previous investigation. Using a time-domain averaging (or eduction) technique, with the spikes as triggering events, they determined educed velocity signals which supported the proposed vortex train model.

Experiments in the wake behind a circular cylinder have been conducted by Bevilaqua [1973] and by Papailiou and Lykoudis [1974]. The vortices shed by a moving cylinder in still mercury, were found to persist at high Reynolds

numbers. An analysis of this observation was done in connection to the entrainment problem.

A comprehensive review of the flow around a circular cylinder has been reported by Morkovin [1964]. This included experimental observations and theoretical studies of various aspects of the problem over an extended Reynolds number range.

In summary, there is considerable evidence that the mixing regions of turbulent free shear flows may be characterized by the presence of relatively coherent vortex-like structures. The passing frequency of these organized patterns when expressed through the Strouhal number fd/U, takes values of about 0.6 for round jets and of the order of 1 for plane jets (there are fewer experimental observations for the latter, though).

There are no reports in the literature on how the two mixing layers of a plane jet interact when merging together, nor on how they may affect the far field self-preserving region.

3.3 Externally Disturbed Plane Jets

Besides being capable of generating noise, turbulent jets are known to be sensitive to acoustic inputs. Indeed, the latter effect when considering a flow with low Reynolds number in the verge to become turbulent has been known for a long time, as observed by Leconte [1858]. At higher

Reynolds numbers, the effects go from altering the process of vortex formation, growth and coalescence in the initial region, as described by Rockwell [1971] and Becker and Massaro [1968], to a direct interaction between the acoustic field and the turbulent flow.

A comprehensive report, including their own experiments with water and air jets, was published by Chanaud and Powell [1962]. In a more recent investigation, Simcox and Hoglund [1971] theoretically analized the acoustic field-turbulent flow interaction for the plane jet. Glass [1968] reported experiments performed in a supersonic air jet where the sound waves generated in downstream positions affected, through an acoustic feedback process, the initial portions of the jet, changing the effective exchange coefficients and therefore the rate of jet spread and decay.

Goldschmidt and Kaiser [1971] conducted experiments applying pure acoustic waves of various frequencies to the self-preserving region of a plane turbulent jet. Their concluding results were that self-preservation of the flow is maintained, and that at specific frequencies, the spreading rate is increased (with an accompanying faster decay of the centerline velocity) and the geometric virtual origin is shifted.

Considerable interest in the above mentioned aspects of turbulent jets has arisen from the current technology on fluidic control devices. Particularly, in respect to the

dynamic response of fluidic amplifiers, the loss of performance at high frequencies is believed to be related to changes of the turbulent jet characteristics when subjected to periodic initial disturbances. This was pointed out by Stiffler [1971] in his study of the dynamic characteristics of the mean velocity profile of a plane jet.

Binder and Favre-Marinet [1972] reported experiments done on a plane jet subjected to relatively large amplitude transverse blowing pulses in the nozzle near region. The pulses were generated with a cylindrical rotating pressure chamber, provided with a blowing slot on each side of the nozzle, and were alternatively periodic. A higher rate of spreading and higher mean velocity decay at the centerline were found, when compared with the undisturbed jet.

It is seen therefore, that turbulent jets are sensitive to a considerable extent, to external disturbances, either in the form of pure acoustic tone or as localized gross blowing inputs. The initial region of the jet is particularly affected resulting perhaps, in changes of any possible relationship between the coherent structures in this region and the flapping behavior far downstream of the jet.

CHAPTER 4

EXPERIMENTAL SETUP AND PROCEDURES

4.1 Experimental Setup

All the experiments and measurements pertaining to this work were done in one of the existing turbulent plane jet setups at the Ray W. Herrick Laboratories of Purdue University. In the next paragraphs a description of the experimental setup, which was essentially the same used by Ott [1972] and Young [1973], is followed by a detailed account of the instrumentation and measurement procedures used in this investigation.

The facility consisted of a vertical rectangular nozzle of 0.635 x 30.48 cm (aspect ratio 48) supplied with air by a 1/4 HP squirrel-cage blower. A flexible duct connector between the blower outlet and the plenum chamber was employed in order to avoid the transmission of vibrations from the blower. The plenum chamber of dimensions 10.25 cm width, 30.48 cm height and 67.5 cm long, was provided with a series of honeycombs and screens to ensure uniform flow. The test section downstream of the nozzle exit was confined between two 90.2 x 122 cm plywood horizontal plates (Figure 4.1). In this way, a turbulent jet with Reynolds number based on the slot width (0.635 cm) and exit velocity (2.43×10^3 cm/sec)

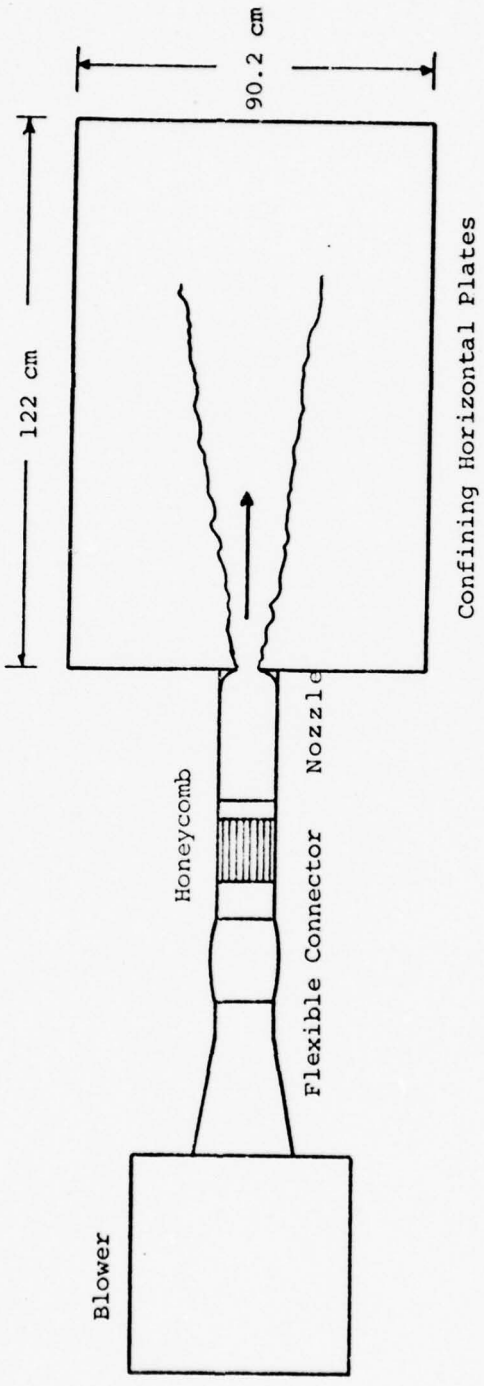

Figure 4.1 Schematic Diagram of Setup

of approximately 10^4, was obtained.

The existing two-dimensional traversing mechanism, with range 152.4 cm in the longitudinal x-direction and 76.2 cm in the lateral y-direction, was modified by installing two 10 turns precision potentiometers for lateral independent positioning of the probes. (Figure 4.2). Once the potentiometers were calibrated, positioning of probes within ± 0.01 cm was obtained.

In order to measure mean velocity profiles and to check self-preservation of the flow, a pair of Pitot-tubes (0.1 cm internal diameter) were manufactured. The Pitot-tubes were used together with a pressure transducer and a X-Y plotter, the former previously calibrated against a micromanometer (Figures 4.3 and 4.4).

Traverses were done at various longitudinal positions. The resulting mean velocity profiles appear in Appendix A, where the self-preserving characteristics of the flow are also presented.

Two DISA 55A01 constant-temperature anemometers with DISA 55A22 and DISA 55F11 probe supports and "home-made" plated tungsten sensing elements (0.0002 cm diameter), were used to obtain the velocity signals at any two points in the flow. In computing normalized crosscorrelations between these signals, calibration of the hot-wires was excluded. It sufficed to measure the root-mean-square value of each signal and divide as noted in equation (2.17). A true root-

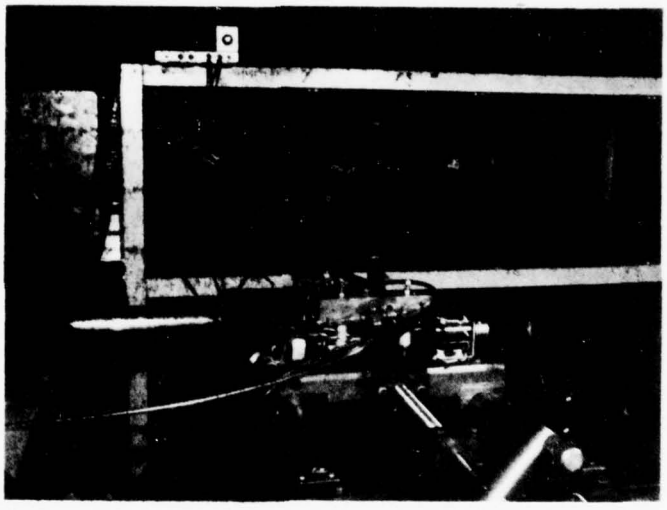

Figure 4.2 Traversing Mechanism

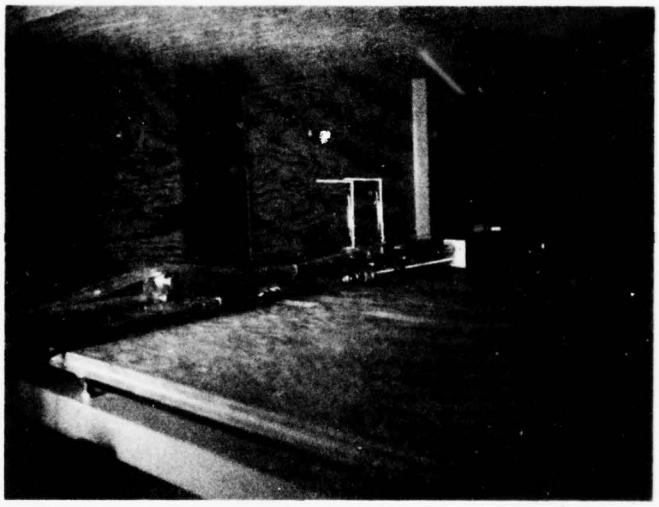

Figure 4.3 Hot-Wire Probes and Pitot-tubes

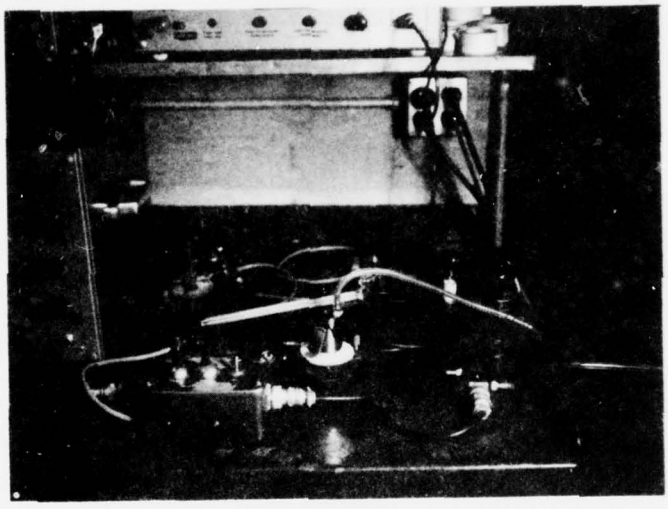

Figure 4.4 Micromanometer and Pressure Transducer

mean-square voltmeter B&K 215 was used for this purpose.

Preliminary crosscorrelation function measurements were done using a SAICOR Correlator and Probability Analyzer, model SAI-42. This digital on-line processing instrument, provides a correlation computation at 100 incremental lag points simultaneously. By using the resume capability of the instrument, an average of various correlation samples can be determined, although the process is slow and tedious.

In order to overcome the above disadvantage and to have additional computational features, the use of a Hewlett-Packard 5452A-2114B Fourier Analyzer System, was preferred. It consists of the following elements: an analog-to-digital converter with a wide range of sampling characteristics; an 8K words memory minicomputer which includes the Fast Fourier Transform algorithm among its software; and a display, a teleprinter and a fast paper tape puncher units. Depending on the data block size used, a more complete picture of the correlation function could be obtained, that is, including more lag points. Also by programming the system, any number of samples could be taken for a particular situation and therefore a better estimate of the correlation function was obtained. Detailed block diagrams and listings of the programs used in this investigation are presented in Appendix B.

Finally, auxiliary equipment like two SKL302 low-pass filters to avoid aliasing in the analog-to-digital

conversion, a EI500 X-Y Plotter, a general purpose oscilloscope and digital voltmeters, were also used. (Figures 4.5, 4.6, 4.7).

4.2 Experimental Procedures

The measurement procedure was essentially the same in all experiments. After having carefully positioned and aligned the probes, a warm up period (for the instrumentation) of at least one hour was allowed. At the beginning of each run, a quick average correlation based on 10 or 20 samples was determined with the Fourier analyzer. In this way, proper scaling and sampling parameters for the analog-to-digital converter were determined (the cut-off frequencies of the low-pass filters were set to just avoid aliasing. Generally 1 kHz, but no less than 600 Hz, was used for these frequencies). After this preliminary operation the analyzer was reprogrammed and up to four estimates of the correlation function were determined for each run at each point of interest. Each estimate included 250 samples and took about 20 minutes to be obtained.

Four kinds of velocity correlation measurements were taken. These are labelled Type I, II, III and IV, respectively. Figures 4.8, 4.9, 4.10 and 4.11 show schematically how the probes were positioned for each measurement type, respectively. Table 4.1 gives the various values of the x and y coordinates used in positioning the probes for each type of measurement.

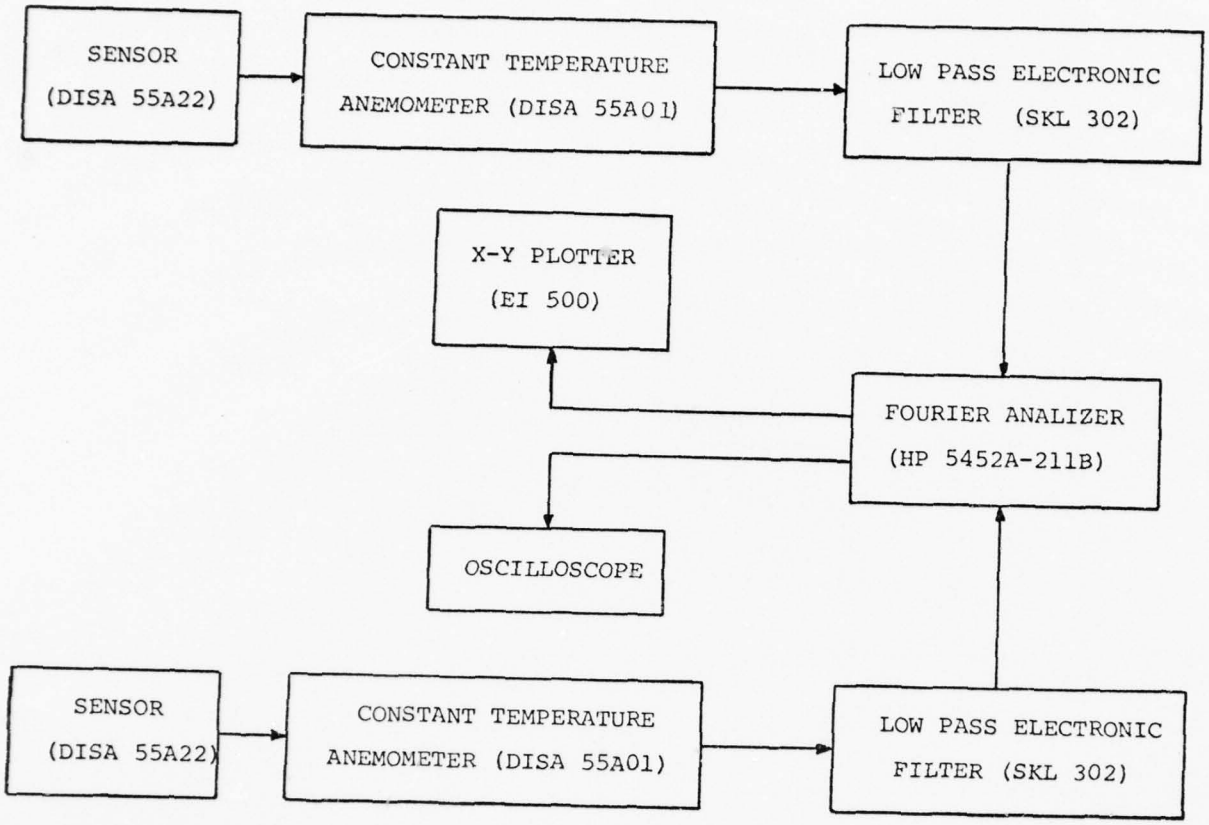

Figure 4.5 Block Diagram of Instrumentation

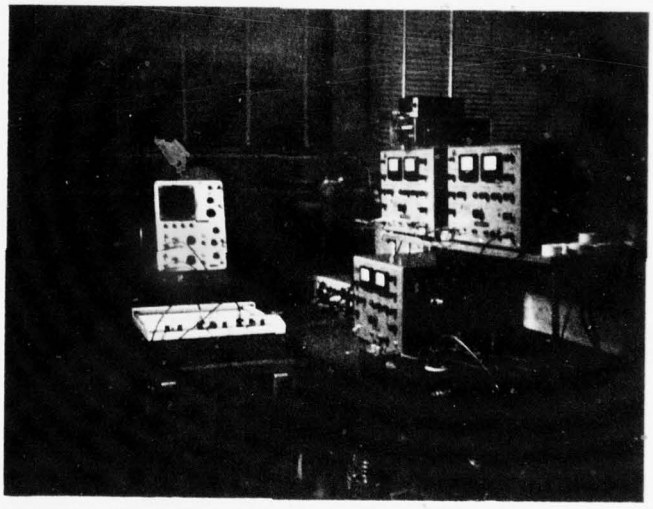

Figure 4.6 Instrumentation

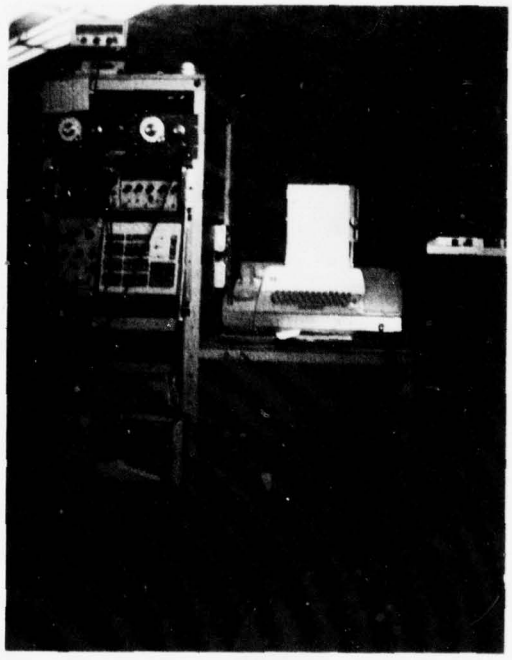

Figure 4.7 HP Fourier Analizer

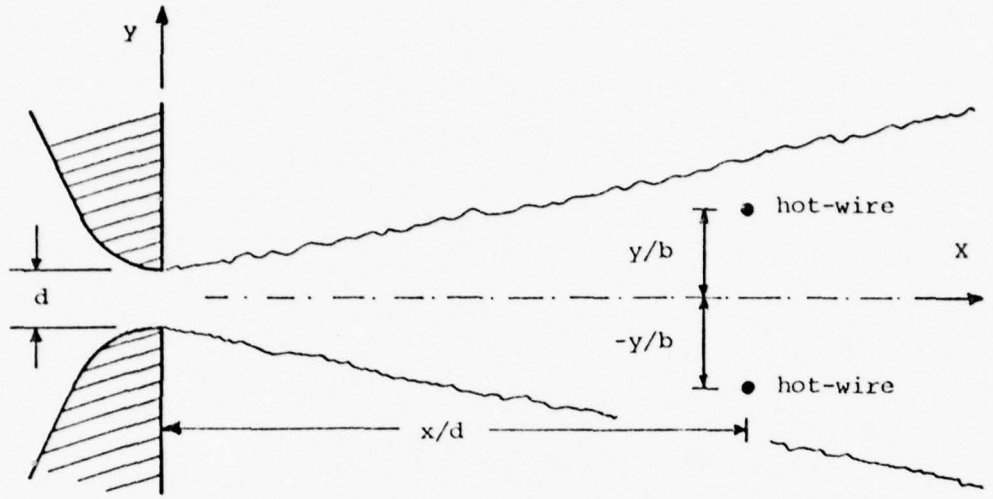

Figure 4.8 Measurements Type I

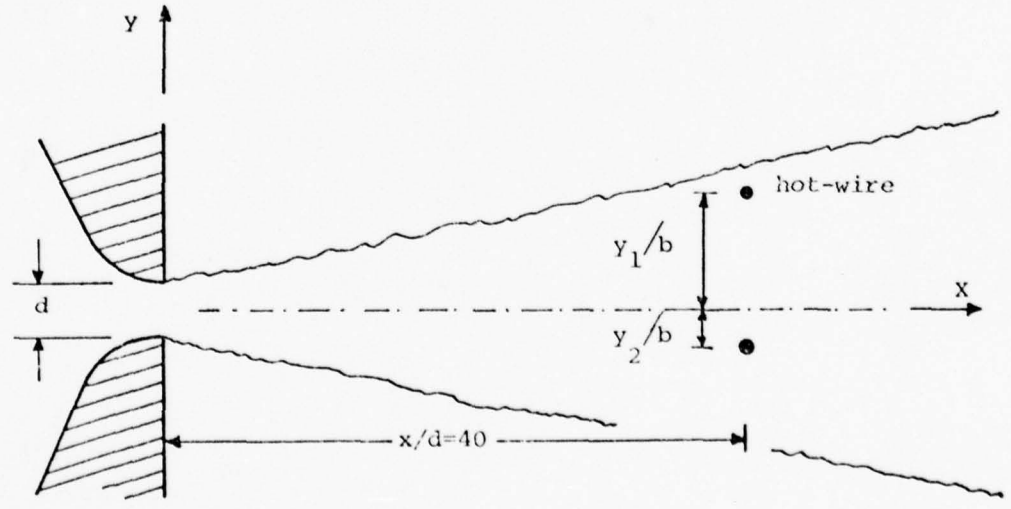

Figure 4.9 Measurements Type II

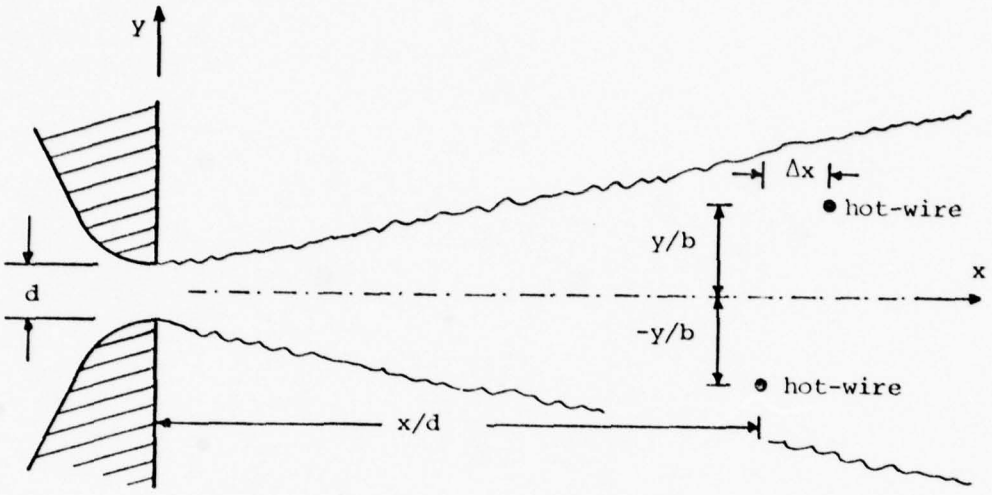

Figure 4.10 Measurements Type III

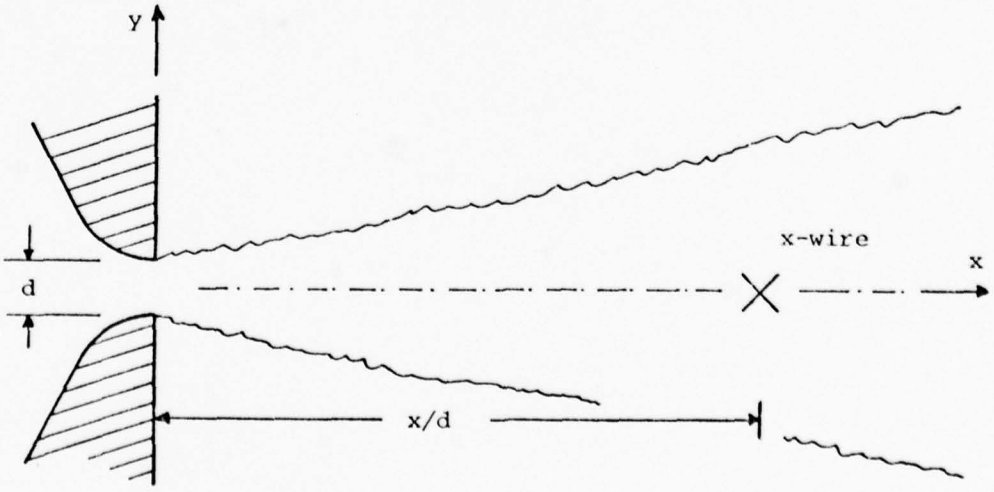

Figure 4.11 Measurements Type IV

Table 4.1 Probe Configurations.

MEASUREMENTS TYPE	x/d	y_1/b	y_2/b	$\Delta x/d$
I	10,20,30,40,60,80,100 ✓ ✓ ✓	0.5 0.75 1.0 1.25	-0.5 -0.75 -1.0 -1.25	—
II	40 ✓ ✓ ✓ ✓	0.25 0.5 0.75 1.0 1.25	-0.5,-0.75,-1.0,-1.25 -0.25,-0.75,-1.0,-1.25 -0.25,-0.5,-1.0,-1.25 -0.25,-0.5,-0.75,-1.25 -0.25,-0.5,-0.75,-1.0	—
III	20,30,40 10,20,30,40	0.65 1.0	-0.65 -1.0	2,4,6,8,10 ✓
IV	10,20,30,40,60,80	0	0	—

Measurements Type I (Figure 4.8) consisted of cross-correlations between x-component velocity signals obtained from probes set at two points symmetrically apart with respect to the centerline of the jet. These measurements were performed at x/d stations of 10, 20, 30, 40, 60, 80 and 100; the probes were positioned at y/b values of 0.5, 0.75, 1.0 and 1.25 approximately, for each x/d station.

Corresponding to the Type II runs (Figure 4.9), crosscorrelations were measured by setting the probes at points with different opposite lateral coordinate y/b. The Type II runs were limited to x/d = 40. However, a wide number of combinations for the lateral coordinates y_1/b and y_2/b were included.

The third type of measurements, Type III (Figure 4.10), was obtained by holding one probe at a given x/d station and placing the second probe at the opposite side of the jet but at a different x/d position. The longitudinal separation between probes Δx, was varied from 0 to 5.1 cm in steps of 1.27 cm. Three x/d stations (20, 40 and 60) for the fixed probe were investigated.

Finally, the measurement procedure of the Type IV (Figure 4.11) was different from those already described. For this case the autocorrelation function of the y-component velocity at the centerline of the jet, was measured for x/d positions of 20, 30, 40, 60 and 80. Instead of two normal hot-wires, an x-wire type DISA 55A38 was employed for these

measurements. Detailed analysis on how the autocorrelation was estimated for this case is given in Appendix B, together with the program used to process the data with the Fourier analyzer.

Measurements were also taken at the mouth of the jet to attempt to determine any instabilities in the blower feeding the nozzle. Preliminary and limited observations were also made in the presence of a low frequency acoustic disturbance. These are noted in Chapter 7.

As a last series of experiments, modification of the electrical motor and pulleys driving the blower, allowed runs at Reynolds numbers of 7900 and 15100. These included measurement of crosscorrelations at x/d stations of 40, 60 and 80, with the probes symmetrically positioned with respect to the jet centerline (Type I measurements).

The objetive in all the measurements (Types I to IV) was to first determine whether indeed there is a flapping motion of the jet and secondly to attempt to diagnose its origin.

CHAPTER 5

EXPERIMENTAL RESULTS

In this chapter the experimental results are presented. In order to have a better depiction of the flapping behavior first some general properties are reported and then various characteristics (as resulted from the experiments) are separately considered. The various types of measurements, tabulated on Table 4.1, are reported in the sections that follow as needed rather than chronologically. Generally the type I measurements were taken to determine flapping frequency and amplitude. The type II measurements were taken to assure that the motion was transversely coherent. The absence of "weaving" of the flow past a fixed vortex street type structure was noted through type III measurements. They indeed confirmed the uniform sideways motion of the entire flow field and gave an approximate wave velocity (or convective velocity). The type IV measurements were taken to insure that the sideways motion was also noted at the jet centerline.

Additional measurements at different Reynolds numbers are reported in the last part of this chapter.

5.1 General Characteristics of the Flapping Motion

All measured crosscorrelation functions between x-components of the velocities at two points on opposite sides of the centerline of the jet, are persistent and repeatable. These correlation estimates present some general features which will be examined in the following paragraphs.

The two most important characteristics, indicating the existence of an oscillating (in the average) lateral motion or flapping of the jet, are: an invariably negative value of the correlation function at zero time delay and an alternate succession of positive and negative values as the time delay between the two signals increases. Examples of these correlations (as obtained directly from the Fourier analyzer through an x-y plotter), are given in Figures 5.1 to 5.4. The correlation functions shown in Figures 5.1 and 5.2 were obtained with the hot-wire probes positioned symmetrically apart with respect to the jet centerline at $x/d = 40$, $y/b = \pm 1.0$ and $x/d = 100$, $y/b = \pm 1.0$, respectively (Type I). Figures 5.3 and 5.4 show correlations taken at $x/d = 40$, with the probes asymmetrically positioned (Type II): Figure 5.3 corresponds to $y_1/b = 0.75$, $y_2/b = -0.5$ (Note that for $\tau > 0.128$ sec in Figures 5.1 and 5.2 and for $\tau > 0.064$ sec in Figures 5.3 and 5.4, that is, the second half of all records, the correlation function is not significant. This is due to the wrap-around error inherent in the analyzer performance, as explained in Appendix B).

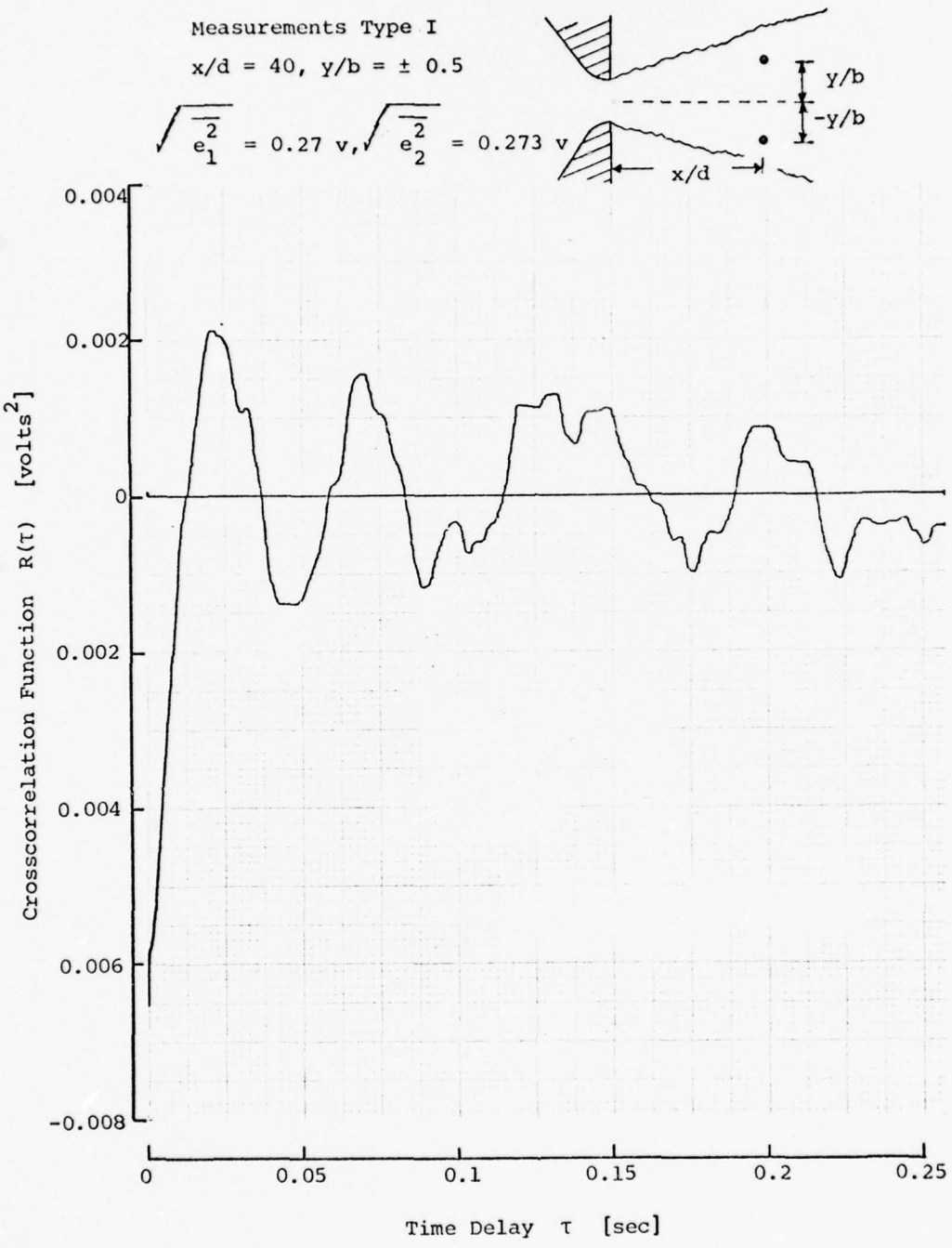

Figure 5.1 An Example of Crosscorrelation Function for x/d = 40, y/b = ± 0.5

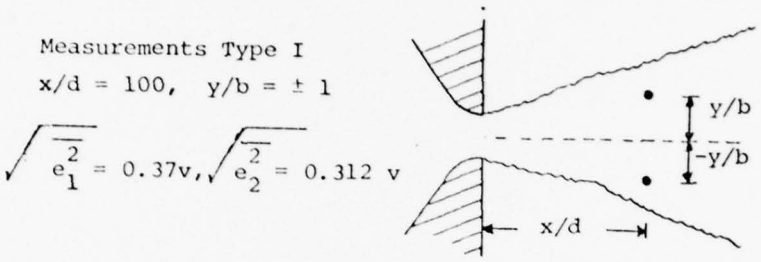

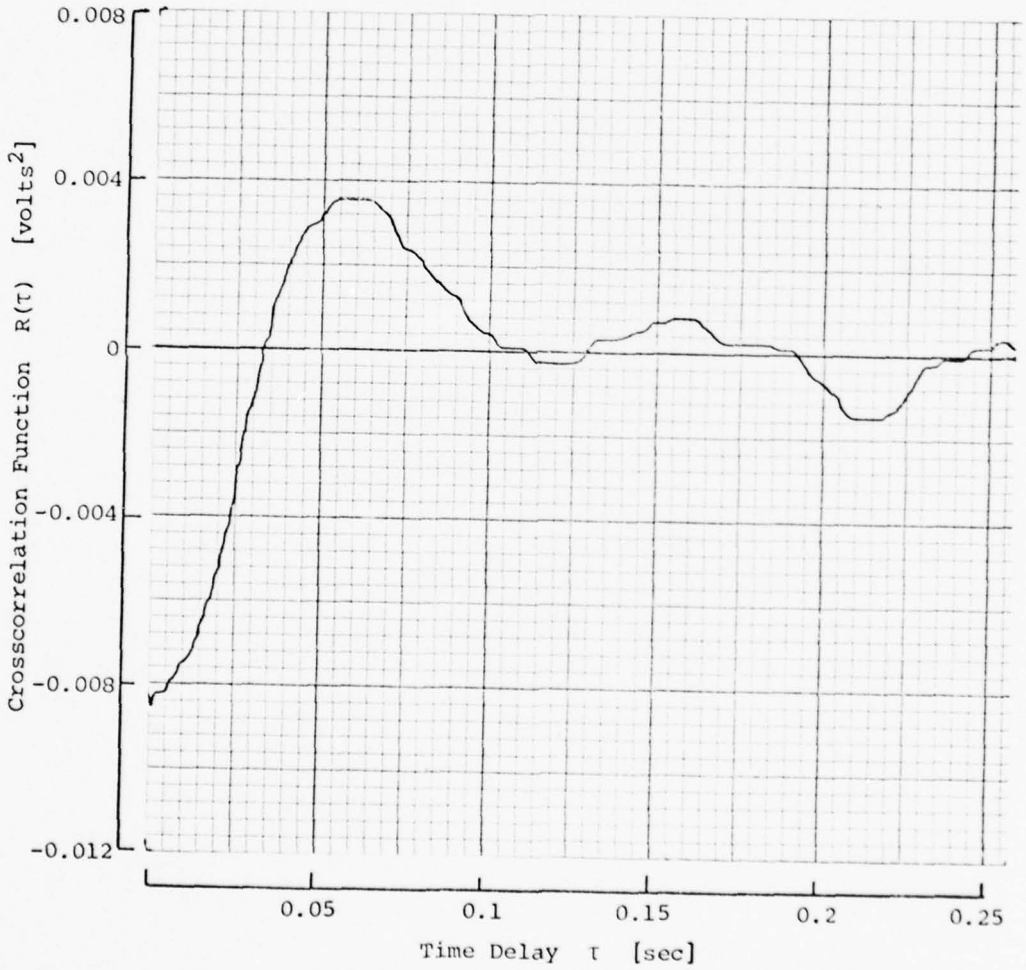

Figure 5.2 An Example of Crosscorrelation Function for x/d = 100, y/b = 1

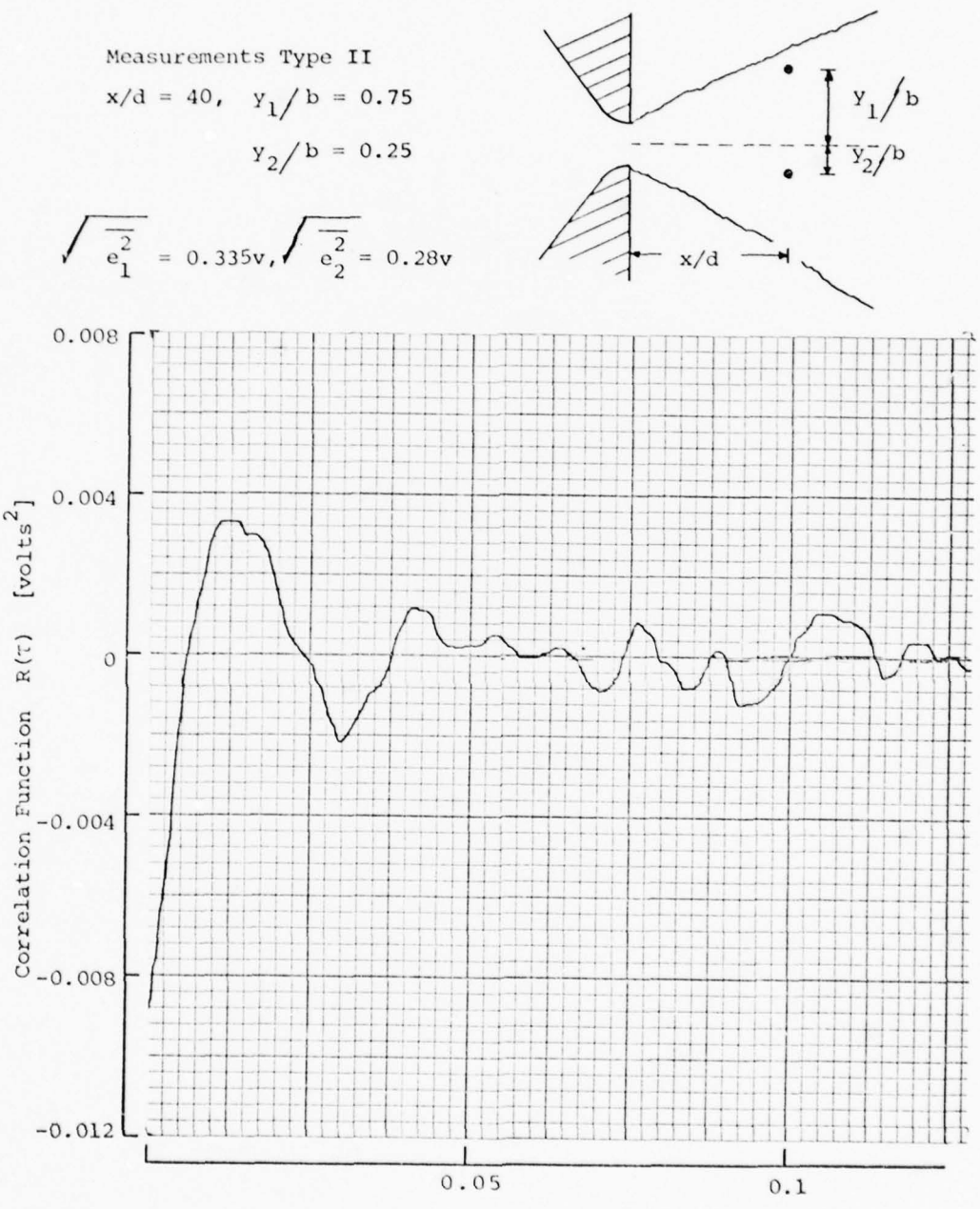

Figure 5.3 An Example of Crosscorrelation Function for x/d = 40, $y_1/b = 0.75$, $y_2/b = -0.25$

Measurements Type II

$x/d = 40$, $y_1/b = 1.25$

$y_2/b = -0.5$

$\sqrt{\overline{e_1^2}} = 0.41v$, $\sqrt{\overline{e_2^2}} = 0.342v$

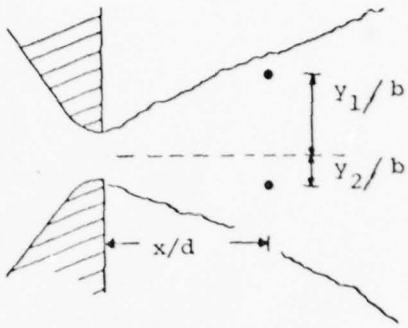

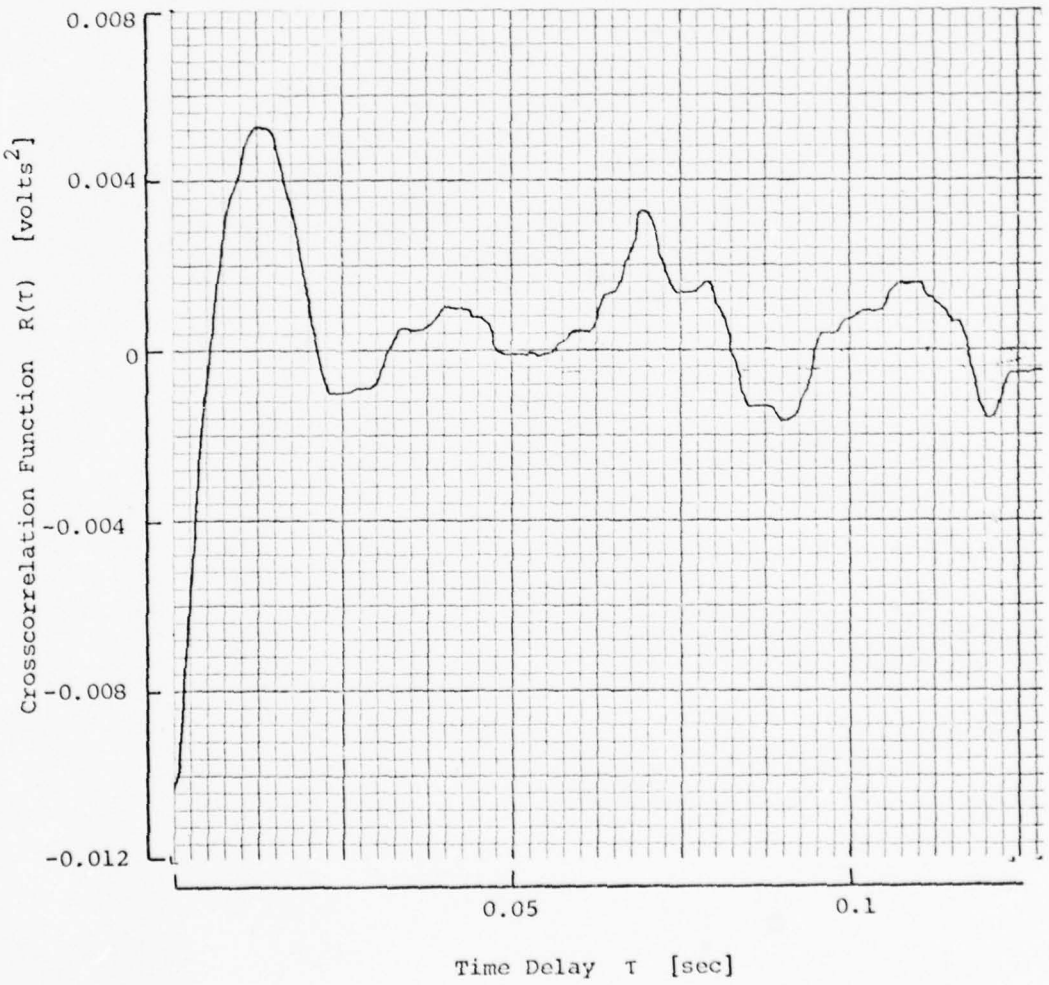

Figure 5.4 An Example of Crosscorrelation Function for $x/d = 40$, $y_1/b = 1.25$, $y_2/b = -0.5$

The correlations exhibit a certain periodicity. This is related to and gives a measure of the flapping frequency. (Simultaneously, the magnitude of the correlation at $\tau = 0$ would give a measure of the amplitude of the oscillatory-like flapping motion). The times between local maxima or local minima (see for instance Figure 5.1) are generally not equal. However, the time to the first maximum is clearly measurable and it suggests the definition of a frequency of flapping, f_1, as illustrated schematically in Figure 5.5. On the other hand, an average time between local maxima and minima, beyond the first local maximum, can be found. With it a second frequency f_2, as also illustrated in Figure 5.5, can be determined. These two frequencies are essentially the same, although within some experimental scatter, as noted in the beginning of the next section.

5.2 Characteristics of the Flapping Frequency along the Longitudinal and Lateral Coordinates

Type I Measurements

A complete survey of crosscorrelation functions was done after setting both probes on opposite sides of the jet centerline (measurements Type I). The resulting frequencies of flapping are plotted as a Strouhal number, fd/U_o. Figures 5.6 and 5.7 present the results for f_1 and f_2, respectively. The flapping frequency (given by f_1 and f_2) is noted to decrease as x/d increases.

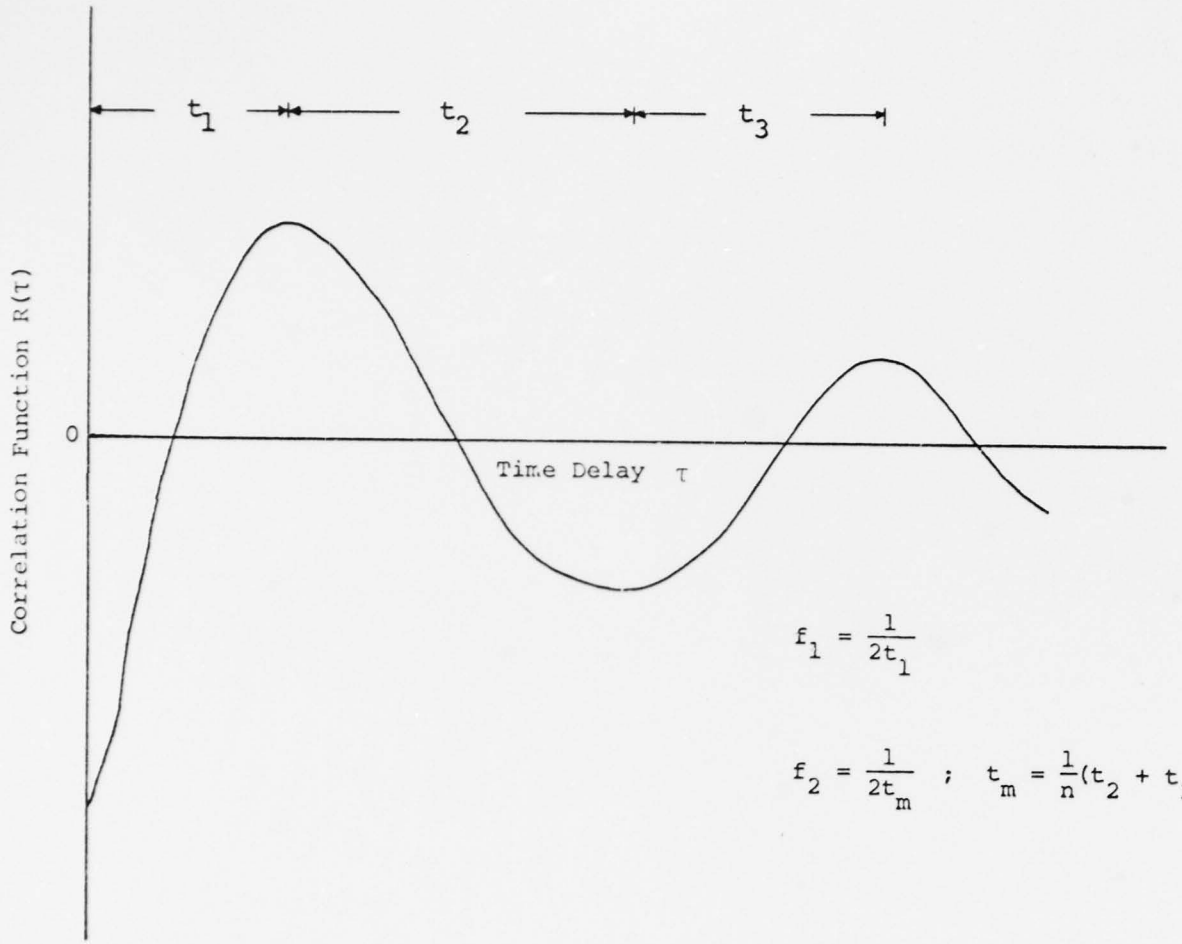

$$f_1 = \frac{1}{2t_1}$$

$$f_2 = \frac{1}{2t_m} \quad ; \quad t_m = \frac{1}{n}(t_2 + t_3 + \ldots + t_n)$$

Figure 5.5 Definition of Flapping Frequency

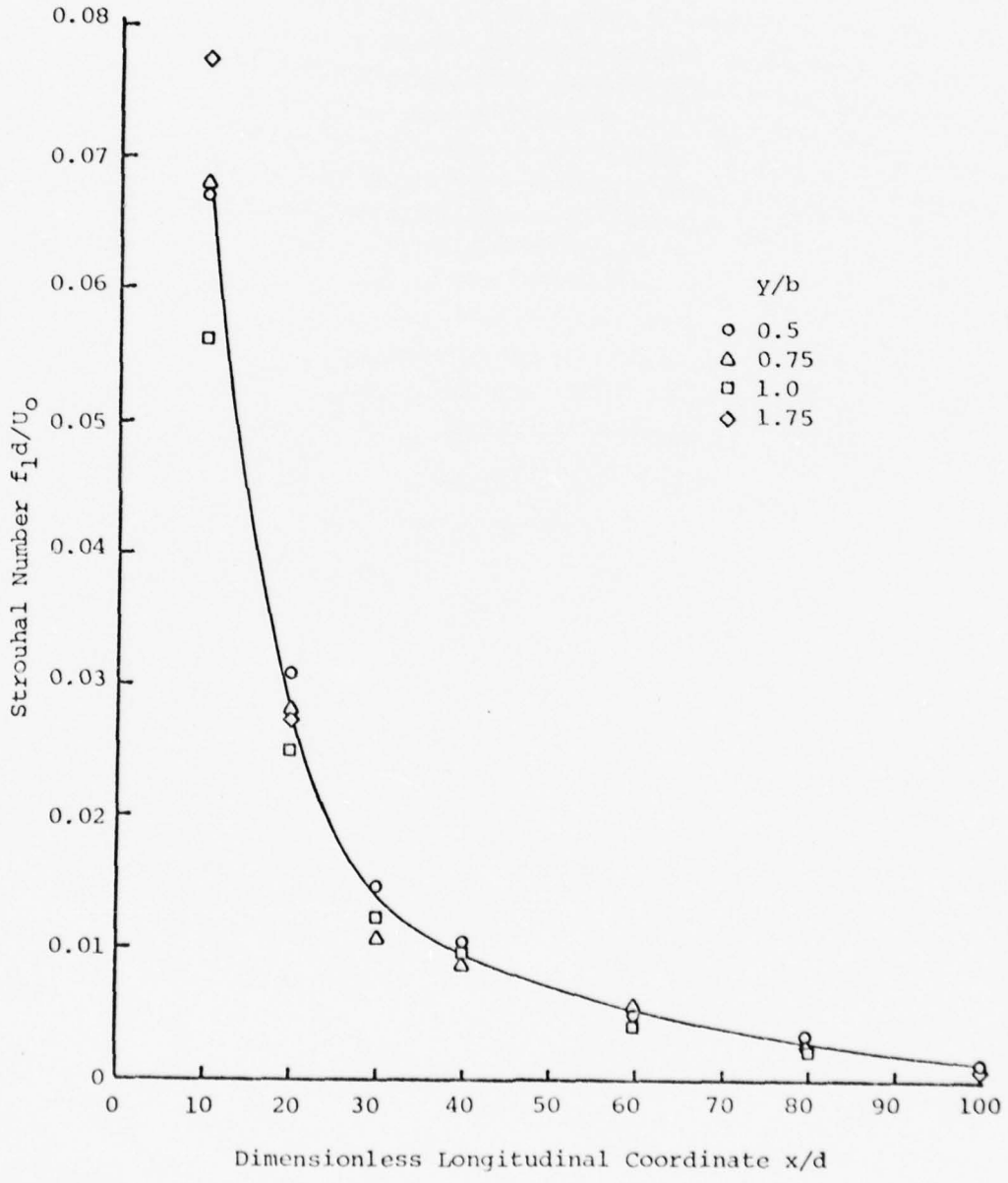

Figure 5.6 Strouhal Number $f_1 d/U_o$ vs. x/d

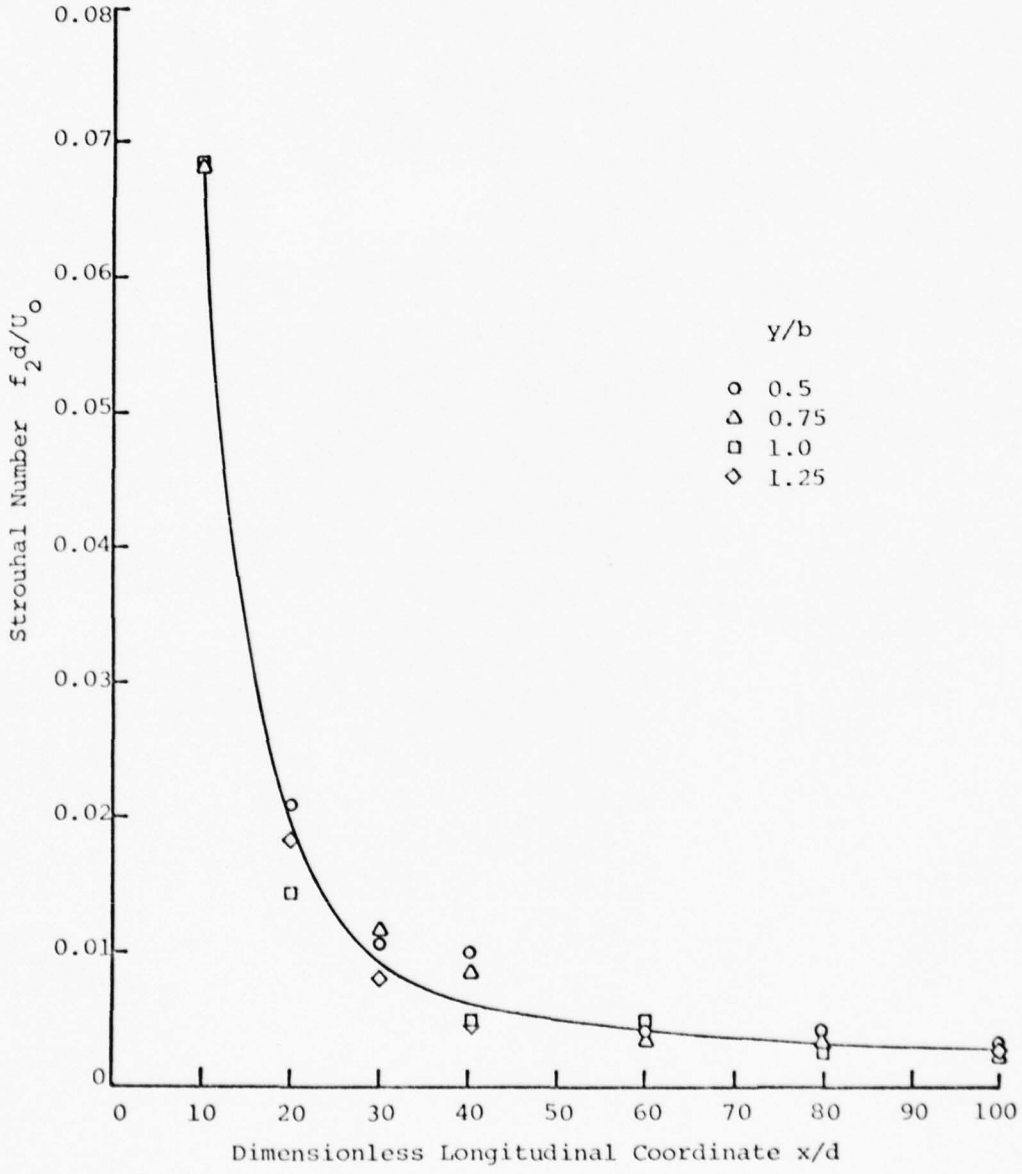

Figure 5.7 Strouhal Number $f_2 d/U_o$ vs. x/d

On the other hand, the flapping frequency does not seem to depend on the lateral coordinate. This is noted both by the collapse of the data points on Figures 5.6 and 5.7 and by the plot in Figure 5.8. This is so at least for $x/d > 30$ where the jet becomes self-preserving in terms of mean velocity and turbulence intensity (Bradbury [1965], Gutmark and Wygnanski [1976]). The data points corresponding to x/d values of 10 and 20 show a large amount of scatter. The reason for this could be error in positioning the probes at these small x/d stations and insufficient time resolution in the correlations computed by the analyzer, as compared with larger x/d points at lower velocities.

Several scaling parameters for f (both f_1 and f_2) were considered. The intent was to exhibit any possible similarity and self-preservation for the flapping frequency. The various jet coordinates, length and velocity scales (x, y, d, b, U, U_m) were combined in this search. The best results are shown in Figures 5.9 to 5.15.

Figure 5.9 shows the variation of $\frac{f_1 y}{U}$ against y/d for each x/d, where U is the local mean velocity at each pair of points of coordinates x/d, $\pm$ y/d (where the cross-correlation was measured). Figure 5.10 presents a collapse of all curves in Figure 5.9, using y/b instead of y/d for the abscissa.

The same data, but in somewhat different form, is presented in Figure 5.11 when the parameter $\frac{fy}{U} \Big/ \frac{y}{b}$ is plotted

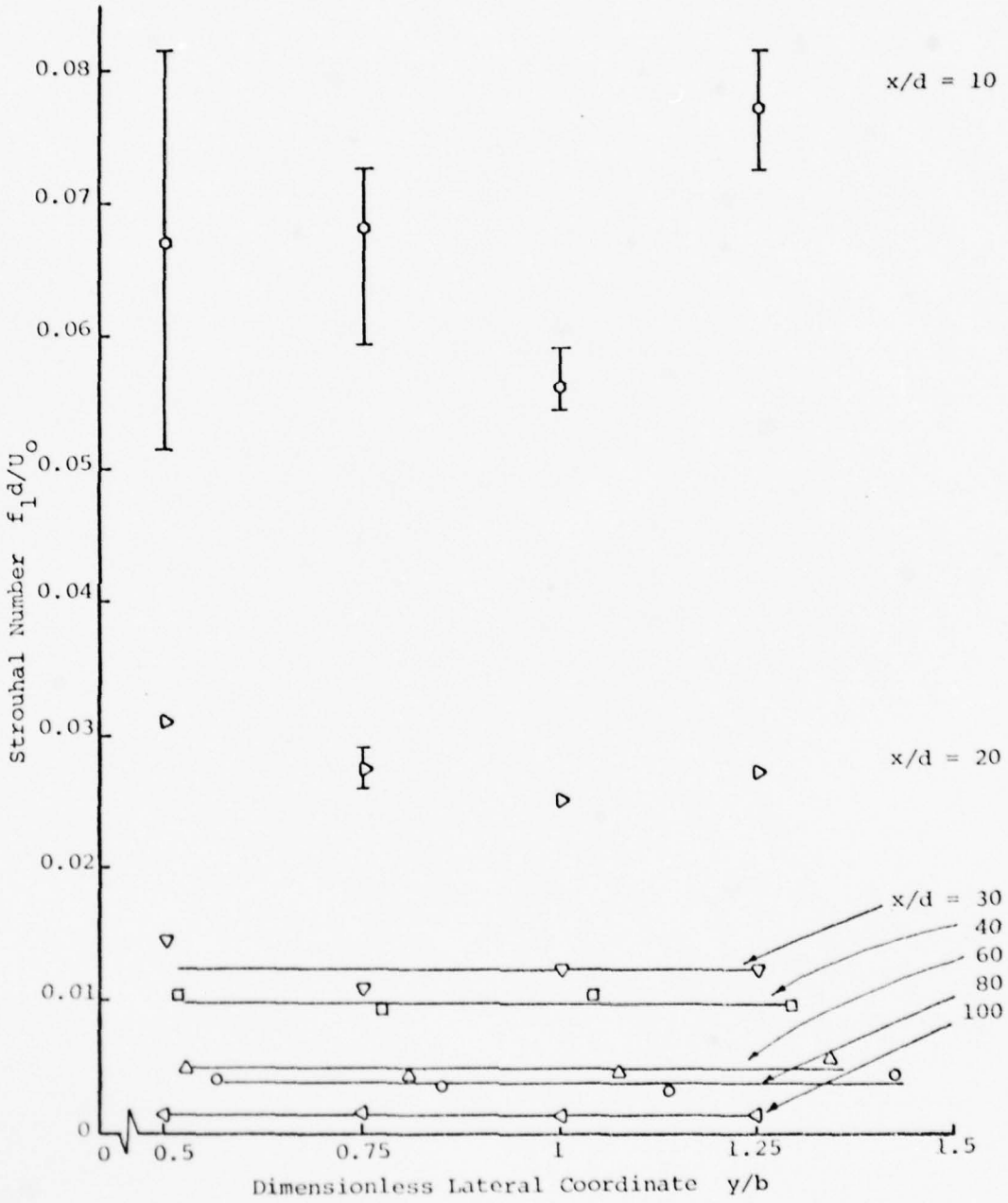

Figure 5.8 Strouhal Number $f_1 d/U_o$ vs. y/b

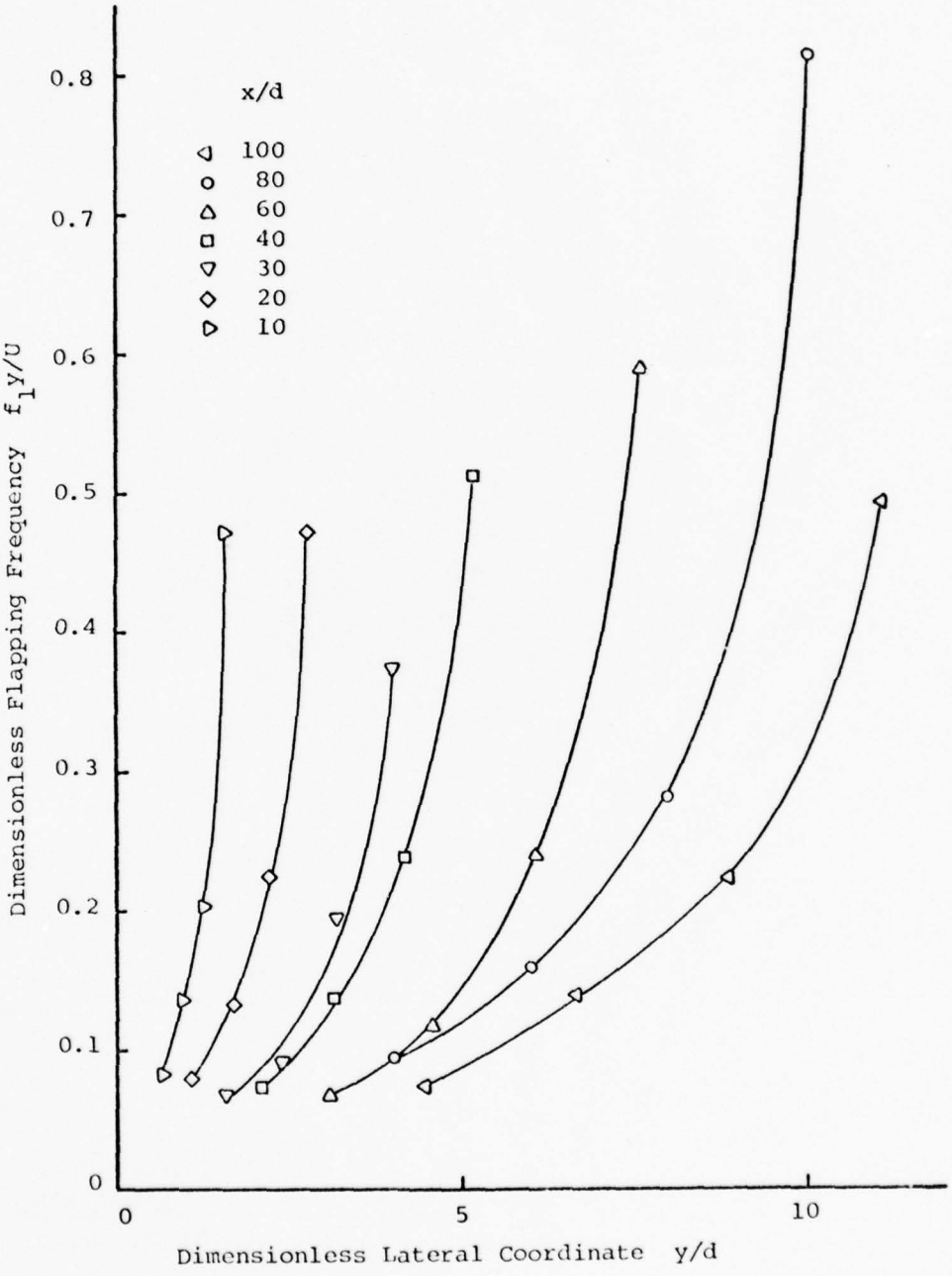

Figure 5.9 Dimensionless Flapping Frequency $f_1 y/U$ vs. y/d

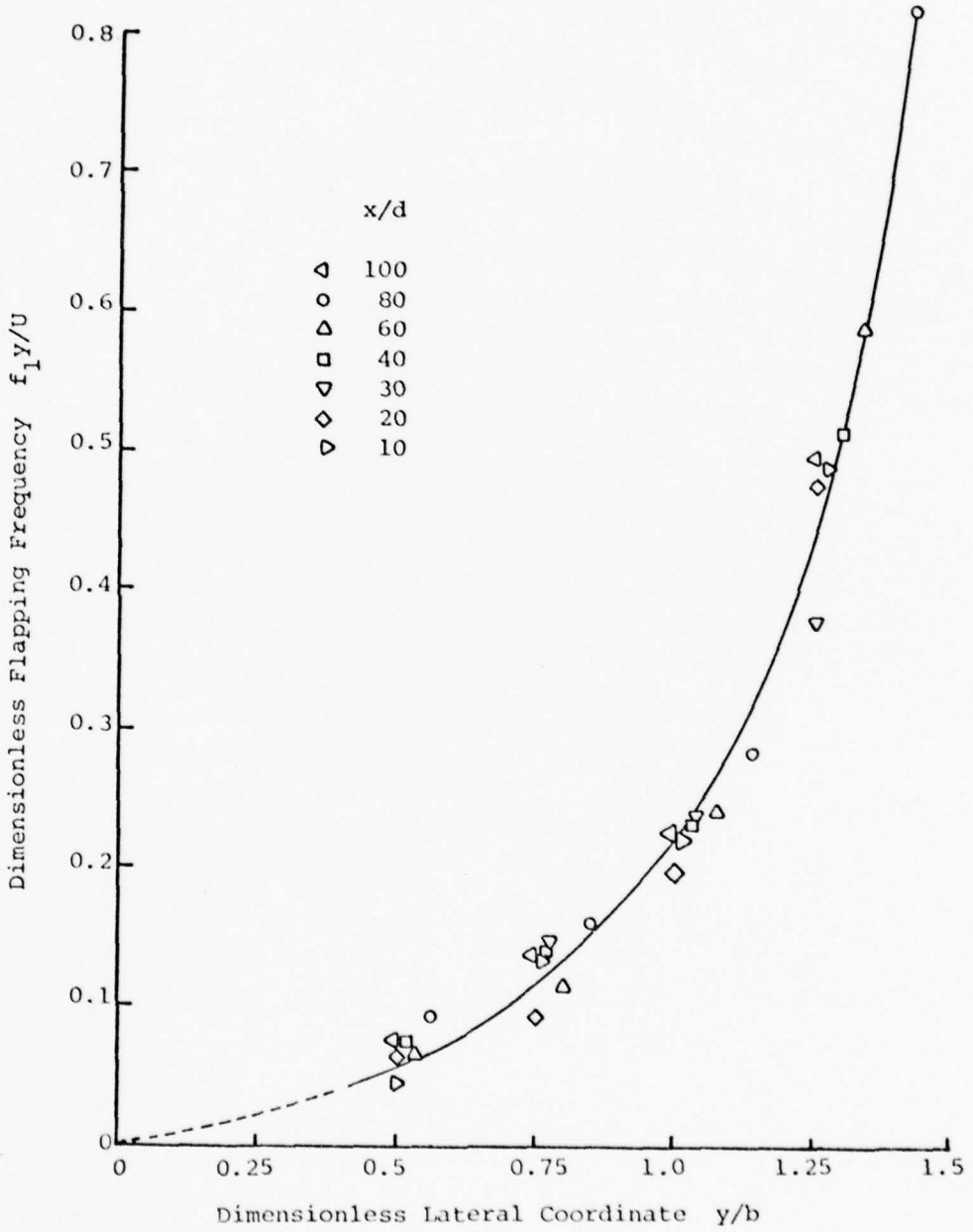

Figure 5.10 Dimensionless Flapping Frequency $f_1 y/U$ vs. y/b

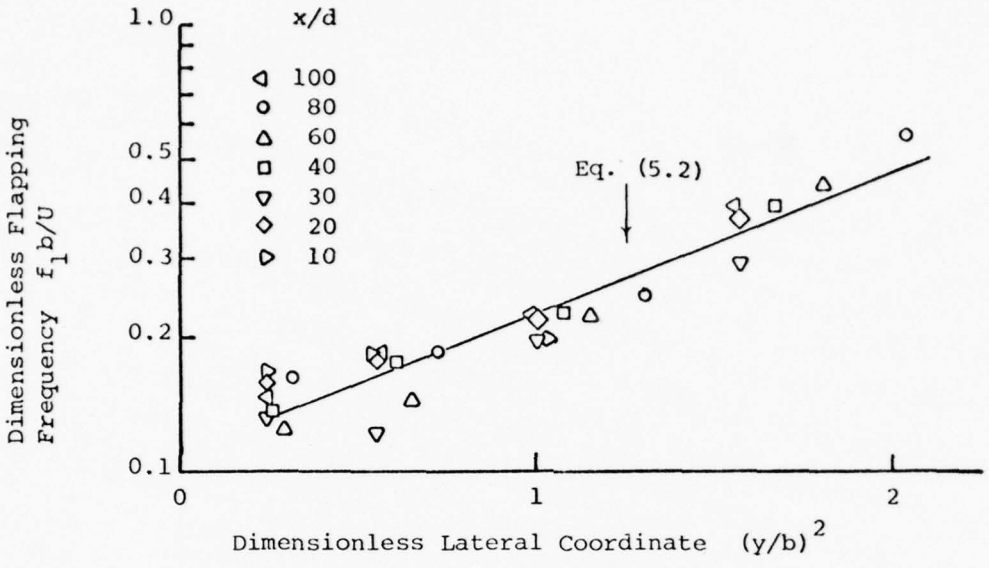

Figure 5.11 Dimensionless Flapping Frequency $f_1 b/U$ vs. $(y/b)^2$

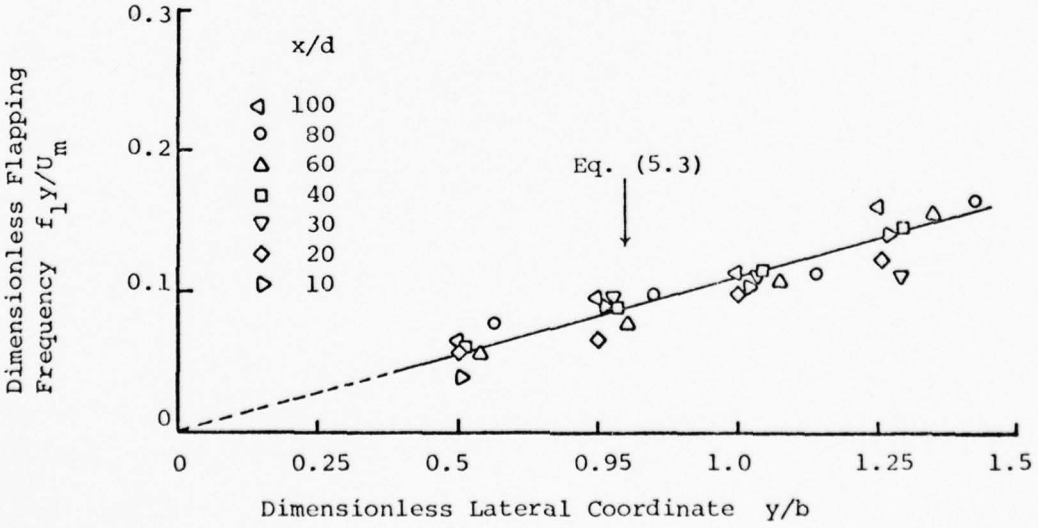

Figure 5.12 Dimensionless Flapping Frequency $f_1 y/U_m$ vs. y/b

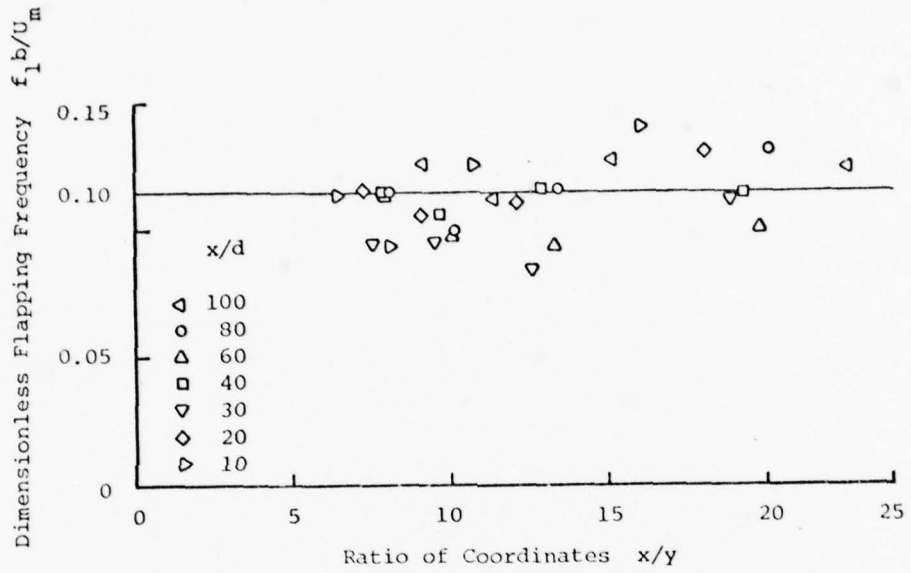

Figure 5.13 Dimensionless Flapping Frequency $f_1 b/U_m$ vs. x/y

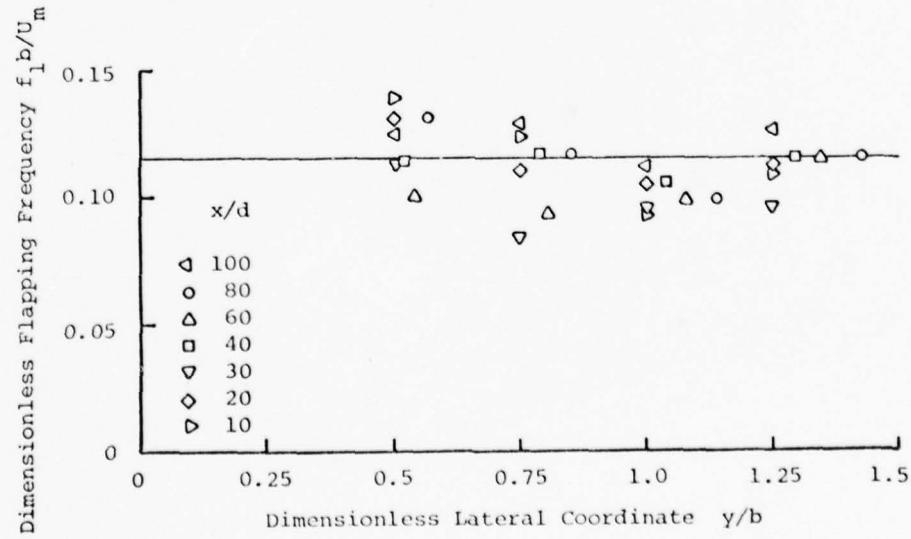

Figure 5.14 Dimensionless Flapping Frequency $f_1 b/U_m$ vs. y/b

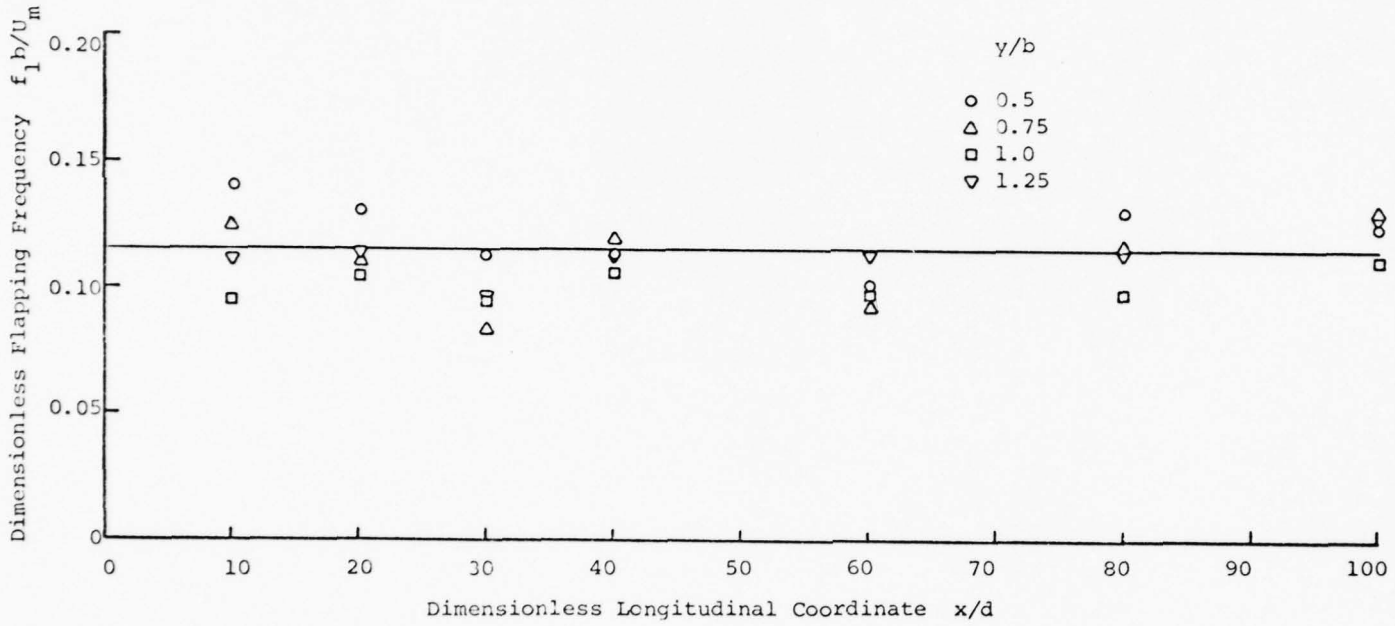

Figure 5.15 Dimensionless Flapping Frequency $f_1 b/U_m$ vs. x/d

Figure 5.2 An Example of Crosscorrelation Function for x/d = 100, y/b = 1

against $(y/b)^2$, using a logarithmic scale for the ordinate. The data points follow approximately a straight line, that is:

$$\ln \frac{fy/U}{y/b} \sim \left(\frac{y}{b}\right)^2 \tag{5.1}$$

or

$$\frac{fy}{U} = 0.11 \frac{y}{b} \exp 0.72 \left(\frac{y}{b}\right)^2 \tag{5.2}$$

Figure 5.12 relates fy/U_m (where U_m is the center-line mean velocity at a given x/d) to y/b. A fit of the type:

$$\frac{fy}{U_m} \simeq 0.11 \frac{y}{b} \tag{5.3}$$

appears satisfactory.

Actually both equations (5.2) and (5.3) represent the same trend. In effect, if Reichardt's solution for the self-preserving mean velocity profile is recalled (equation (2.4), Chapter 2):

$$\frac{U}{U_m} = \exp \left[- (0.8326 \frac{y}{b})^2\right] \tag{2.4}$$

or:

$$\frac{U}{U_m} = \exp \left[- k \left(\frac{y}{b}\right)^2\right] \tag{5.4}$$

it may be combined with (5.2) to give (5.3).

Moreover, equation (5.3) may also be written as:

Figure 5.3 An Example of Crosscorrelation Function for x/d = 40, $y_1/b = 0.75$, $y_2/b = -0.25$

$$\frac{fb}{U_m} = 0.11 \tag{5.5}$$

which is the result shown in Figures 5.13, 5.14 and 5.15.

The flapping frequency then, attains approximate self-preservation if scaled with the jet half-width b and the mean velocity at the centerline.

Using this result, a replotting of the correlation functions was done through a computer Calcomp system. The abscissa τ was modified to a dimensionless time delay $\tau U_m/b$ and the ordinate was divided by the product of the r.m.s. values of the signals (to have a normalized crosscorrelation function). Figures 5.16 to 5.19 show these results for y/b values of 0.5, 0.75, 1, and 1.25 respectively, each one including x/d stations larger than 30 (the plots for x/d = 10 and 20 were purposely omitted. They did not show the same trend).

It is interesting to note that not only does the flapping frequency exhibit approximate self-preservation and similarity for x/d > 30, but so does the magnitude of the crosscorrelation function (at least for the first half-period). As an example, the values of $\underline{R}(0)$, where:

$$\underline{R}(0) = \frac{\overline{u(y,t)\,u(-y,t)}}{\sqrt{\overline{u^2(y,t)}}\sqrt{\overline{u^2(-y,t)}}} \tag{5.6}$$

are plotted in Figure 5.20. A trend is noted and a relationship of the form:

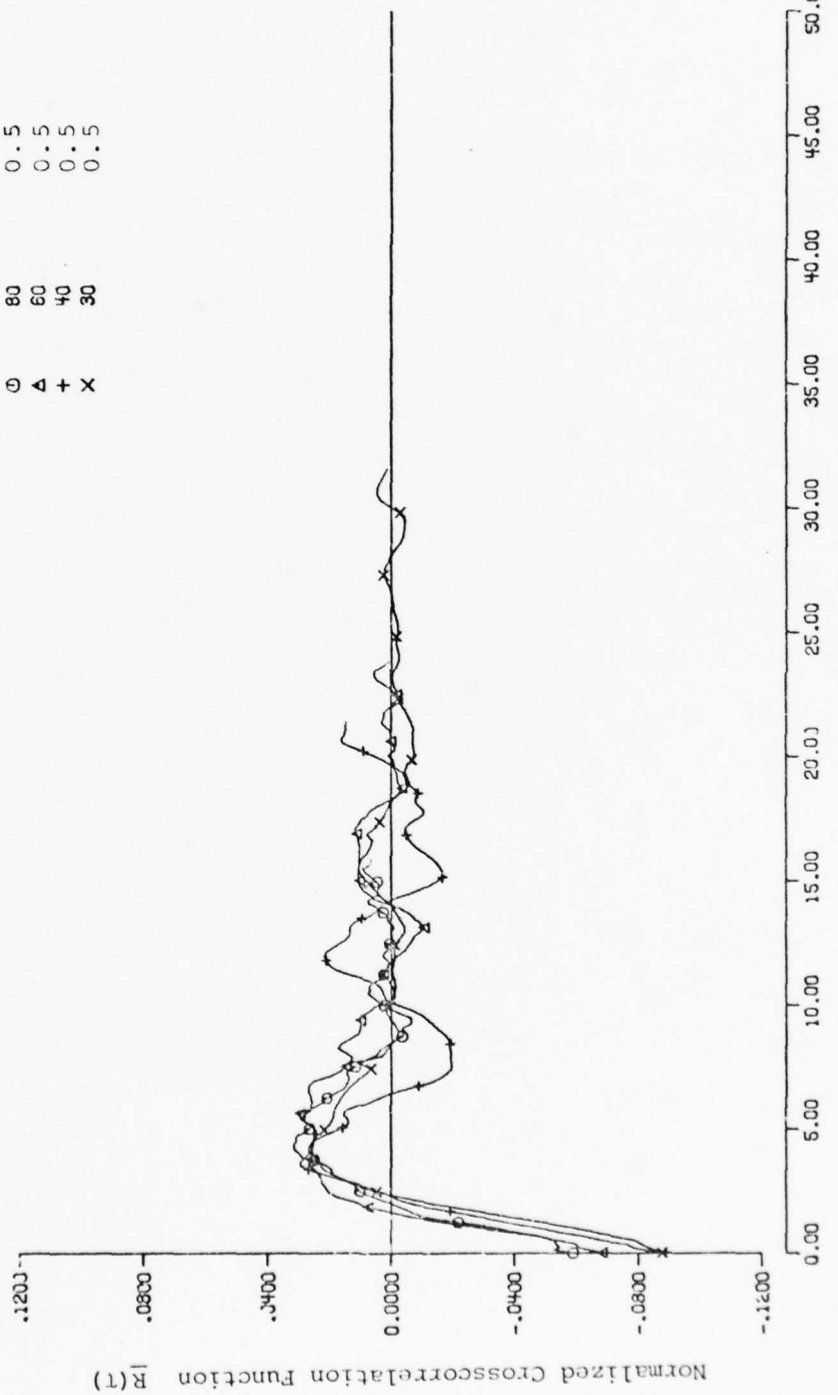

Figure 5.16 Normalized Crosscorrelation Functions

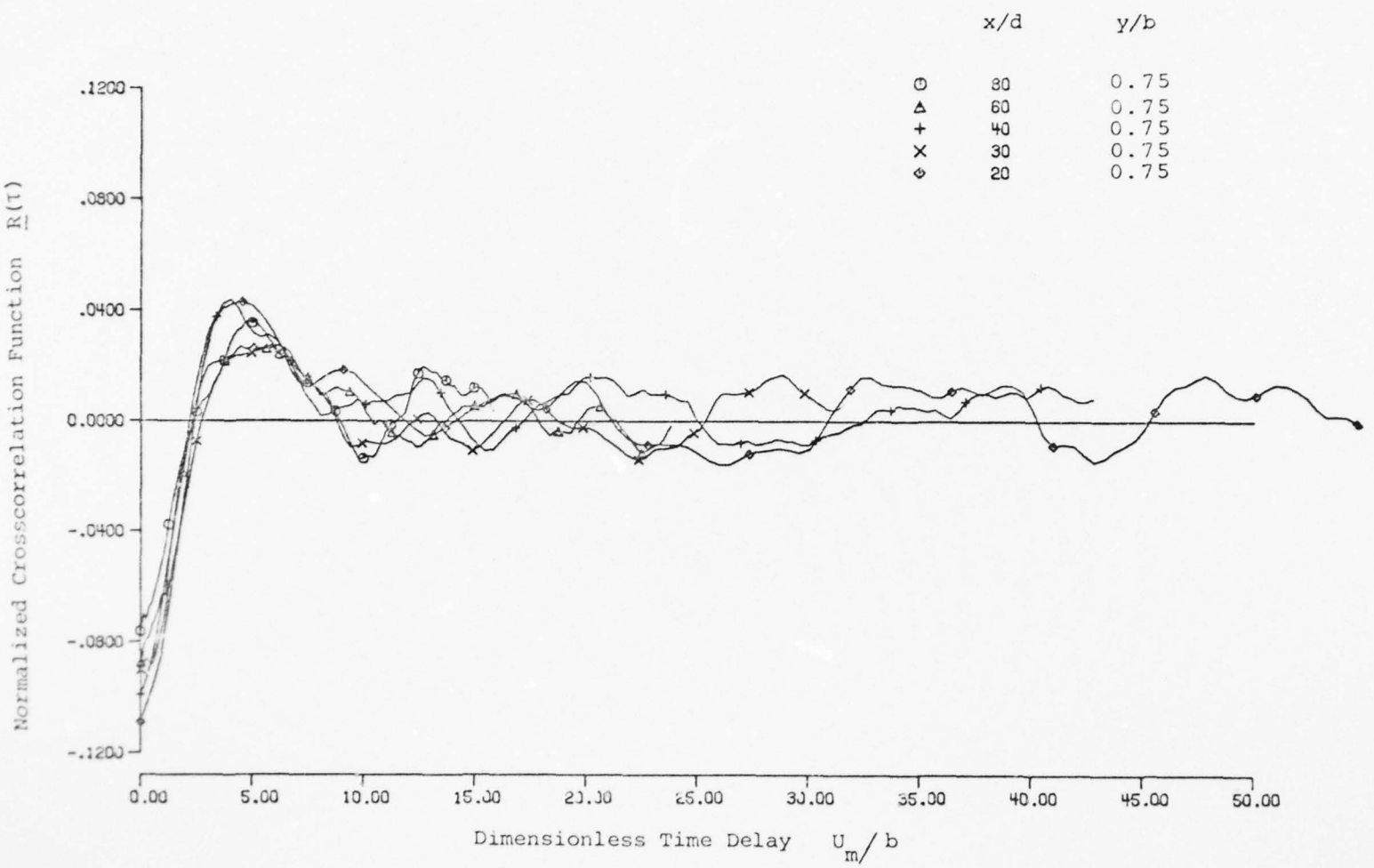

Figure 5.17 Normalized Crosscorrelation Functions, y/b = 0.75

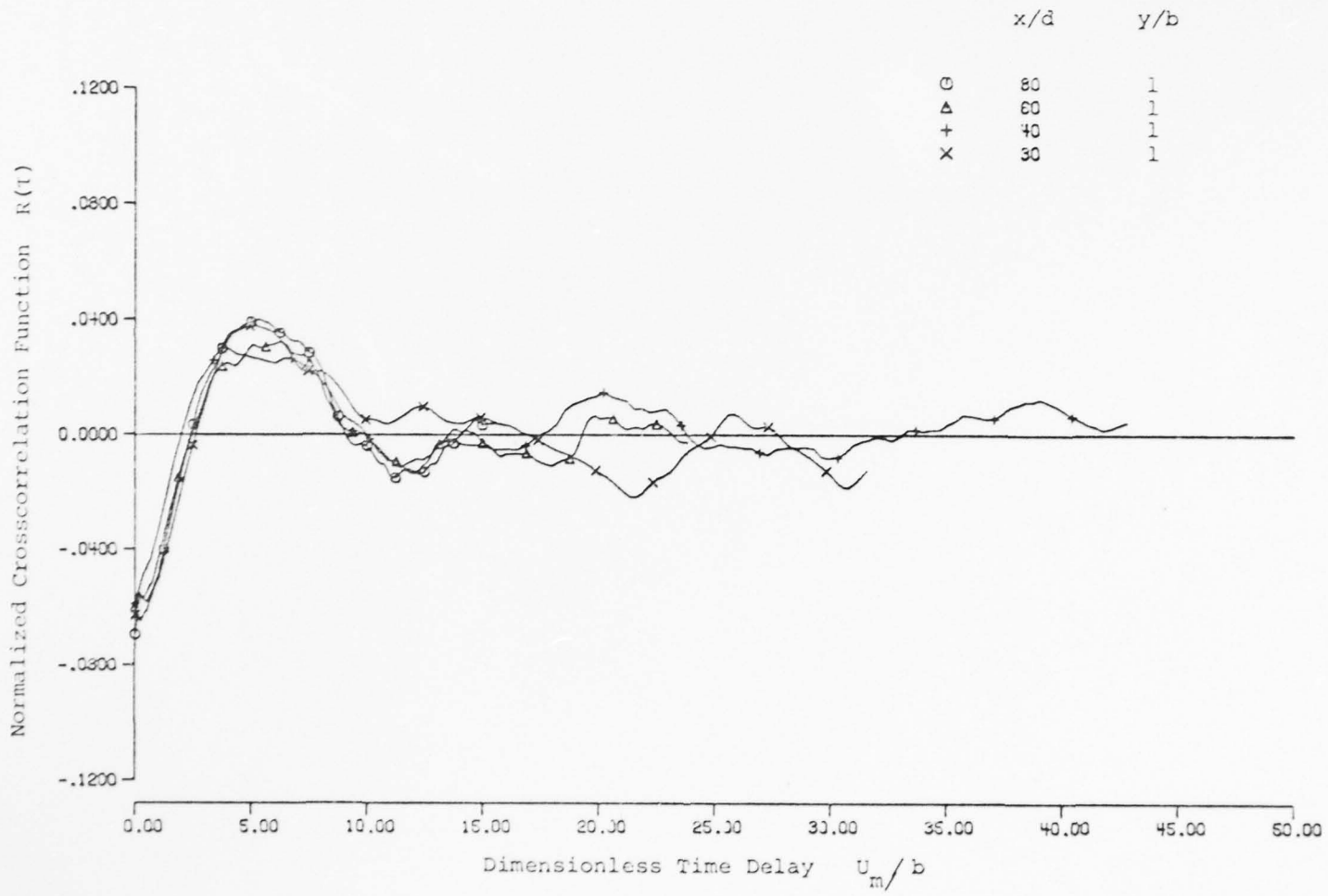

Figure 5.18 Normalized Crosscorrelation Functions, y/b = 1

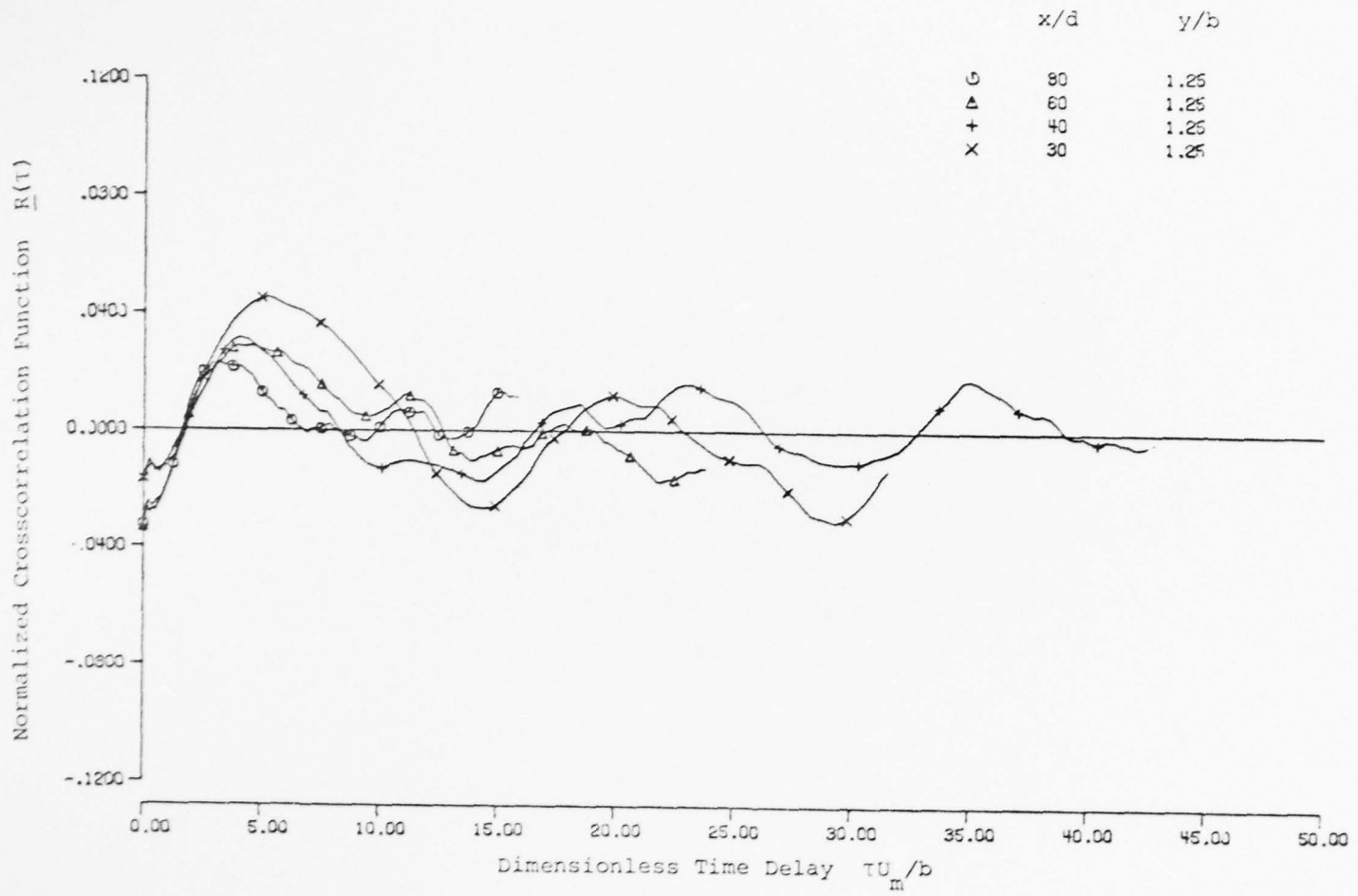

Figure 5.19 Normalized Crosscorrelation Functions, y/b = 1.25

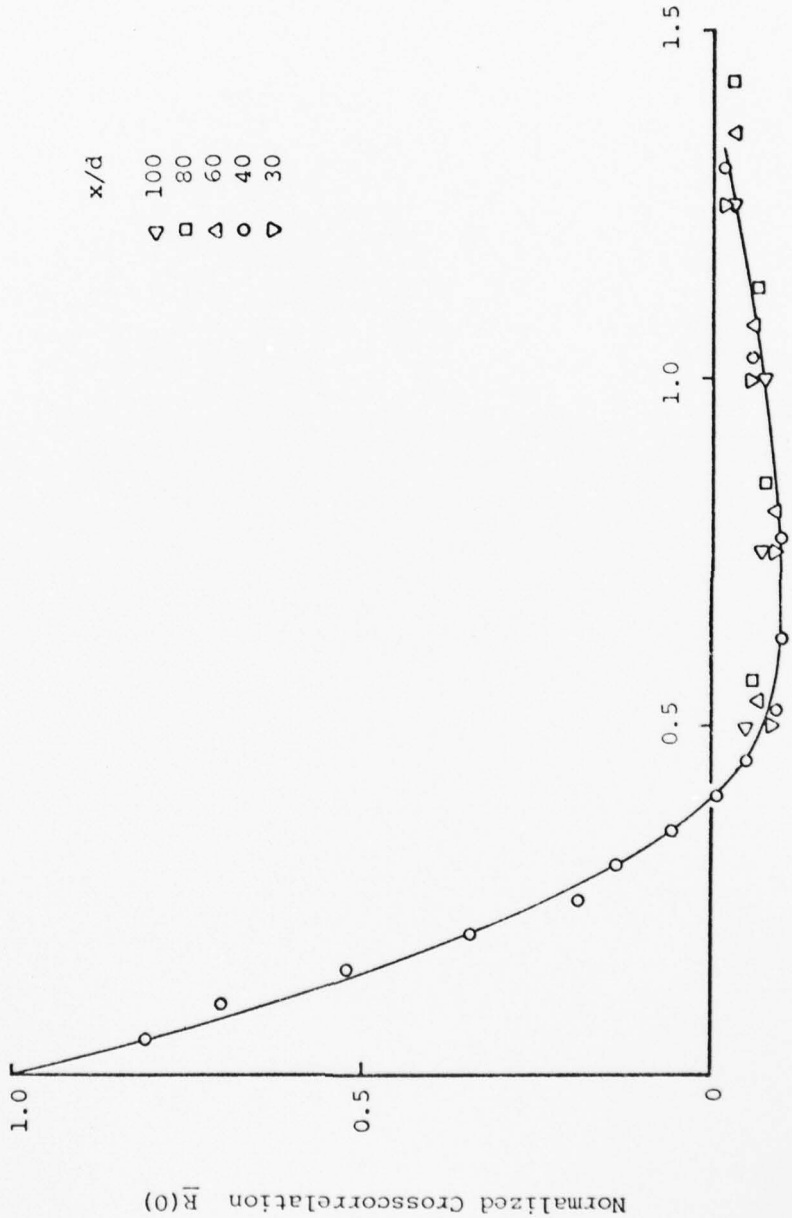

Figure 5.20 Normalized Crosscorrelation $\underline{R}(0)$ vs. y/b

$$\underline{R}(0) = (1-k_1\, y/b)\, \exp\,(-k_2\, y/b) \qquad (5.7)$$

seems to be satisfied. Self-preservation, however, is far from perfect. In this respect it should be remembered that the more complicated a statistical quantity is, the longer it takes to reach self-preservation (Tennekes and Lumley [1972]). The best fits for the coefficients in equation 5.7 appear to be $k_1 = 2.5$, $k_2 = 2.9$. These are not shown on Figure 5.20. It does make sense to expect that for small y/b the typical lateral correlation function is obtained (Hinze [1959]), whereas for $y/b > 0.35$ the negative values attributed to flapping become predominant.

A detailed survey of correlation functions was performed with both probes at $x/d = 40$ but at equal $|y/b|$ locations. This was done in order to have a better picture of the flapping behavior across a given longitudinal coordinate and extend the results of Figure 5.20. Figures 5.21 a, b, c, c, e and f show a sequence of such functions for and increasing separation distance between the two symmetrically set probes. The curves corresponding to $\pm\, y/b < 0.35$ shown in Figure 5.21 a, b, and c, presented a positive value for $\underline{R}(0)$. Note however, that $\underline{R}(0)$ decreases as the separation distance between probes increases (this is an expected result as commented later). Moreover, at $\pm\, y/b = 0.35$ the value of $\underline{R}(0)$ is smaller that the values of $R(\tau)$ corresponding to slightly positive and negative time delays (Figure 5.21c). At $\pm\, y/b = 0.4$, $\underline{R}(0)$ is aproximately zero and the correlation function takes a kind

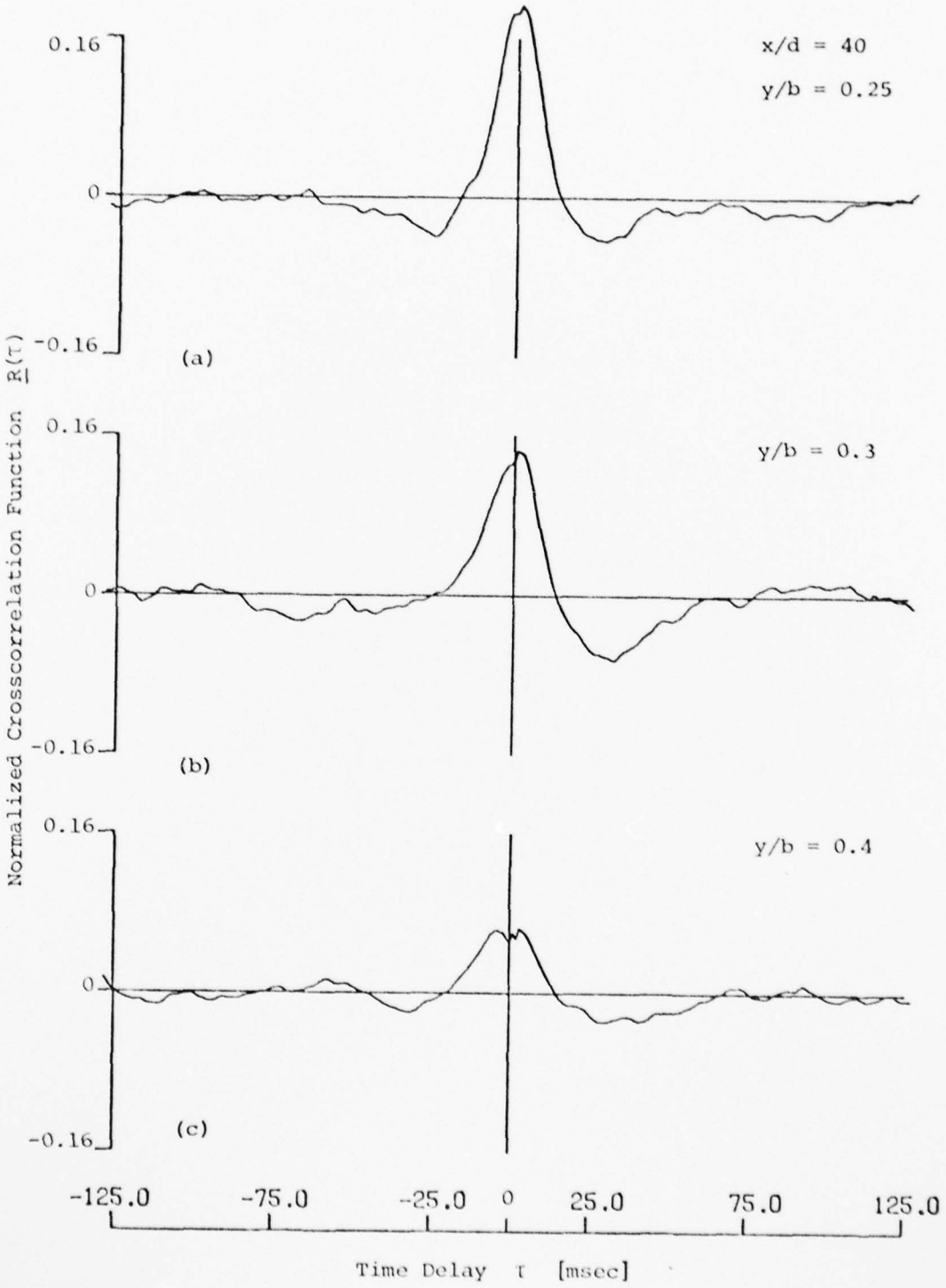

Figure 5.21 Type I Crosscorrelation Functions

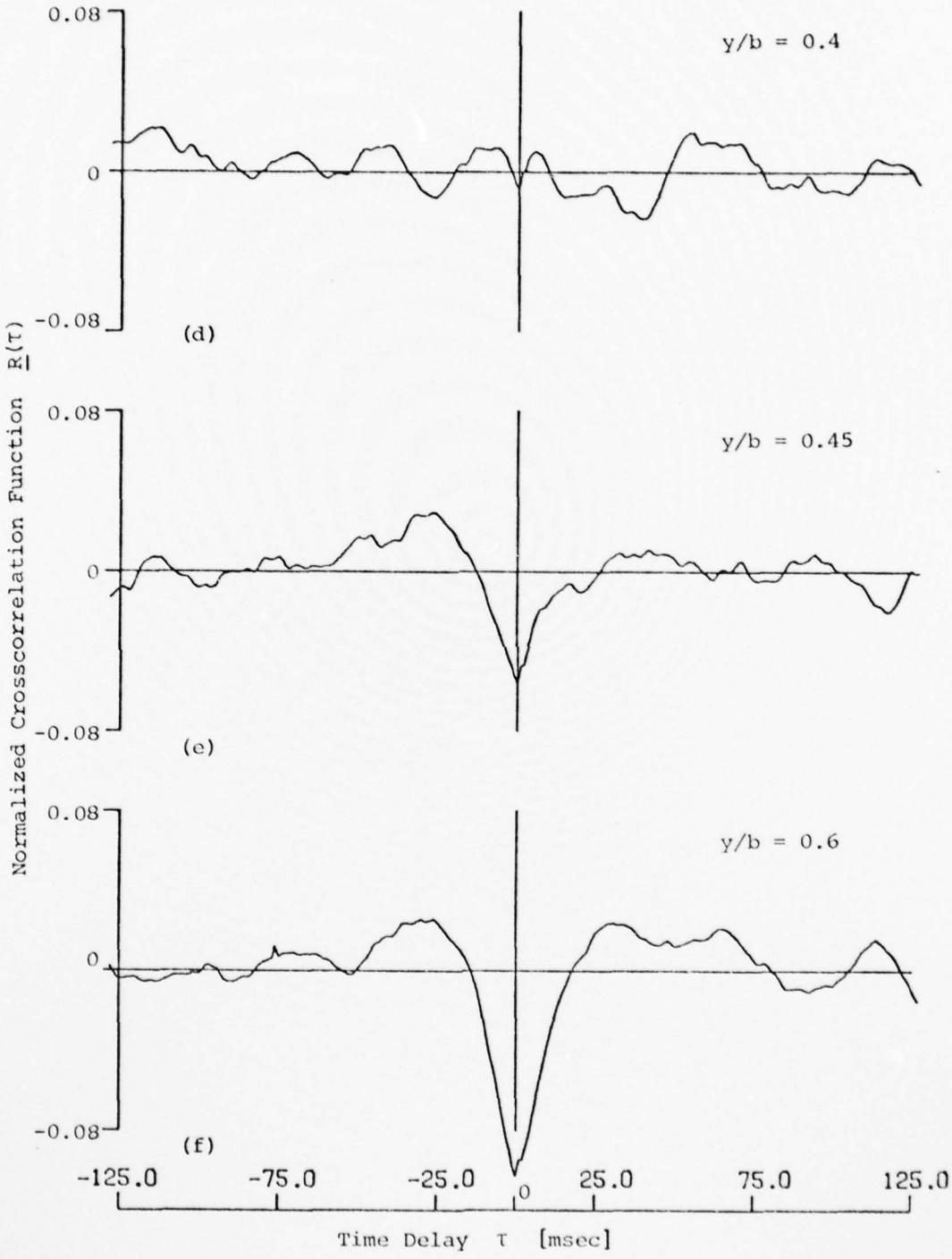

Figure 5.21 (continued)

of transitional shape (Figure 5.21d). Finally, for $\pm$ y/b > 0.45, the correlations characterizing the flapping behavior were obtained (Figures 5.21 e and f). The values of $\underline{R}(0)$ in Figures 5.21 correspond to the values in the plot of Figure 5.20.

Type II Measurements

It was mentioned before that the flapping frequency did not exhibit a preferred dependence on the lateral coordinate (Figure 5.8). This was one of the results of the Type I measurements (those performed with the probes symmetrically positioned with respect to the jet centerline).

A question may still arise as to whether the motion, interpreted as flapping, is instead due to a "weaving" of the mean flow through an impressed vortex type structure. To determine that possibility Type II measurements were taken with the sensors at different lateral locations (sample plots are shown in Figures 5.3 and 5.4). The presence of any such structures would have to give further changes in the sign of the correlation at $\tau = 0$. This was not noted. Furthermore no dependence of the flapping frequency on lateral location was observed either.

The results of measured flapping frequency are combined in Figure 5.22 (compare with Figures 5.13, 5.14 and 5.15). The average value of the parameter fb/U_m is constant and compares well with that obtained from the Type I measurements.

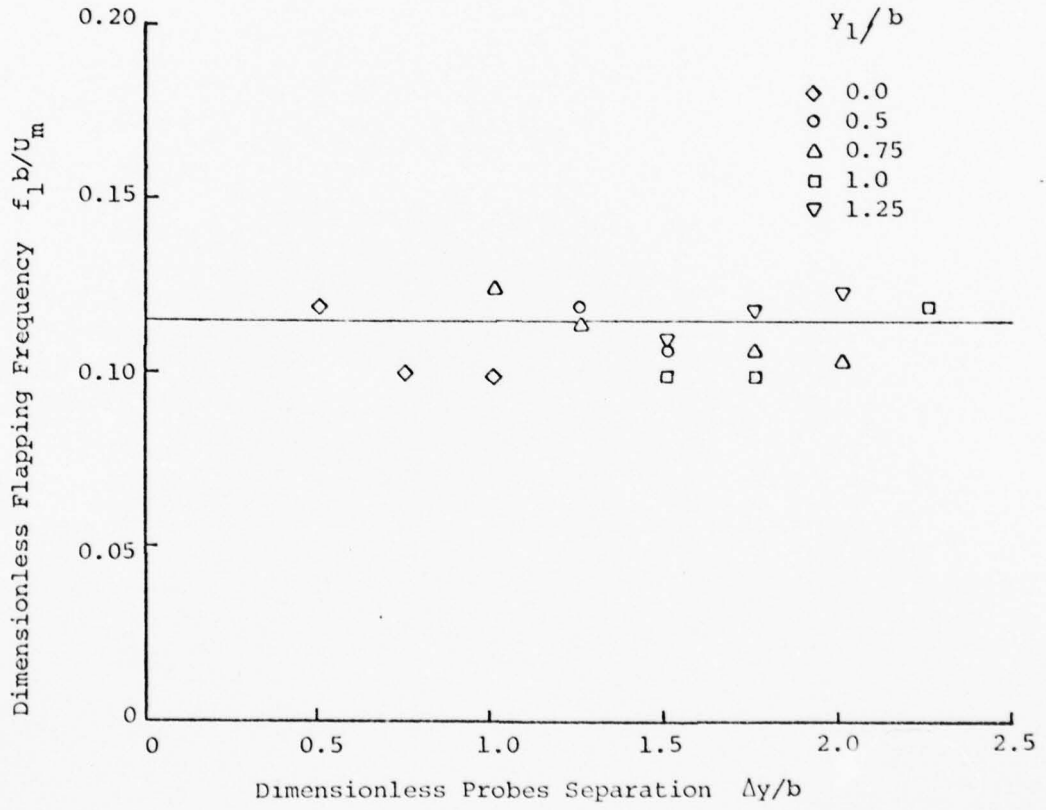

Figure 5.22 Dimensionless Flapping Frequency $f_1 b/U_m$ vs. $\Delta y/b$

It seems therefore, that the frequency of flapping when expressed as fb/U_m, is a single value characteristic for each x/d station, independently of the points considered in measuring the crosscorrelation, for $|y/b| \geq 0.5$.

The amplitude of the correlation function at zero time delay $\underline{R}(0)$, is however, a function of y/b as shown in the sequence of correlations of Figure 5.21. This is an expected result, since $\underline{R}(0)$ as defined and obtained by varying the separation distance between probes, is equivalent to the space-correlation:

$$R(y,\Delta y) = \frac{\overline{u(y+\frac{1}{2}\Delta y)\ u(y-\frac{1}{2}\Delta y)}}{\sqrt{\overline{u^2(y+\frac{1}{2}\Delta y)}}\ \sqrt{\overline{u^2(y-\frac{1}{2}\Delta y)}}} \qquad (5.8)$$

for y = 0. In equation (5.8), $y = \frac{1}{2}(y_1+y_2)$ and Δy is the separation between probes.

Further analysis was done of the Type I and Type II data at x/d = 40. The objective was to obtain space-correlations in a form similar to equation (5.8). The results are presented in Figure 5.23. The lateral coordinate of the middle-point between probes ($y = \frac{1}{2}(y_1+y_2)$) and the separation distance $\Delta y = y_1-y_2$, are nondimensionalized by the jet half-width b. Note that the space-correlation function never attains a negative value for $y/b \geq 1.0$, but approaches zero asymptotically as the probe separation $\Delta y/b$ increases.

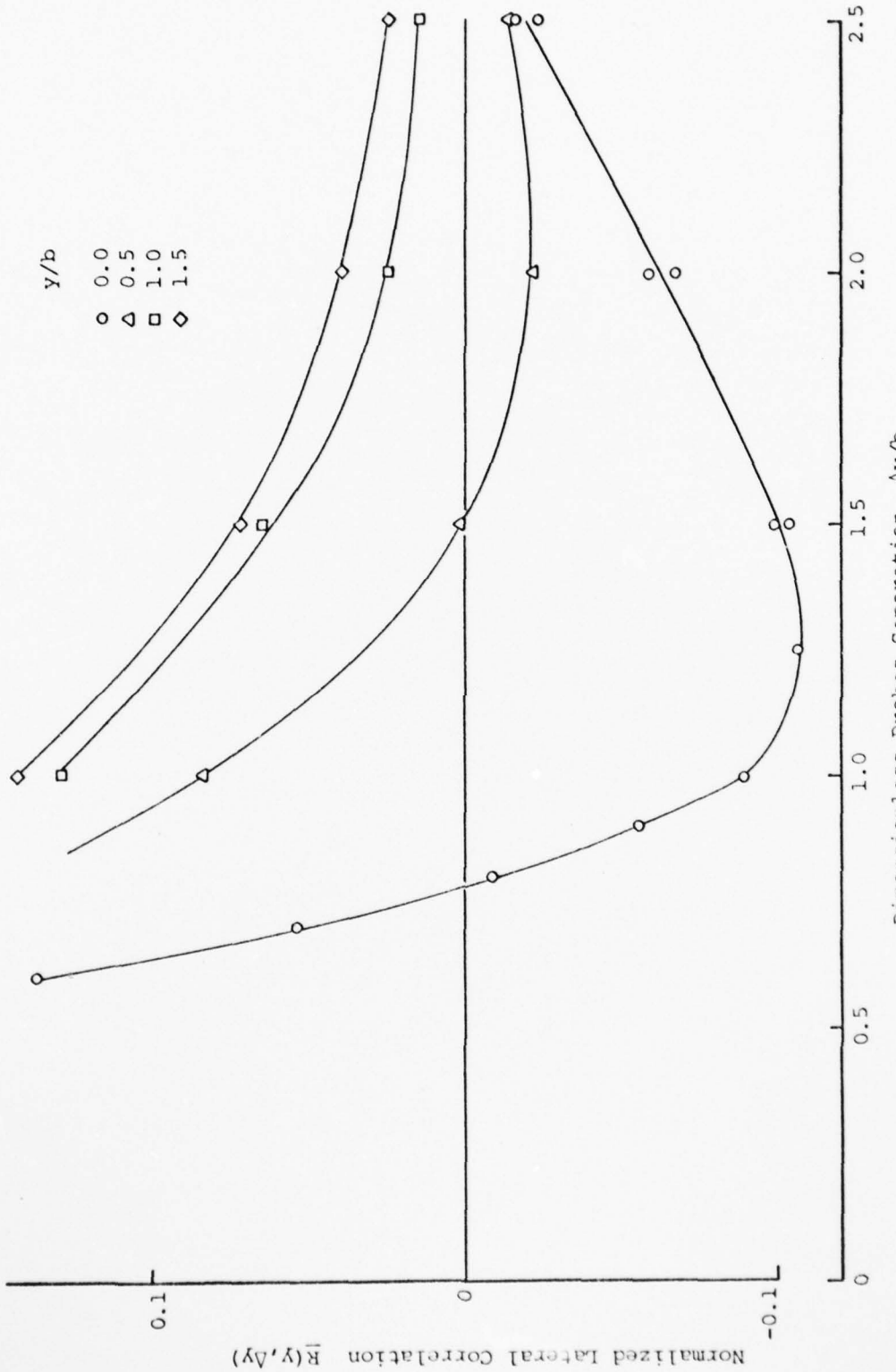

Figure 5.23 Normalized Lateral Correlation $\underline{R}(y,\Delta y)$ vs. $\Delta y/b$

The same curves are presented in Figure 5.24 with a smaller scale in order to compare them with similar results reported by Gutmark and Wygnanski [1976]. Further comments on this comparison are presented in Chapter 6.

5.3 Amplitude of Flapping

An estimate of the amplitude of flapping can be done by assuming a sinusoidal bodily displacement of the mean velocity profile of the jet from its mean location.

In effect, the instantaneous displacement of the mean velocity profile may be assumed as:

$$\varepsilon = \varepsilon_m \sin 2\pi ft \tag{5.9}$$

where f is the frequency of flapping and ε_m is the amplitude to be estimated.

If e is the instantaneous a.c. voltage of the hot-wire anemometers, then for an essential linear response, the correlation function can be expressed as:

$$\underline{R}(\tau) = \frac{\overline{e(x,y,t)\ e(x,-y,t+\tau)}}{\sqrt{\overline{e^2(x,y,t)}}\ \sqrt{\overline{e^2(x,-y,t+\tau)}}} \tag{5.10}$$

Furthermore, for sufficiently small values of ε, the nonrandom component of e can be approximated by:

$$e = \frac{\partial E}{\partial y}\,\varepsilon \tag{5.11}$$

where E is the d.c. voltage output of the anemometers. Substituting (5.9) in (5.11) and (5.11) in (5.10), one

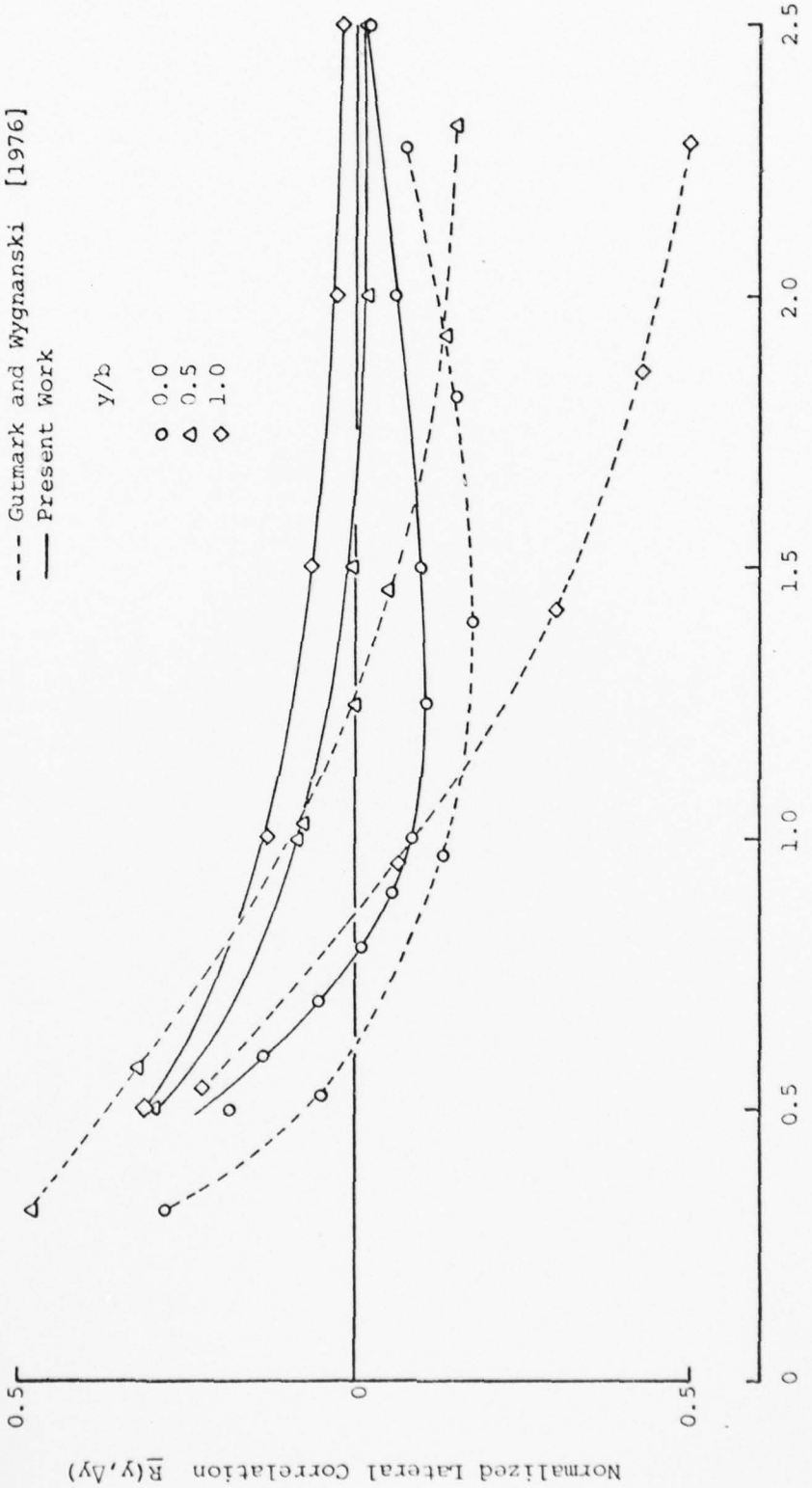

Figure 5.24 Normalized Lateral Correlation $\underline{R}(y,\Delta y)$ vs. $\Delta y/b$

obtains:

$$\underline{R}(\tau) = \frac{-\left(\frac{\partial E}{\partial y}\right)^2 \varepsilon_m^2 \tfrac{1}{2}\cos 2\pi f\tau}{\overline{e^2}} \tag{5.12}$$

On the other hand, an empirical cooling law for the hot-wires, may be expressed as:

$$\frac{E^2}{R_w(R_w-R_f)} = k_1 + k_2 U^{\frac{1}{2}} \tag{5.13}$$

or

$$E^2 = A + BU^{\frac{1}{2}} \tag{5.14}$$

where $A = k_1 R_w(R_w-R_f)$, $B = k_2 R_w(R_w-R_f)$, k_1 and k_2 are empirical constants and R_w and R_f are the operating and cold resistance of the hot-wire, respectively.

Differentiating (5.14) with respect to U:

$$2E\frac{\partial E}{\partial U} = \tfrac{1}{2}BU^{-\frac{1}{2}}$$

or:

$$\frac{\partial E}{\partial U} = \frac{1}{4}\frac{BU^{-\frac{1}{2}}}{E} \tag{5.15}$$

combining (5.14) and (5.15), one gets:

$$\frac{\partial E}{\partial U} = \frac{1}{4U}\frac{E^2-A}{E} \tag{5.16}$$

Thus, writing $\frac{\partial E}{\partial y} = \frac{\partial E}{\partial U}\frac{\partial U}{\partial y}$ and substituting in (5.12) after using (5.16):

$$\underline{R}(\tau) = - \frac{\left[\frac{1}{4U} \frac{E^2-A}{E} \frac{\partial U}{\partial y}\right]^2 \varepsilon_m^2 \frac{1}{2} \cos 2\pi f\tau}{\overline{e^2}} \tag{5.17}$$

At $\tau = 0$, the last expression reduces to:

$$\underline{R}(0) = \frac{1}{2} \frac{\left[\frac{1}{4U} \frac{E^2-A}{E} \frac{\partial U}{\partial y}\right]^2 \varepsilon_m^2}{\overline{e^2}}$$

from which, a relationship is obtained for ε_m:

$$\varepsilon_m = \frac{[2R(0)]^{\frac{1}{2}}}{\frac{1}{4U} \frac{E^2-A}{E} \frac{\partial U}{\partial y}} \tag{5.18}$$

Furthermore, expressing ε_m, U and $\frac{\partial U}{\partial y}$ in dimensionless form by using the half-width b and the mean velocity at the centerline U_m of the jet, (5.18) reduces to:

$$\frac{\varepsilon_m}{b} = \frac{[2R(0)]^{\frac{1}{2}}}{\frac{U_m}{4U} \frac{E^2-A}{E} \frac{\partial (U/U_m)}{\partial (y/b)}} \tag{5.19}$$

Finally, assuming a mean velocity profile as given by Reichardt (equation 2.4, Chapter 2):

$$\frac{U}{U_m} = \exp\left[-(0.8326 \frac{y}{b})^2\right] \tag{2.4}$$

and taking derivatives, one obtains:

$$\frac{U_m}{U} \frac{\partial (\frac{U}{U_m})}{\partial (\frac{y}{b})} = - 1.39 \frac{y}{b} \tag{5.20}$$

AD-A071 260 PURDUE UNIV LAFAYETTE IND RAY W HERRICK LABS F/G 20/4
AN EXPERIMENTAL STUDY OF THE FLAPPING MOTION OF A TURBULENT PLA--ETC(U)
AUG 76 J G CERVANTES DE GORTARI N00014-75-C-1048
UNCLASSIFIED HL-78-40 NL

2 OF 2
AD A071260

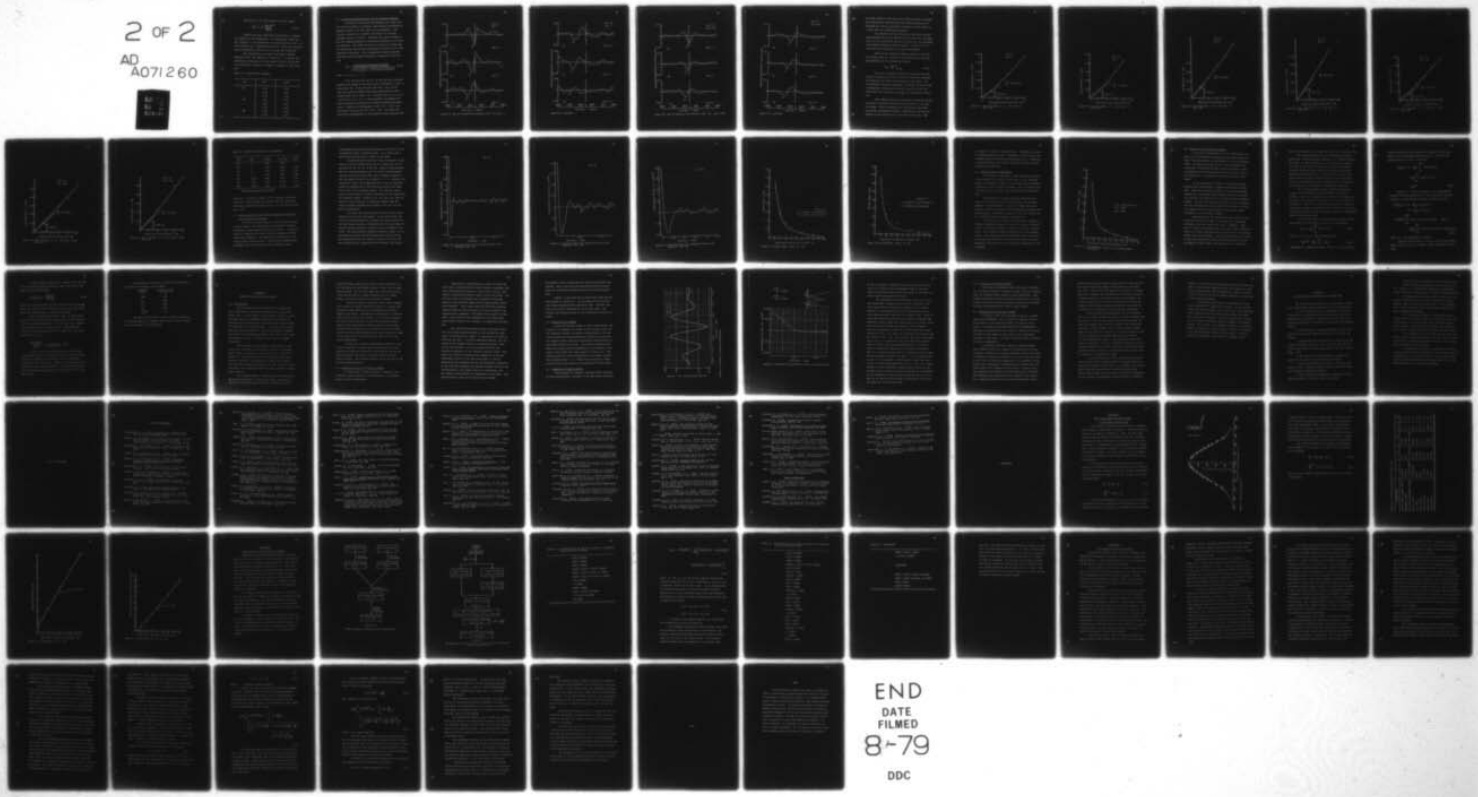

END
DATE FILMED
8-79
DDC

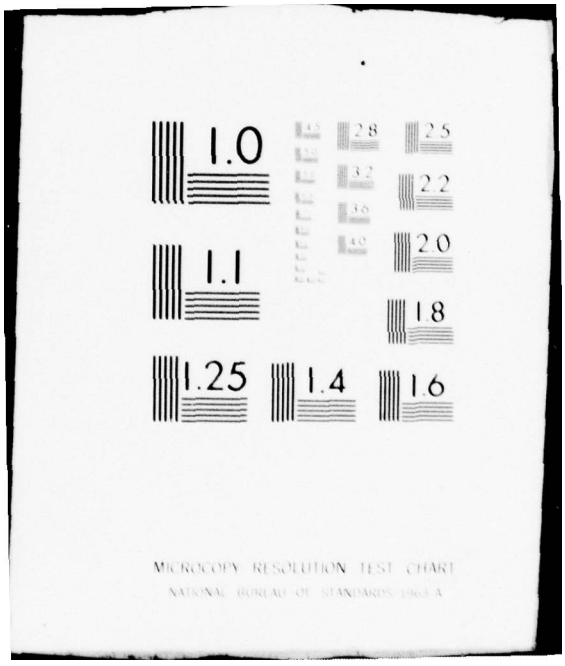
1.0
1.1
1.25
1.4
1.6
2.8
3.2
3.6
4.0
2.5
2.2
2.0
1.8
MICROCOPY RESOLUTION TEST CHART
NATIONAL BUREAU OF STANDARDS 1963-A

Expression (5.20) substituted in (5.19) gives:

$$\frac{\varepsilon_m}{b} = 4.07 \frac{[\underline{R}(0)]^{1/2}}{\frac{E^2-A}{E}\frac{y}{b}} \qquad (5.21)$$

Limited data was taken which included d.c. voltage (E) values for the anemometers. An approximate value for the constant A was estimated, by extrapolating to $U^{1/2} = 0$, the straight line represented by (5.14). This was obtained from measurements of the type I at x/d of 80, 60 and 40.

The approximate ε_m/b values calculated through equation (5.21) are tabulated in Table 5.1. As noted, the amplitude of flapping is in the order of 15% to 23% of the jet half-width, and does not appear to depend on x/d nor on y/b.

Table 5.1 Amplitude of Flapping

x/d	y/b	ε_m/b
80	1.13	0.18
	0.85	0.21
	0.56	0.18
60	1.07	0.17
	0.80	0.19
	0.53	0.23
40	1.03	0.15
	0.77	0.16

5.4 Convection Characteristics of the Flapping Behavior

A series of correlation measurements were done with the hot-wire probes at different longitudinal coordinates on opposite sides of the jet (Type III measurements). The original intent was to further investigate the uniform flapping motion of the jet. The data also gives insight on how the flapping behavior is convected downstream of a given x/d position. One probe was set at a fixed x/d station and the second was successively positioned at steps of 2d in the downstream direction. The corresponding crosscorrelation functions were determined according to equation (5.22) below:

$$\underline{R}(\tau) = \frac{\overline{u(x/d,y/b,t)\; u((x/d)+2n,-y/b,t+\tau)}}{\sqrt{\overline{u^2(x/d,y/b,t)}}\;\sqrt{\overline{u^2((x/d)+2n,-y/b,t+\tau)}}} \qquad (5.22)$$

with n = 0, 1, 2, ..., 5

Four x/d stations (10, 20, 30 and 40) were surveyed, keeping both probes at the same lateral coordinate ± y/b = 1. Three more (20, 30 and 40) were done with ± y/b = 0.65. Each x/d station included downstream separations for the second probe, up to 10d(n = 5). Figures 5.25 a, b, c, d, e, f and 5.26 a, b, c, d, e, f show examples of sequences of such correlation functions for increasing downstream separation. Figure 5.25 corresponds to x/d = 10, ± y/b = 1.0, and Figure 5.26 to x/d = 20 ± y/b = 0.65. As noted, the time delay corresponding to the negative probe (pointed with

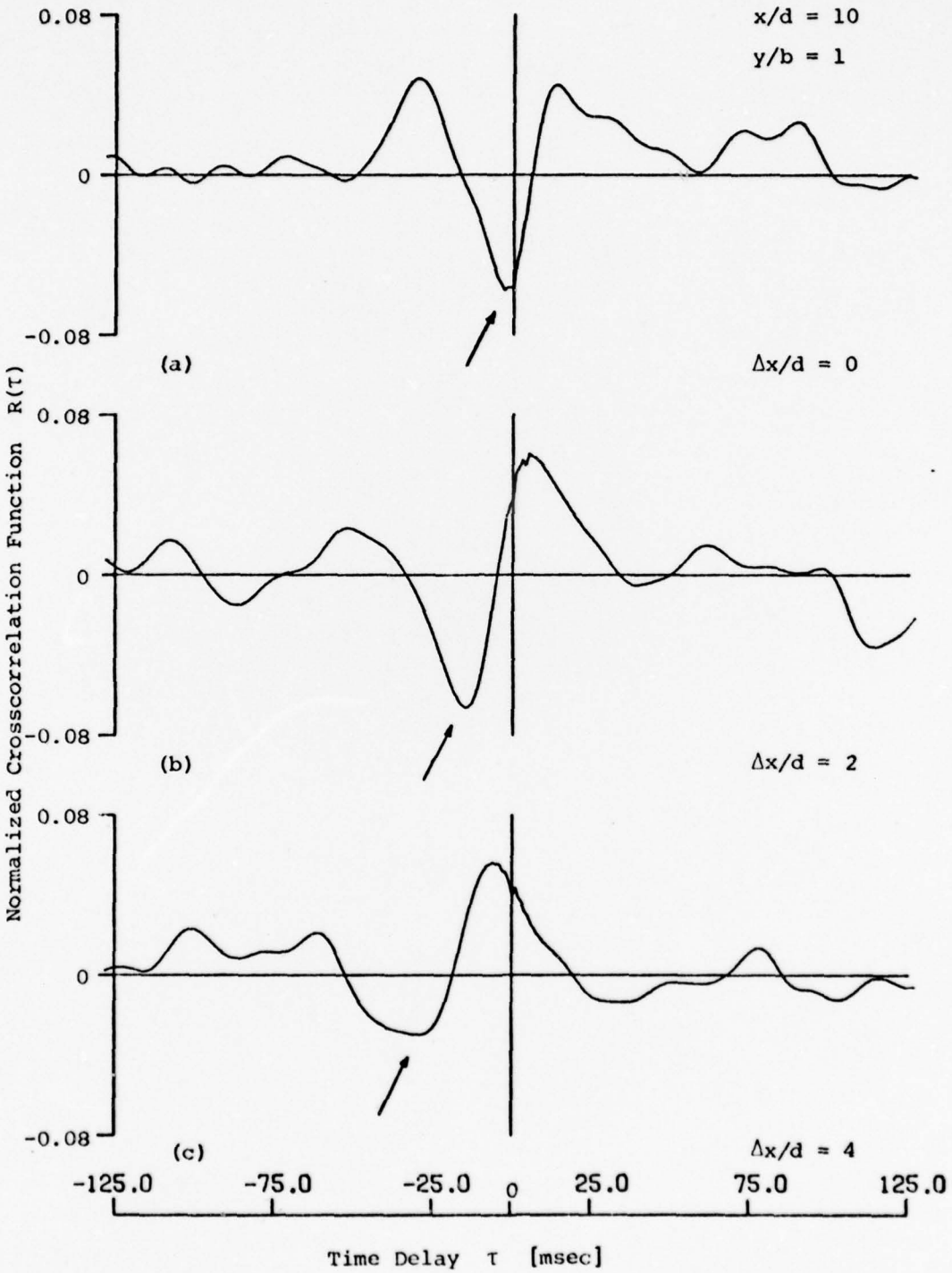

Figure 5.25 Type III Crosscorrelation Functions x/d = 10, y/b = 1

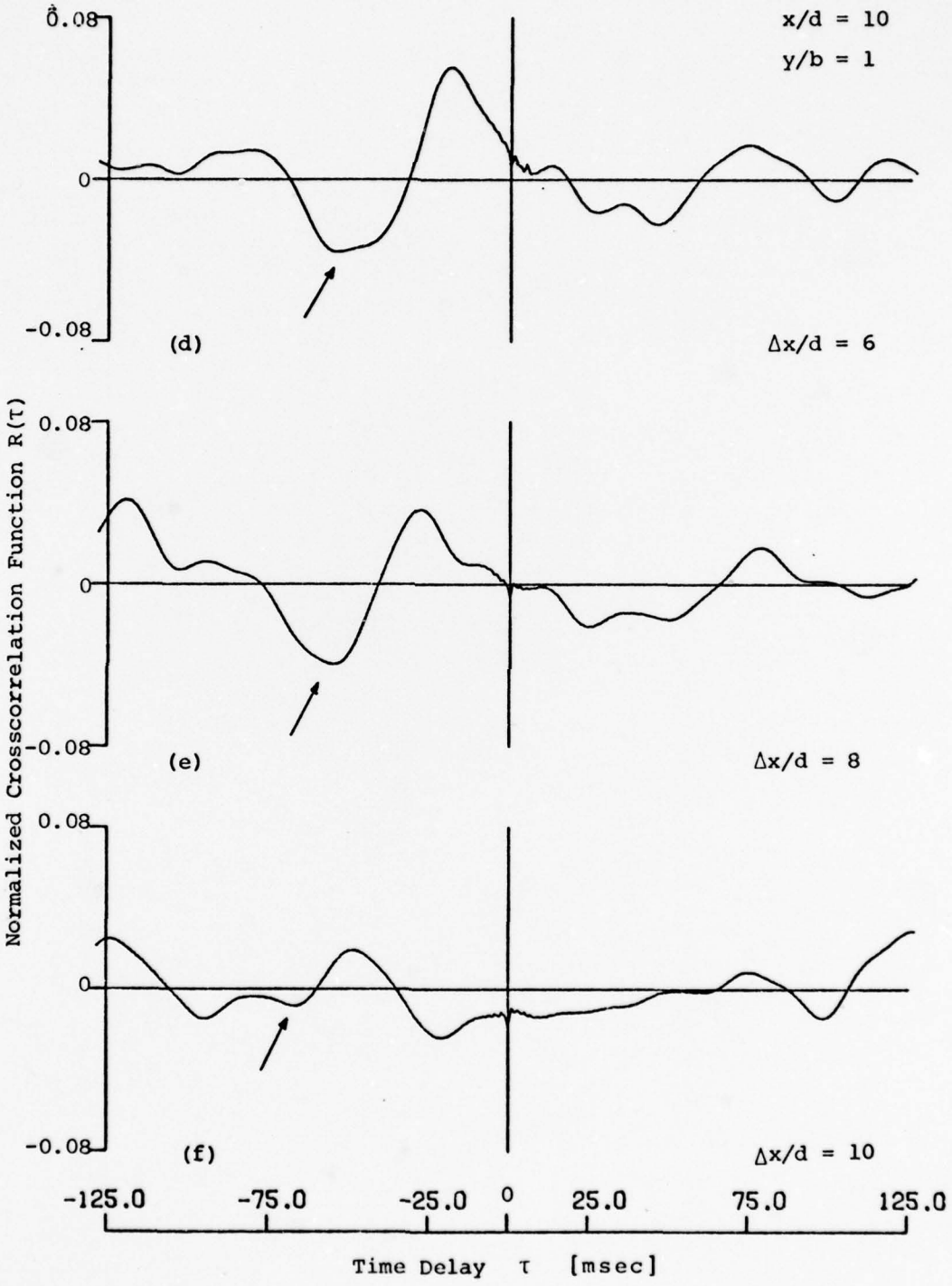

Figure 5.25 (continued)

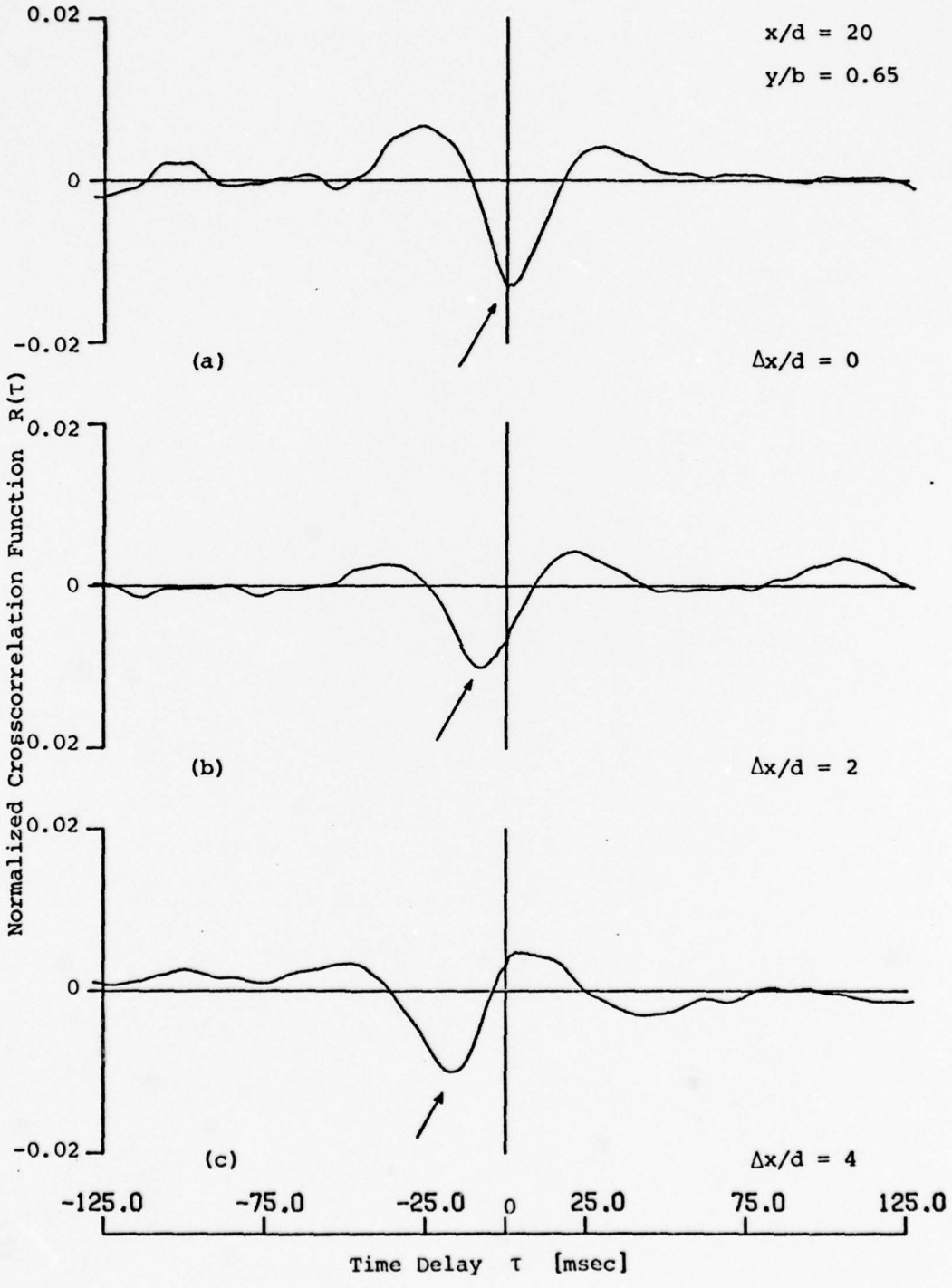

Figure 5.26 Type III Crosscorrelation Functions, x/d = 20 , y/b = 0.65

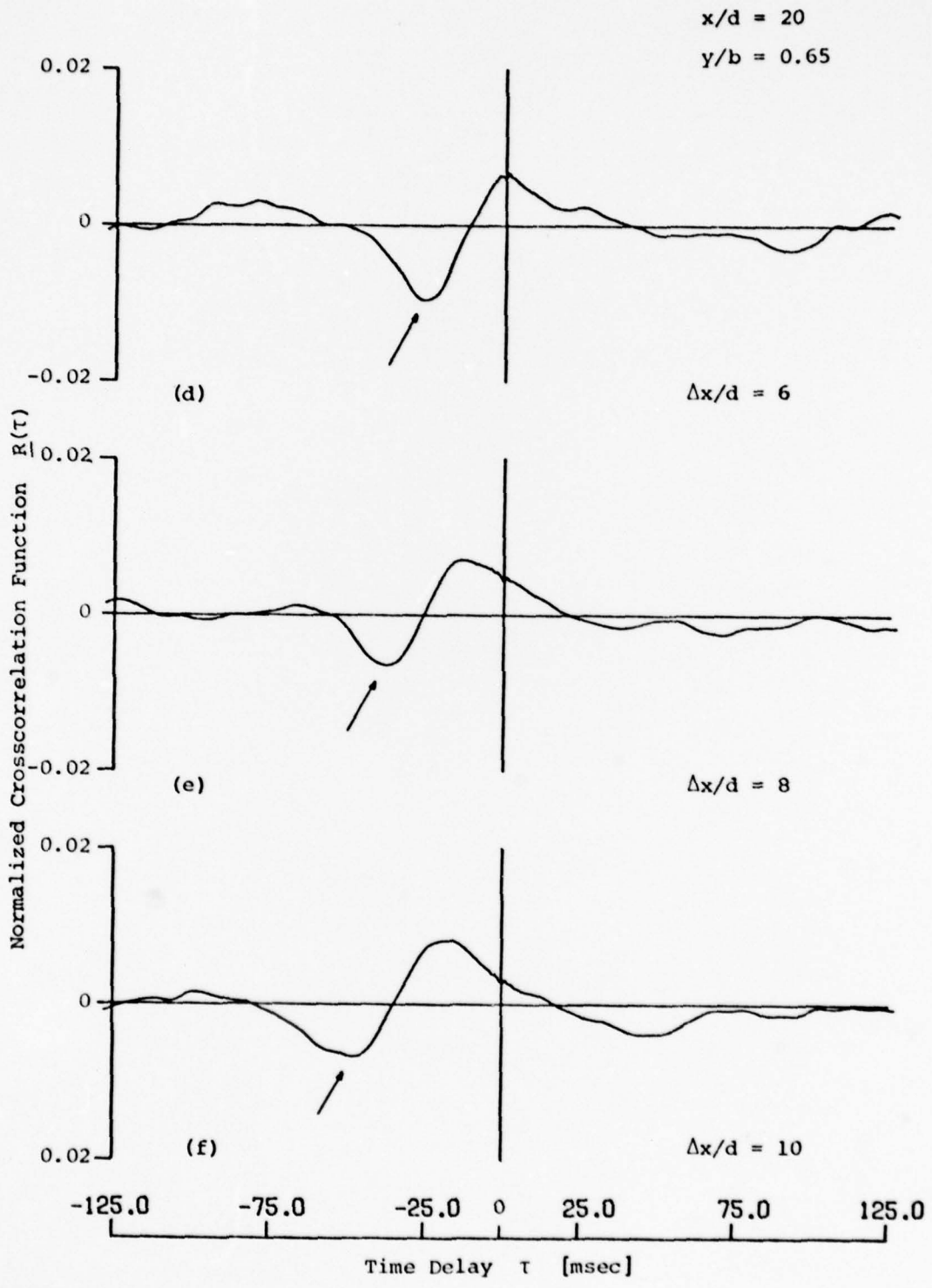

Figure 5.26 (continued)

an arrow) shifts as the separation between probes increases. This effectively indicates that the flapping behavior as detected at a given longitudinal position can be sensed at a later time at a downstream position.

An indication of the velocity of convection of the flapping behavior can be obtained by plotting the time delay shift in the correlation functions against the corresponding longitudinal separation between probes. Figures 5.27 to 5.33 show this result for each case investigated.

Based on the separation between probes Δx and the time delay shift $\Delta\tau$, a velocity of convection of the flapping behavior can be defined as follows:

$$U_{cf} = \frac{\Delta x}{\Delta \tau} \Bigg|_{\Delta x \to 0} \qquad (5.23)$$

This can be roughly obtained by extrapolating the curves in Figures 5.27 to 5.33 to zero separation distance and computing the ratio in expression (5.23) above. The corresponding flapping convective velocities divided by the corresponding local mean velocities (U_{cf}/U), and by the centerline mean velocities (U_{cf}/U_m) are tabulated in Table 5.2.

Also indicated are the convective velocities (of the turbulent structure) measured by Young [1973] in the same jet setup. These velocities were obtained by measuring space-time correlations between longitudinal velocity components at two points on the same side of the jet. The

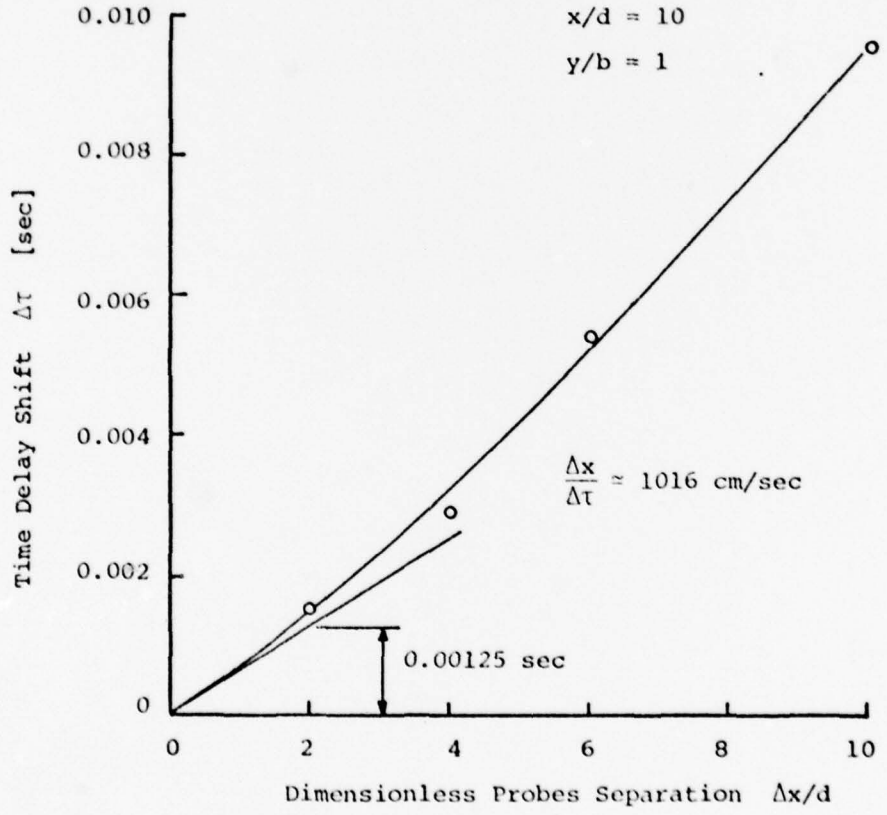

Figure 5.27 Time Delay Shift $\Delta\tau$ vs. $\Delta x/d$, $y/b = 1$, $x/d = 10$

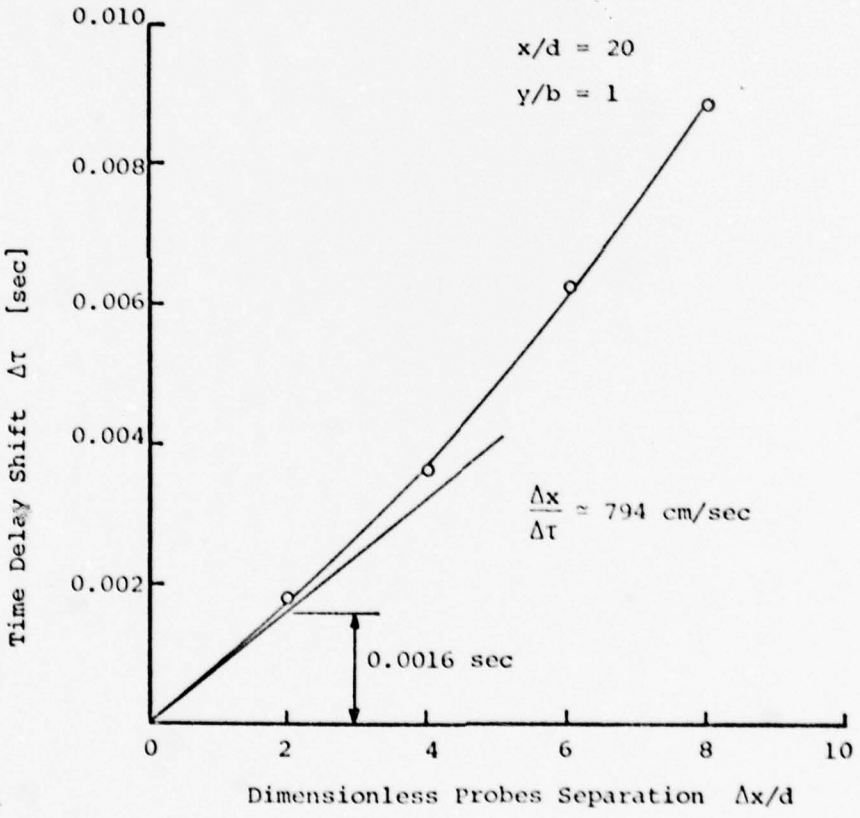

Figure 5.28 Time Delay Shift $\Delta\tau$ vs. $\Delta x/d$, $y/b = 1$, $x/d = 20$

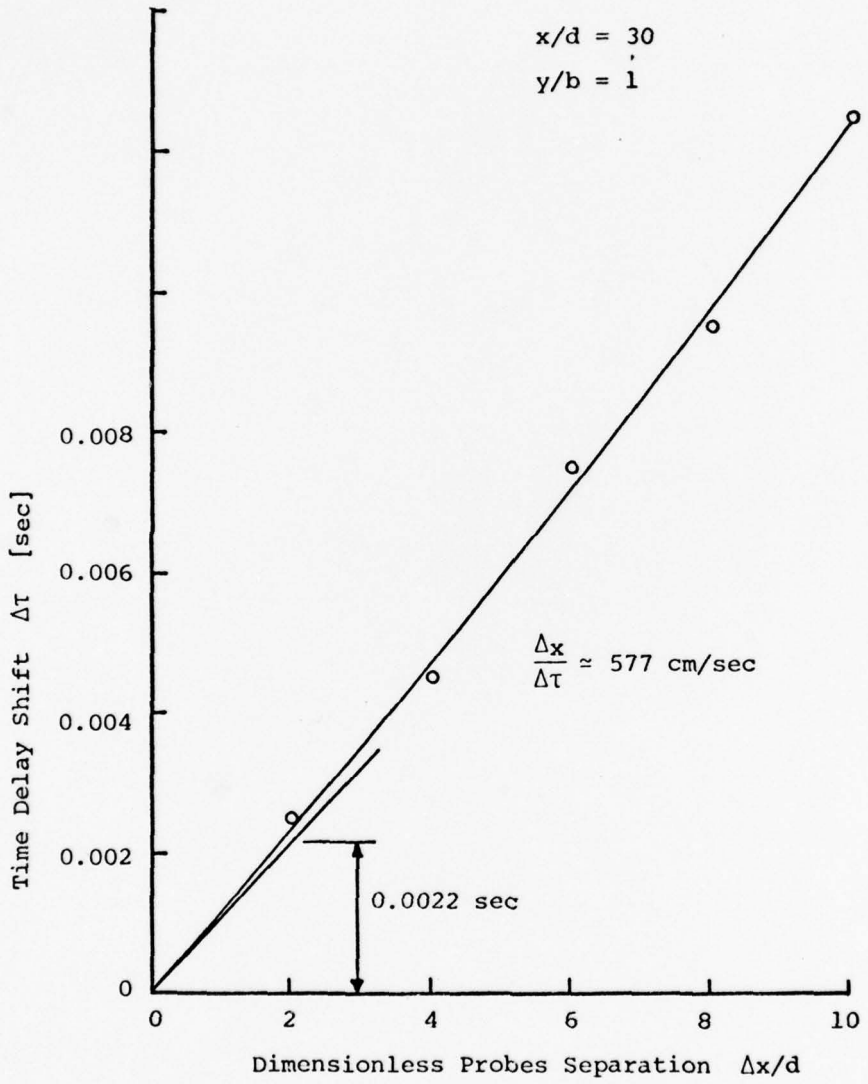

Figure 5.29 Time Delay Shift $\Delta\tau$ vs. $\Delta x/d$, $y/b = 1$, $x/d = 30$

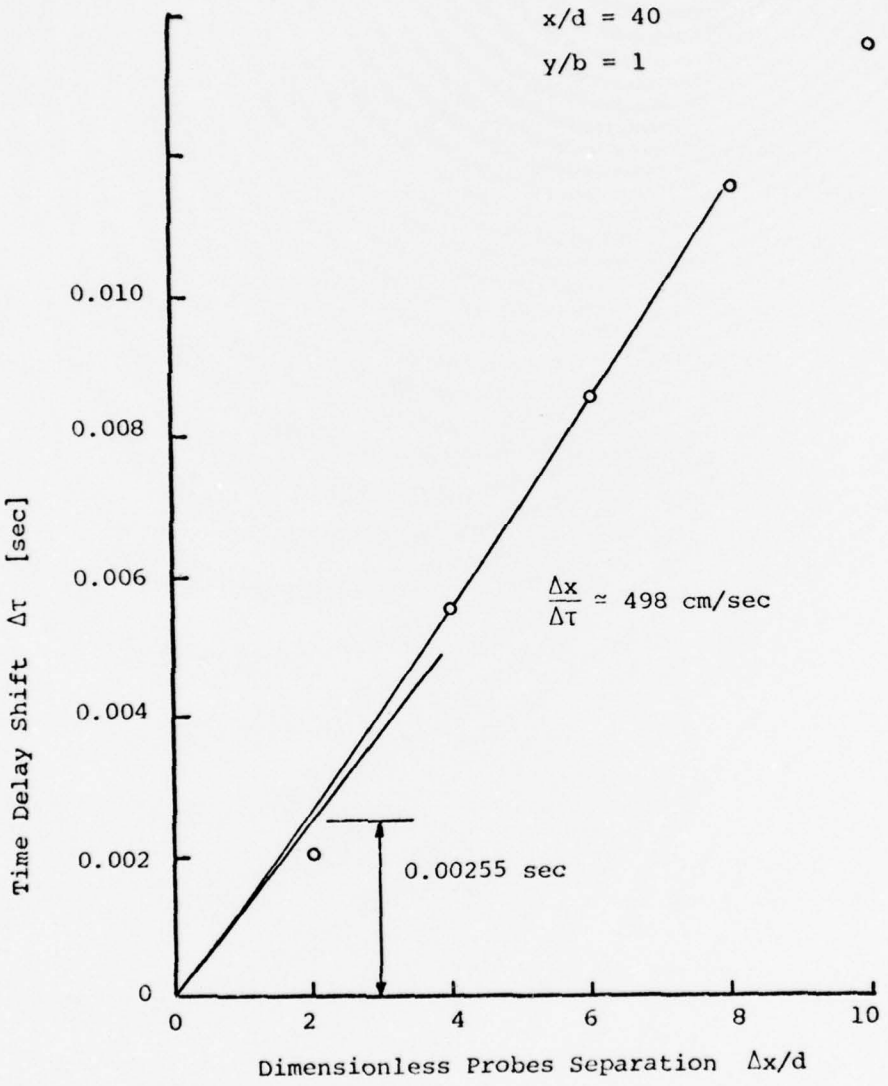

Figure 5.30 Time Delay Shift $\Delta\tau$ vs. $\Delta x/d$, $y/b = 1$, $x/d = 40$

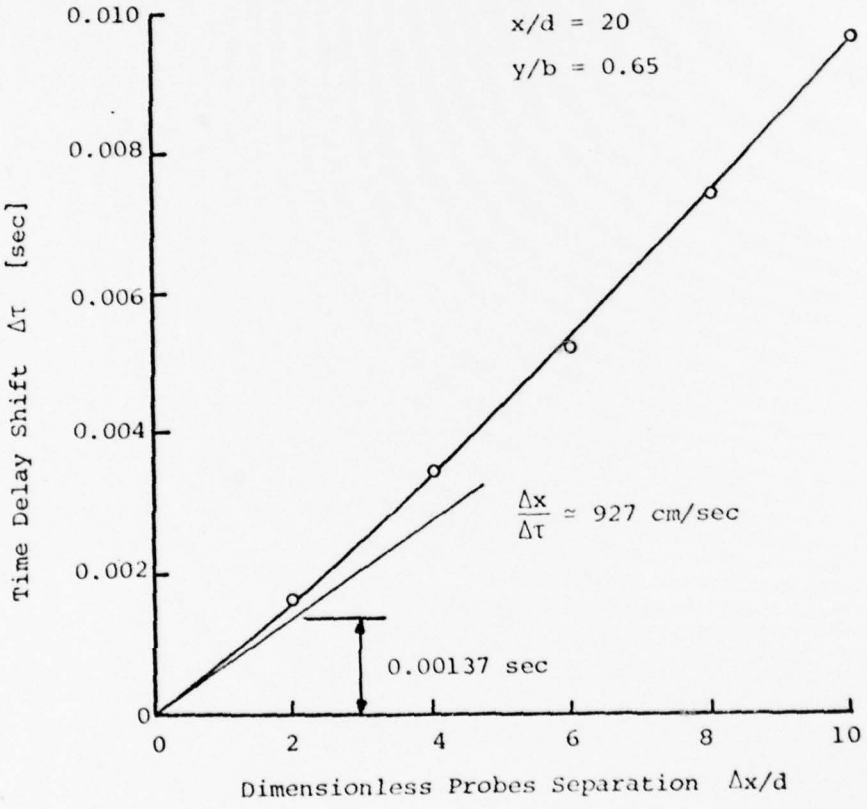

Figure 5.31 Time Delay Shift $\Delta\tau$ vs. $\Delta x/d$, $y/b = 0.65$, $x/d = 20$

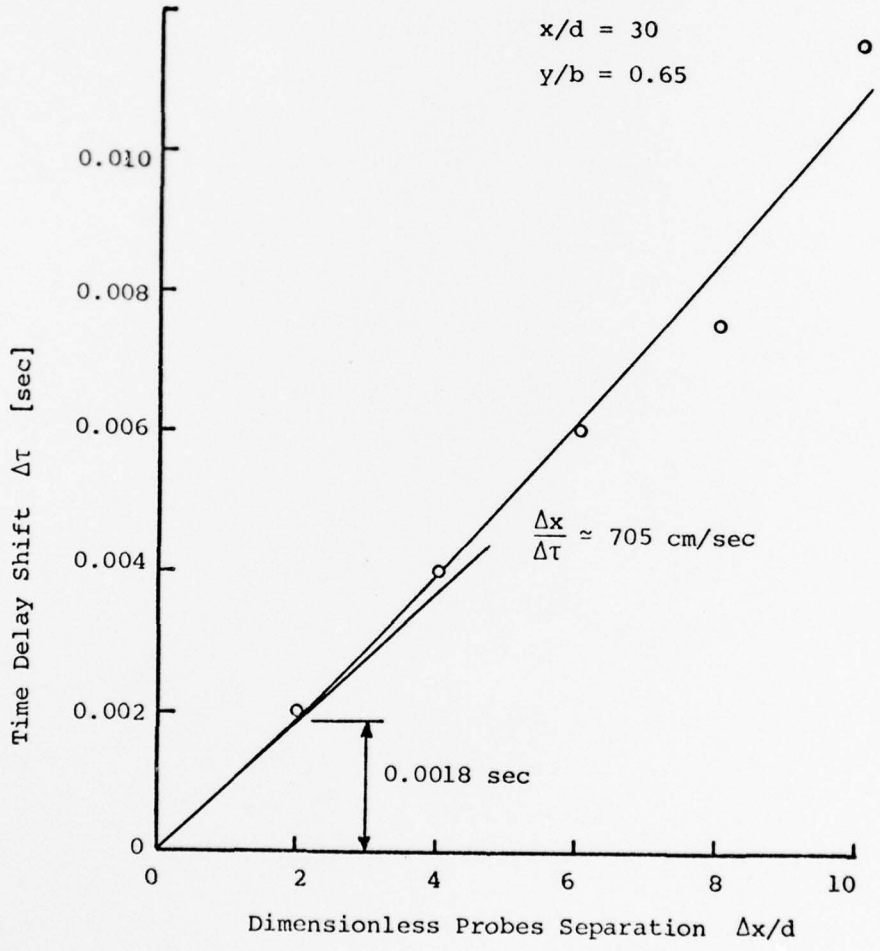

Figure 5.32 Time Delay Shift $\Delta\tau$ vs. $\Delta x/d$, $y/b = 0.65$, $x/d = 30$

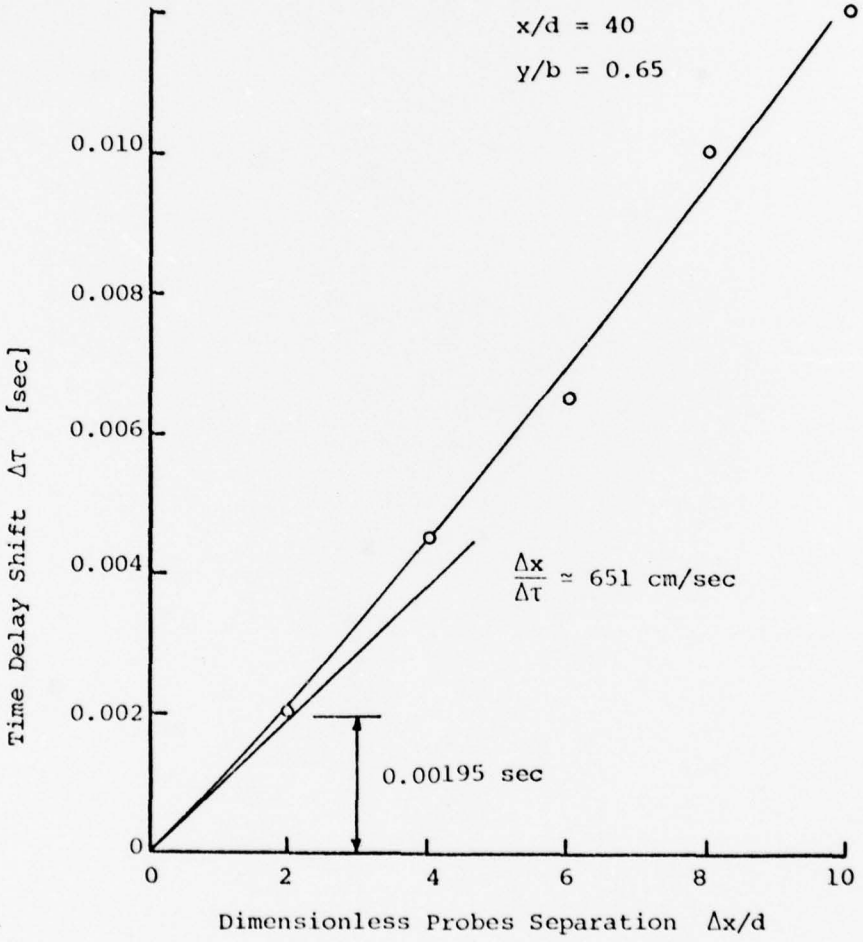

Figure 5.33 Time Delay Shift $\Delta\tau$ vs. $\Delta x/d$, $y/b = 0.65$, $x/d = 40$

Table 5.2 Convective Velocities of Flapping

x/d	y/b	U_{cf}/U	U_{cf}/U_m	U_c/U*
10	1	1.16	0.58	
20	1	1.28	0.64	1.68
30	1	1.15	0.57	1.43
40	1	1.23	0.61	1.58
20	0.65	0.99	0.74	1.18
30	0.65	0.94	0.70	1.1
40	0.65	1.01	0.75	1.18

*Measurements by Young [1973].

direction. As noted in Table 5.2 the flapping convective velocities resulted about 30% smaller than the convective velocities measured by Young for y/b = 1, and about 20% for y/b = 0.65.

5.5 Autocorrelation of the Lateral Component Velocity at the Centerline of the Jet

All the results presented in the previous sections of this chapter, were obtained for longitudinal velocity components, easily measured with normal wires. In the presence of flapping the lateral velocity components should show similar behavior. To obtain such measurements, two x-wire probes should be used. Although the equipment was available, the use of four hot-wire anemometers and

corresponding signal processing equipment would have led to considerably larger averaging times. As a result only a spot-check was made with a single x-wire probe.

Autocorrelation functions of the y-component of the velocity were determined along the jet centerline, at x/d positions of 20, 30, 40, 60 and 80. (Type IV measurements). The data should obviously give the normal autocorrelation function for small delay times, with a maximum (equal to the mean square value of the signal) at $\tau = 0$. However, for large delay times, the flapping motion (if at all present) should be accompanied by alternatively positive and negative values of the autocorrelation. The results, with a single x-wire suffer in signal resolution but do indeed show the expected trends. Figures 5.34, 5.35 and 5.36, show examples of such functions as obtained directly from the Fourier analyzer through an x-y plotter, for x/d = 20, 40 and 80 respectively.

As noted, the autocorrelation functions have their maximum value at zero time delay. On the other hand, the curves are characterized by a pseudo-oscillatory nature as the time delay increases, consistent with the previously described crosscorrelation functions of the x-component velocity. The dimensionless flapping frequency, fd/U_o, can be determined as before and characterized by both f_1 and f_2. The determined values are shown in Figures 5.37 and 5.38. The frequencies are compared with the earlier data (Type I

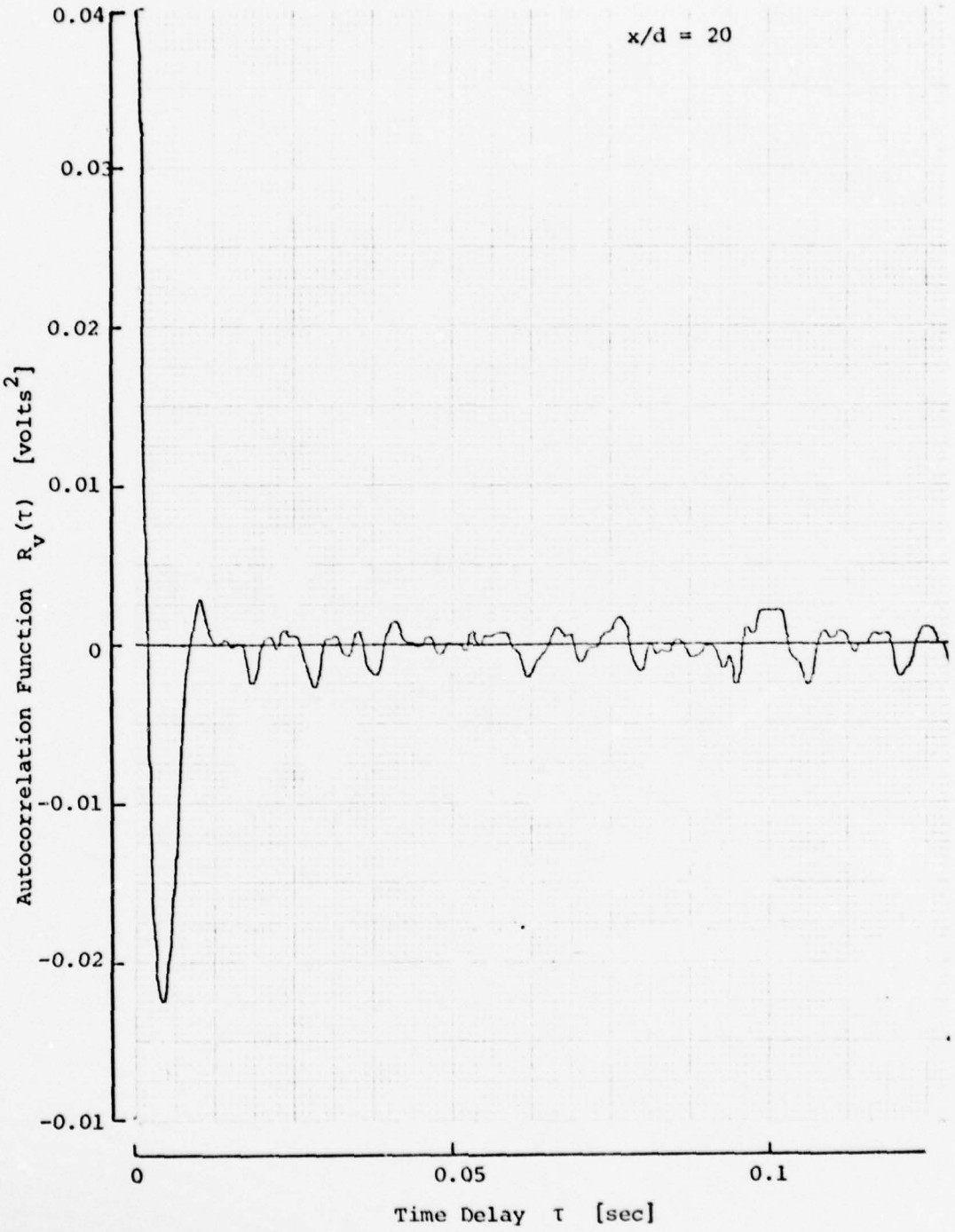

Figure 5.34 Autocorrelation of the v-component Velocity at the Centerline (x/d = 20)

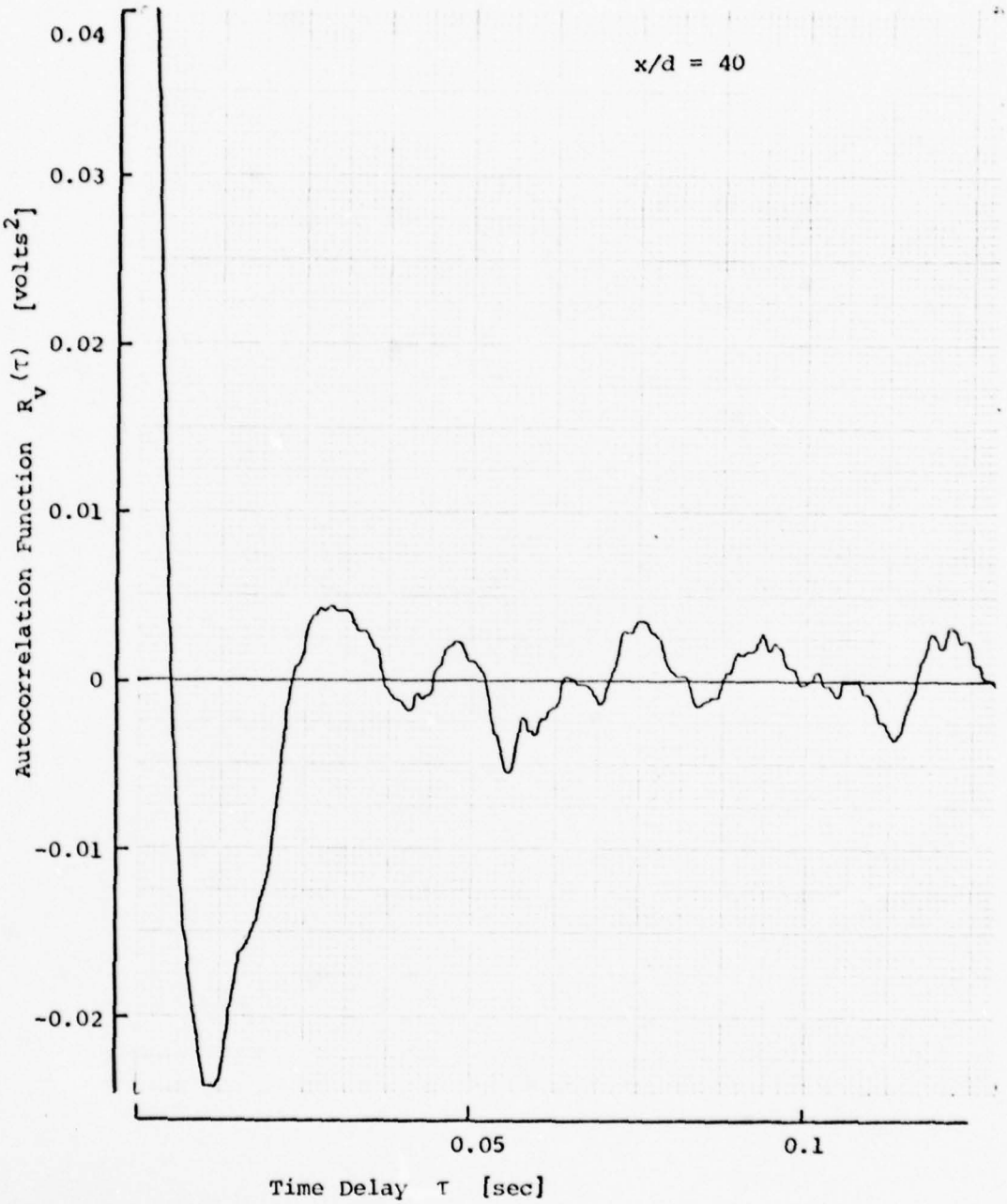

Figure 5.35 Autocorrelation of the v-component Velocity at the Centerline (x/d = 40)

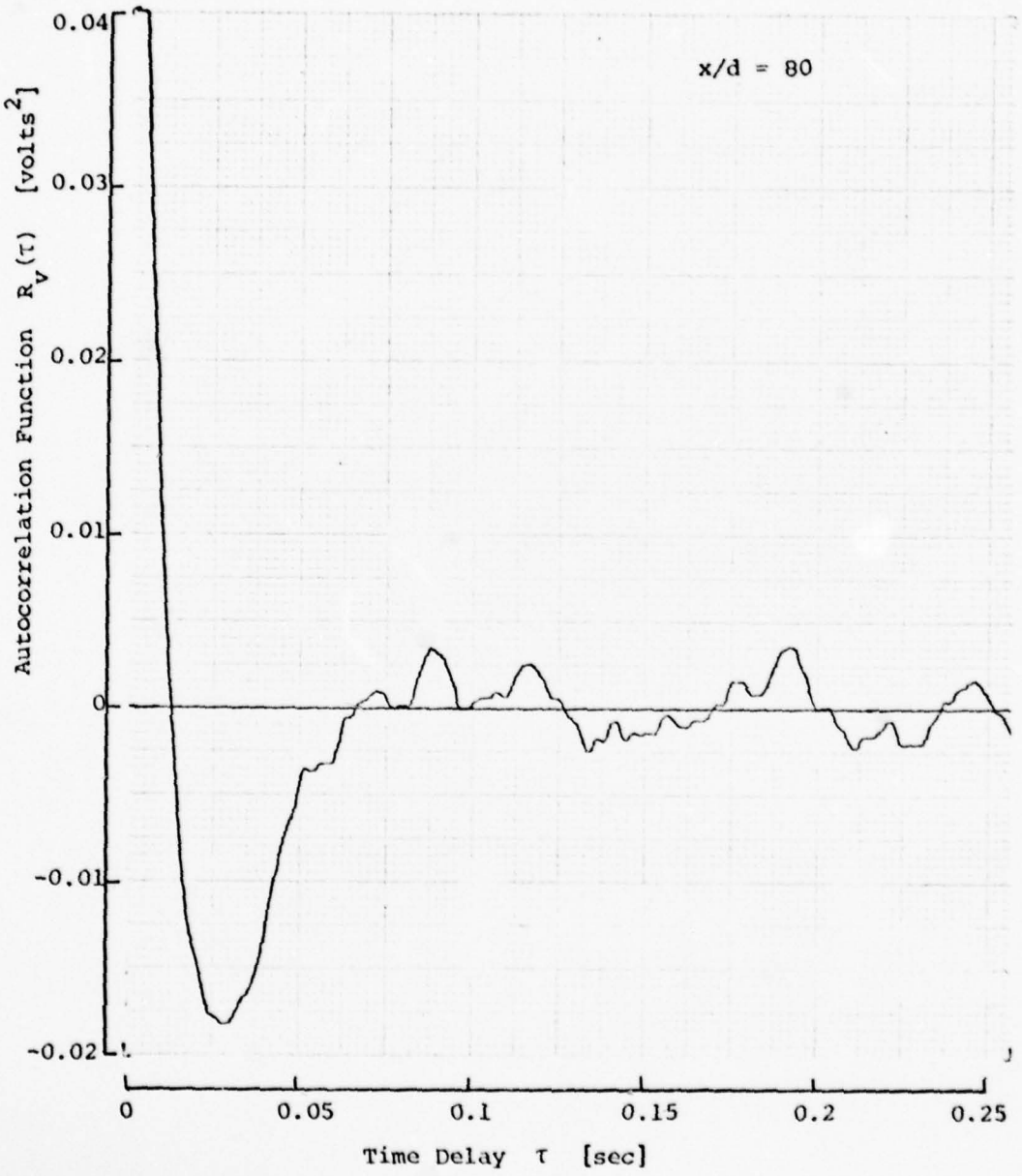

Figure 5.36 Autocorrelation of the v-component Velocity at the Centerline (x/d = 80)

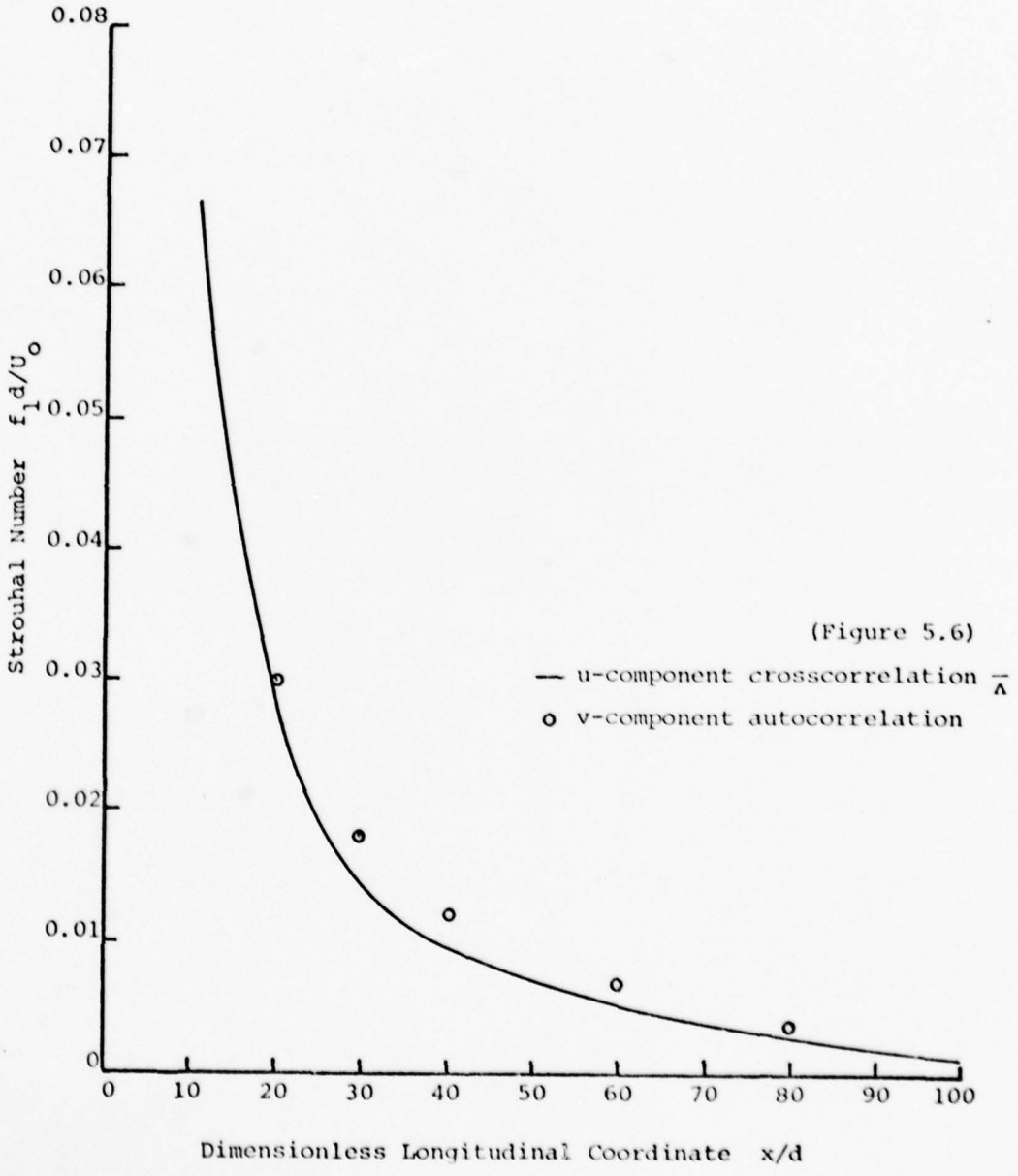

Figure 5.37 Strouhal Number $f_1 d/U_o$ vs. x/d

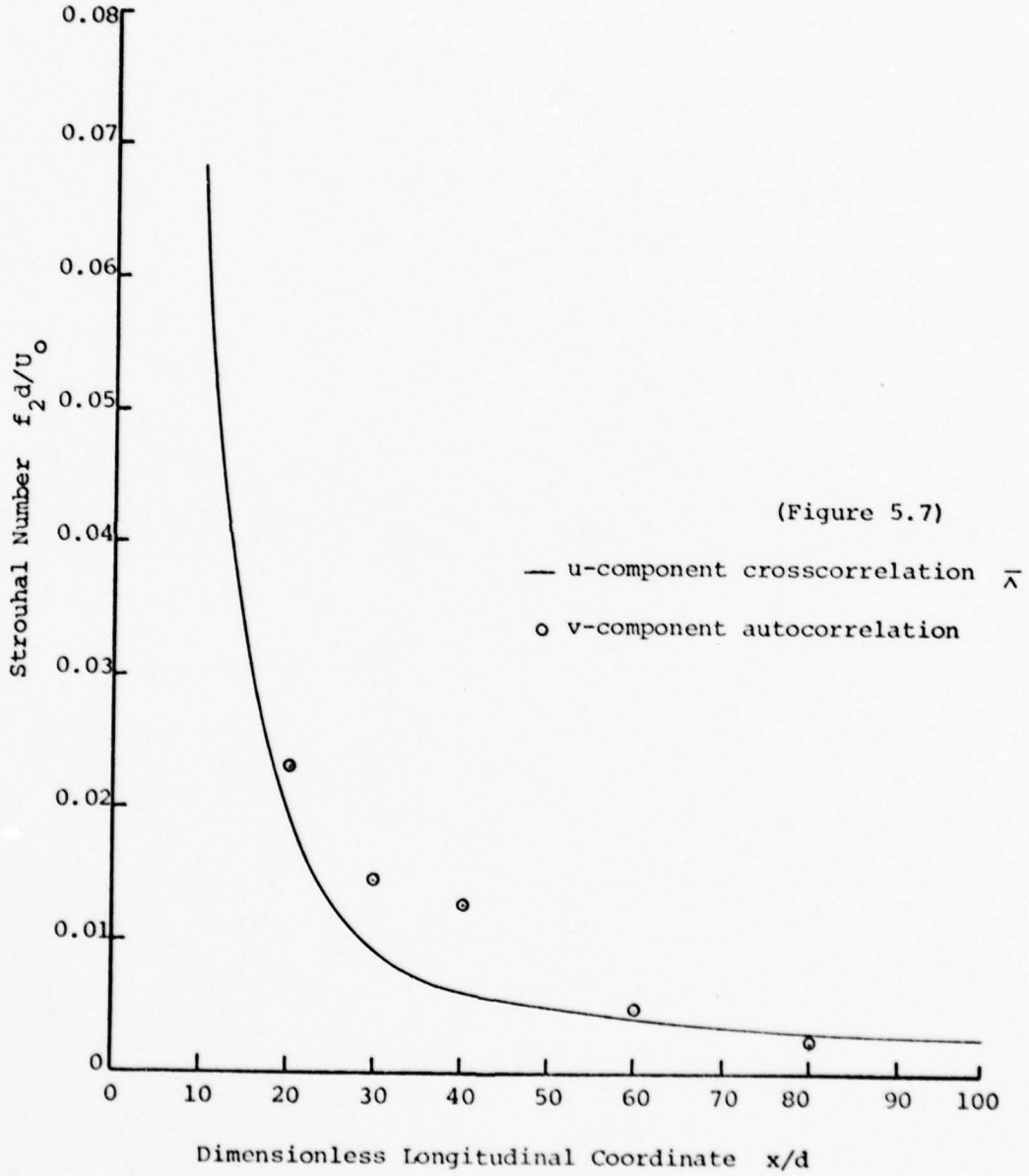

Figure 5.38 Strouhal Number $f_2 d/U_o$ vs. x/d

of Figures 5.6 and 5.7, respectively). Although the values of fd/U_o obtained from the v-component autocorrelations are slightly larger than those corresponding to the u-component crosscorrelations, they indeed confirm the trends and conclusions noted earlier.

5.6 Reynolds Number Independence

A few runs (of the Type I, with symmetrically positioned probes) were taken at different jet exit Reynolds number to determine if there is any strong Reynolds number dependence of the flapping frequency. Due to inherent limitations of the jet setup, only two different values were used.

Measurements of crosscorrelation functions were taken at x/d stations of 40, 60 and 80 for exit Reynolds numbers of 7900 and 15100. Figure 5.39 shows the corresponding results in terms of the dimensionless flapping frequency $f_1 d/U_o$. Included in Figure 5.39 are the results for Re = 10000 previously reported in Figure 5.6.

It is obvious in Figure 5.39, that the frequency of flapping expressed through the parameter $f_1 d/U_o$ is independent of the Reynolds number, at least in the range investigated. This Reynolds number similarity is a well founded result. The flapping behavior characterized by relatively low frequencies should be related to the large-scale components of the flow field, and therefore independent of the viscosity.

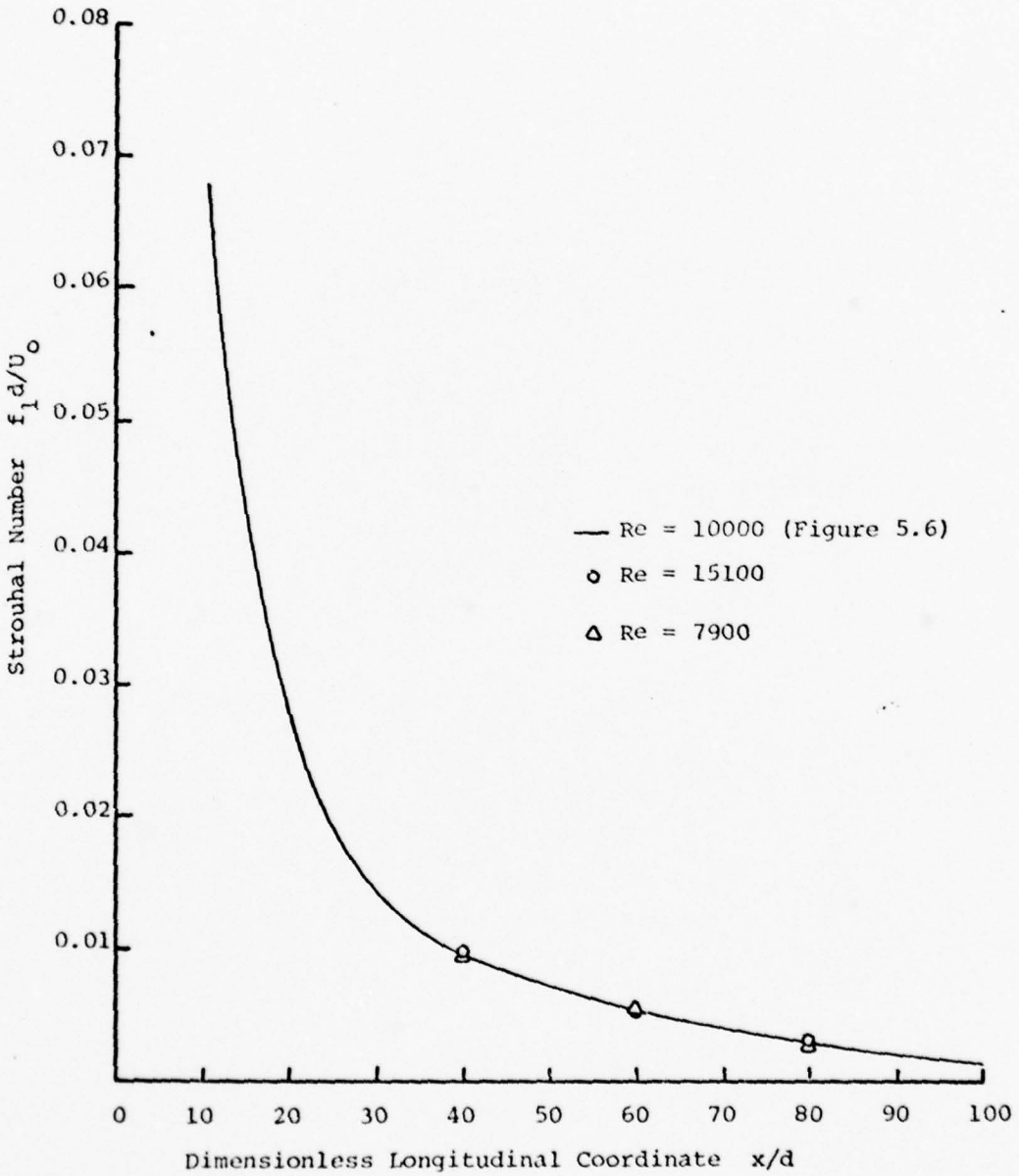

Figure 5.39 Strouhal Number $f_1 d/U_o$ vs. x/d (Reynolds Number Independence)

5.7 Sources of Error and Inaccuracies

Since this investigation is of an experimental nature, it is appropriate to discuss the possible sources of error and uncertainties in performing the reported measurements. The most important aspects to be considered are: inaccuracy in measuring the mean velocity profiles, error in measuring the root-mean-square of the velocity signals, and uncertainty in estimating the crosscorrelation functions.

It was mentioned in Chapter 3 that mean velocity profiles were measured with a home-made total-head Pitot-tube. This was so chosen in order to avoid uncertainties inherent to conventional static-tubes, whose mean readings vary strongly with their size in turbulent flows (Bradshaw [1970]). On the other hand, the selected internal diameter and wall thickness were small enough to interfere as little as possible with the flow but still comply with current standards to give reliable readings.

Measurements of the root-mean-square values of the fluctuating velocities used to normalize the correlation functions, were done with a true r.m.s. voltmeter. This type of instrument theoretically gives very small normalized errors if enough averaging time is allowed (see for instance Bendat and Piersol [1971]). Large averaging times were used in this investigation by setting the time constant of the instrument to high values; the measured r.m.s. values ex-

hibited fluctuations of no more than 5% of the estimated value.

The determination of the uncertainties incurred in estimating a crosscorrelation function is a somewhat difficult task. In the first place, it is necessary to realize that the Fourier analyzer employed in this investigation, computes crosscorrelation function estimates via Fourier Transform methods; that is, a cross-spectrum density function of the two sampled variables is first estimated and then the corresponding inverse transform (the crosscorrelation function) is evaluated, as outlined in Appendix B.

This cross-spectrum density function estimate is however, an inconsistent estimator (Bendat and Piersol [1971]). Thus, it is necessary to perform a smoothing operation over an ensemble of estimates. If a large number of estimates is used (as in this investigation), the number of statistical degrees of freedom in the approximate chi-square distribution of the samples, greatly increasses, reducing any required confidence limit.

On the other hand a crosscorrelation function estimate between two variables $x(t)$ and $y(t)$, defined by:

$$\hat{R}_{xy}(\tau) = \frac{1}{T-\tau} \int_0^{T-\tau} x(t)y(t+\tau)dt \qquad (5.29)$$

for $0 \leq \tau \leq T$, or its digital counterpart:

$$\hat{R}_{xy}(lm) = \frac{1}{N-1} \sum_{n=1}^{N-1} x_n y_{n+r} \qquad (5.25)$$

constitutes an unbiased estimate, (that is, the probability

density function of the estimator is centered at the true value of the correlation function $R_{xy}(\tau)$), since the expected value of (5.24) is given by:

$$E\{\hat{R}_{xy}(\tau)\} = E\left\{\frac{1}{T-\tau}\int_0^{T-\tau} x(t)y(t+\tau)\,dt\right\}$$

$$= \frac{1}{T-\tau}\int_0^{T-\tau} E\{x(t)y(t+\tau)\}\,dt$$

$$= R_{xy}(\tau) \qquad (5.26)$$

However, it is very difficult if not impossible to evaluate the mean-square-error of the correlation function estimate, as given by the variance in equation (5.27):

$$\mathrm{Var}[\hat{R}_{xy}(\tau)] = E\{[\hat{R}_{xy}(\tau)-R_{xy}(\tau)]^2\}$$

$$= E\{\hat{R}^2_{xy}(\tau) - R^2_{xy}(\tau)\}$$

$$= E\left\{\frac{1}{(T-\tau)^2}\int_0^{T-\tau}\int_0^{T-\tau} x(u)y(u+\tau)x(v)y(v+\tau)\,dudv\right\} - R^2_{xy}(\tau)$$

$$= \frac{1}{(T-\tau)^2}\int_0^{T-\tau}\int_0^{T-\tau} E\{x(u)y(u+\tau)x(v)y(v+\tau)\}\,dudv - R^2_{xy}(\tau) \qquad (5.27)$$

where u, v are integration variables.

Equation (5.27) above, involves a mixed fourth order moment of x(t) and y (t) which is quite difficult to calculate.

It may be shown (Kelly et al. [1967]), that for the case of jointly Gaussian processes {x(t)} and {y(t)}, the above variance approaches:

$$\mathrm{Var}[\hat{R}_{xy}(\tau_m)] \simeq \frac{R_{xy}^2(\tau_m)}{B(T-\tau_m)} \tag{5.28}$$

where B is the band width of the analyzed signals (assumed to be the same for both signals), and τ_m is the time delay where the maximum value of correlation occurs.

Thus, following expression (5.28), an approximate value for the normalized mean-square-error can be obtained for the present measurements. For the worst cases (which corresponded to small values of x/d), a band-width of 1 KHz and averaging times of 512 x 1 x10^{-4} sec were used. Therefore at $\tau_m = 0$

$$\frac{\mathrm{Var}[\hat{R}_{xy}(0)]}{R_{xy}^2(0)} \simeq \frac{1}{1\times10^3\times512\times10^{-4}} \simeq 0.02$$

As far as the time delay characteristics of the correlation functions is concerned (used in estimating the flapping frequency), no theoretical error analysis is available in the literature. However, the frequency values obtained in this investigation were repeatable and consistent (particularly with respect to f_1) within ±10% for the worst cases.

In conclusion, the values reported are expected to be within the following error bounds:

Variable	Expected error
U	$\pm$ 5%
$\underline{R}(0)$	$\pm$ 5%
f_1	$\pm$ 10%
f_2	$\pm$ 10%
U_{cf}	$\pm$ 10%
ε_m/b	$\pm$ 5%

The above expectations are best estimates based on the used parameters to compute them as well as observations while performing the measurements.

CHAPTER 6

SUMMARY OF EFFECTS AND DISCUSSION

6.1 Introduction

The objective of this experimental investigation was to characterize the flapping behavior of a plane turbulent jet. In this chapter, the essential features of the flapping motion are summarized and their significance is qualitatively reviewed in the context of the current trends in turbulent shear flow research. It must be underscored that the flapping motion is a natural phenomenon seemingly unrelated to any Coanda-type effects; the latter arise from the tendency of jets to attach to close walls in sudden expansions.

The existence of some kind of organization in the large-scale structure of the initial regions of turbulent shear flows, is nowadays an accepted fact, as reviewed in Chapter 3. Depending on the particular shear flow, these coherent structures are viewed as randomly spaced vortex-like patterns moving and increasing in size in the mean flow direction, and interacting with each other through a coalescence process.

Two comments however, should be made in relation to the above description. In the first place, the state of affairs so described refers to the near-field region of

turbulent shear flows and the effect of this coherence in the far-field self-preserving region, if any, has not been fully studied. On the other hand, the reported investigations for the case of a plane turbulent jet are rather scarce, even with respect to the initial regions.

It may be argued in relation to the second comment, that a plane jet might essentially behave as a double mixing layer, (with each one of its components the mirror image of the other). Although this conception is geometrically true for the initial region, it is a rather simplistic view of the plane jet in its fully developed region. However, the interaction of the two layers, both as they influence the potential core in between, and as they come together in the fully merging region, could account for some of the distinctive characteristics of the plane jet even farther downstream.

In any case, it may be questioned if hidden in the general turbulent structure which characterizes the self-preserving region of a plane jet, there may be any kind of manifestation of the series of events occurring in the initial region. The flapping behavior of the jet may be one of these manifestations.

6.2 Characteristics of the Flapping Motion

At this point if may be helpful to summarize the essential characteristics of such behavior, as concluded based in this investigation.

Beginning at cross-sections at about 20 times the slot width, crosscorrelations taken between u-component velocity fluctuations at points on each side of the jet, presented a distinctive negative value at zero time delay. As the time delay is increased, the correlation functions assume a quasi-periodic shape with an approximately definable frequency. This result indicates that both velocity signals behave (in the average) as if they included a low frequency wave component in antiphase with respect to each other. This could be the consequence of the whole flow field moving (again in the average) in a pseudo-oscillatory way.

The various half-periods between alternative positive and negative peaks detected in the correlation functions, are generally not equal. No explanation is given in this work for this. It may be speculated however, that inasmuch as the flapping motion is characterized by a relatively low frequency, it may be coupled with the low-frequency components of the turbulent velocity field. Any degree of correlation between such components of the two measurement points in the flow field might in turn be affected by the randomness of the high-frequency components. As the time delay between the signals increases from the one corresponding to the highest degree of correlation, the two signals should become less dependent on each other. The quasi-periodic nature of the correlation function

(attributed to the flapping motion) should then become less defined. Recall that only for perfectly periodic signals would the correlation between them be also perfectly periodic.

Support to the above may be derived by examining the data plotted in Figure 6.1. It was obtained by first filtering both signals before processing them. Low-pass filters, with cut-off frequency of 25 Hz, were used. The periodic yet decaying nature of the correlation function is noted.

6.3 Possibility of Puffing

During the earlier stages of this investigation, the existence of "puffing" was raised as the possible cause for the difference between the various half-periods in the correlation functions (and possibly the decaying correlation). This puffing effect might be originated by instabilities in the blower feeding the nozzle. Correlation functions were taken with various probe arrangements in the potential core close to the nozzle exit (see example in Figure 6.2). Any puffing would have to be accompanied by a periodic correlation, positive near $\tau = 0$. These tests revealed no abnormalities which could indicate the existence of this effect.

6.4 Frequency of Flapping Motion

The frequency of flapping, although almost constant at each cross-section, decreases in the downstream direction.

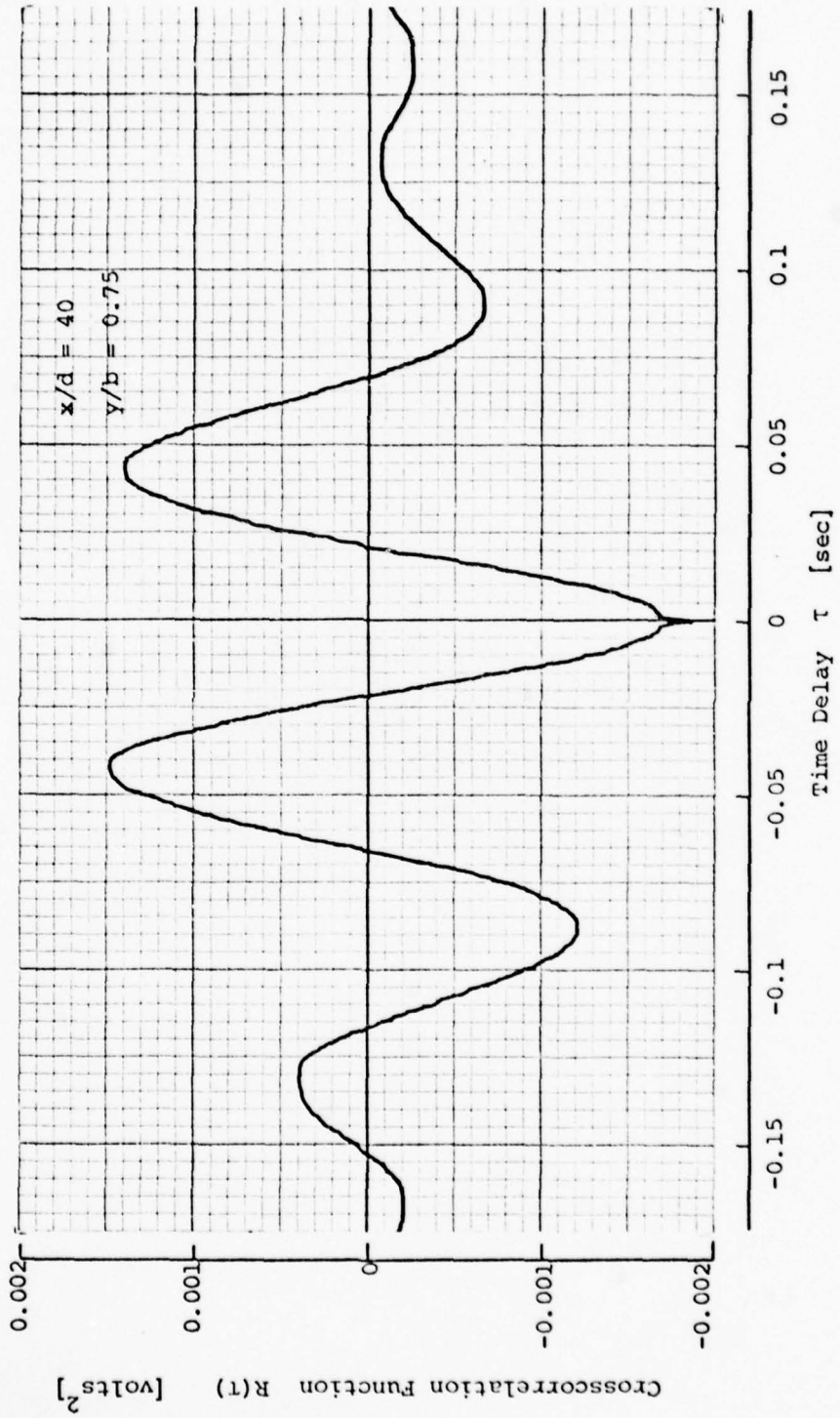

Figure 6.1 An Example of Filtered Crosscorrelation

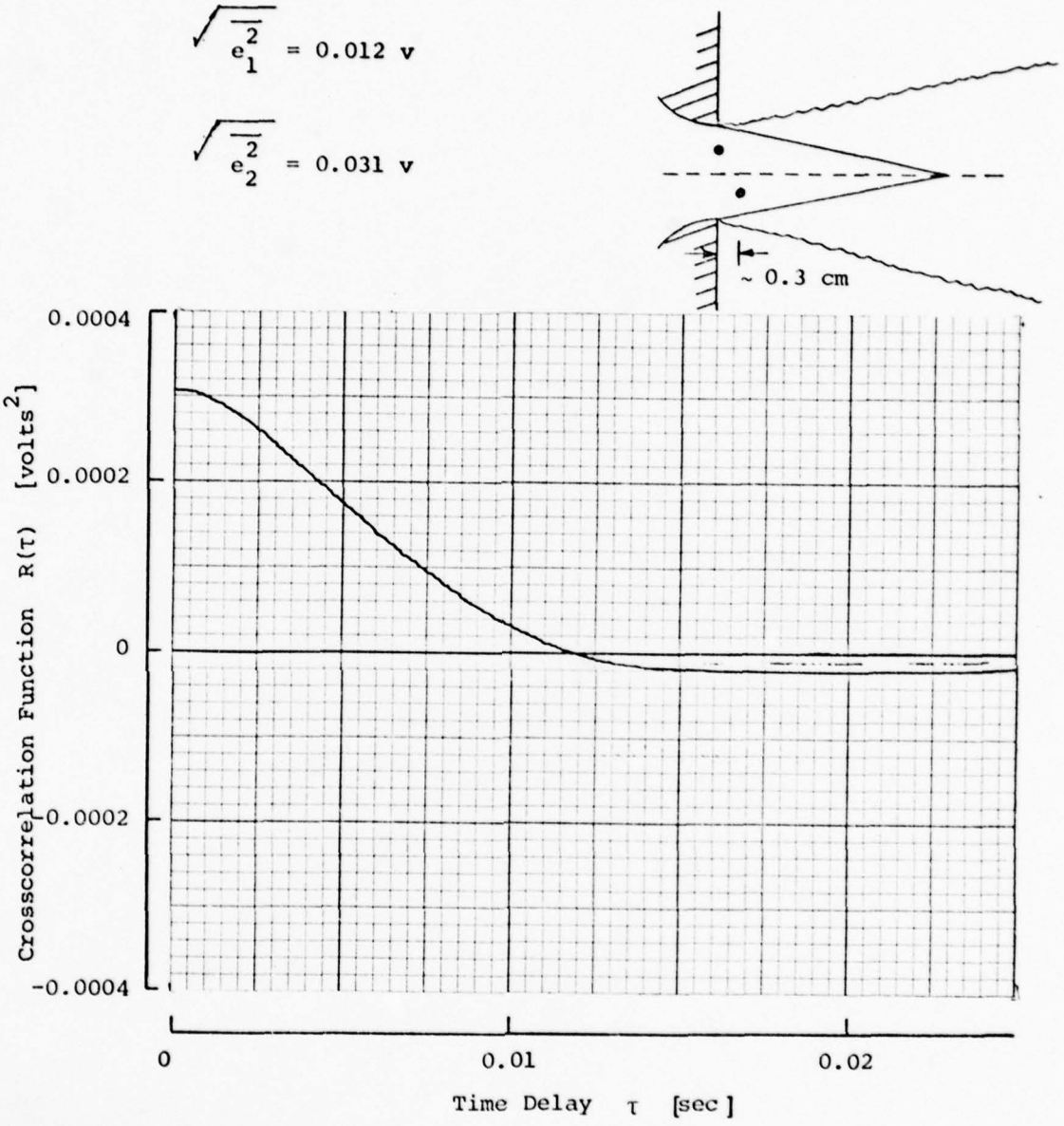

Figure 6.2 An Example of Crosscorrelation Function of the Nozzle Exit.

In the far region it seems to scale quite well by the inverse of a characteristic development time of the mean flow, given by the ratio of the half-width to the mean velocity at the centerline of the jet.

The amplitude of the correlation function at zero time delay $\underline{R}(0)$, depends on the lateral coordinate. For small separations it definitely should, since it corresponds to a space-correlation for varying separation distance between probes (equation 5.8, Figure 5.24). These results when compared with the ones reported by Gutmark and Wygnanski [1976] showed some disagreement (see Figure 5.24). Even though the present work shows the same trends as Gutmark and Wygnanski [1976] for space-correlations corresponding to $y/b \leq 0.5$, there is noticeable disagreement with the cases at $y/b \geq 1.0$. Particularly, the curve corresponding to $y/b = 1.5$ reported by the above mentioned authors, shows a negative dip at approximately $\Delta y/b = 2.3$ with a trend to become more negative as the abscissa increases. This is an unlikely result since it should be realized that having the probes separated by $\Delta y/b = 2.3$ with middle-point at $y/b = 1.5$ corresponds to effectively setting one probe at $y/b = 0.35$ and the second one at $y/b = 2.65$. The latter probe is in the entrainment region totally outside of the turbulent core, and any correlation between the x-component of the velocities at these points should be close to zero. That is not the case with Gutmark and Wygnanski [1976] but is indeed so in the present work.

6.5 Convection of Flapping Motion

Correlation measurements with the probes at different x/d stations and yet on opposite sides of the jet showed that the flapping motion seems to travel downstream. This flapping convection velocity roughly corresponds to the turbulent convective velocity previously measured and reported by other investigators (Ott [1972], Young [1973]).

6.6 Relationship to Wave-Guide Theory

In trying to put the described results in a proper theoretical framework, one is tempted to consider the current efforts in the stability theory of turbulent shear flows. It should be stated however that no mathematical modeling is intended here, but instead a summary of the main features of such theory in the light of the experiments reported in this work. A review of spatial stability theory is given in Appendix C.

A realistic wave-guide model of turbulent shear flows should account for a spatially growing wave of given frequency, attaining its maximum amplitude through some kind of saturation effect and decaying in the mean flow direction. In fact, as Liu [1974] has suggested, it is possible to construct such a wave-guide representation by assuming the turbulent flow to be composed of three parts: the mean flow, the periodic wave component and the small-scale turbulence. The organized wave component may be assumed as the product of an amplitude function to be determined from the kinetic

energy integral equation and a shape function obtained from the linear eigenvalue problem corresponding to the local mean flow. The various flow quantities (assumed to include such wave component) are introduced into the basic equation of motion and time- and phase-averages are performed. An integral equation can in turn be obtained for the kinetic energy of the instability wave and numerical solutions can be sought after considering proper boundary conditions.

Three essential characteristics for the organized wave are obtained through this type of analysis (Merkine and Liu [1975]): (a) the amplitude of the wave increases, attains its maximum value and then decays in the downstream direction, mainly through kinetic energy exchange mechanisms; (b) the lower the frequency of the wave component, the further downstream its maximum amplitude is attained; (c) the sinuous modes (that is, the organized waves oscillating in antiphase, like the u-component velocities in the flapping behavior) have larger amplitude rates and show more delayed saturation values in the downstream direction, than the varicose (or symmetrical) modes.

It is seen therefore, that a wave-guide representation could be used in modeling some of the experimental observations reported in this work. For instance, the sinuous modes (the most amplified ones) predicted by stability theory might account for the pseudo-oscillatory u-components of the velocity (in antiphase) characterizing the flapping

motion. On the other hand, the theoretical result that the lower frequency wave components have the tendency to reach their maximum growth further downstream, might be related to the relatively low and decreasing frequencies associated to the flapping behavior.

In concluding this chapter, a perspective of the plane turbulent jet, might be as follows. In the initial region, the mixing layers, one at each side of the potential core, seem to be characterized by the presence of large-scale coherent structures. As the two layers merge together, the coherent structures interact through a yet unknown process. As a result, the possible existence of organized waves as predicted by stability theory, might be manifested in the far downstream self-preserving region in terms of distinctive phenomena, among them the flapping motion.

CHAPTER 7

CONCLUSIONS AND SUGGESTIONS FOR FURTHER WORK

The following conclusions can be established, based on the experimental results obtained in this investigation:

1) The flapping motion of a turbulent plane jet is a distinctive and measurable natural phenomenon. This was confirmed by spot-checks at two other jet setups and by a previous preliminary investigation (Goldschmidt and Bradshaw [1973]).

2) The frequency of flapping decreases in the longitudinal direction and remains unchanged in the lateral direction.

3) Approximate self-preservation is obtained for the flapping frequency (for $x/d > 30$), if scaled with the centerline mean velocity and the half-width of the jet, giving $fb/U_m \simeq 0.11$.

4) An estimate of the amplitude of flapping gave values in the order of 20% of the jet half-width.

5) The flapping behavior travels in the downstream direction with a velocity about 25% smaller than the turbulent structure convective velocity.

6) The frequency of flapping is independent of the Reynolds number in the range $7900 \leq Re \leq 15100$.

Further work is recommended in the following areas:

1) More accurate measurements are needed for $x/d < 20$. The use of a nozzle with a larger slot would permit better accuracy in positioning the probes at those stations.

2) Simultaneous data acquisition in more than two points of the flow field, can be accomplished by using magnetic tape recording instrumentation. This, together with a large computer, would increase the versatility of data reduction and analysis.

3) A detailed and accurate experimental study is suggested for the initial zone of the turbulent plane jet. Particularly in the region where the two mixing layers merge together. The aim of this investigation would be to get a better insight on how they interact with each other.

4) Preliminary and limited observations with an external acoustic input (frequencies less than 600 Hz) showed no changes in the flapping motion of the jet. More experiments are needed in this respect.

5) Mathematical modeling of turbulent shear flows through stability theory (although in a developing stage) is a promising one. A continuous effort in this area and its possible relationship with the flapping behavior of a turbulent plane jet, is strongly recommended.

LIST OF REFERENCES

LIST OF REFERENCES

Abramovich, G. H. [1963] The Theory of Turbulent Jets. The MIT Press, Cambridge, Mass.

Bashir, J. and Uberoi, M. S. [1974] Experiments on Turbulent Structure and Heat Transfer in a Two Dimensional Jet, The Physics of Fluids, 18, 4, 405.

Batchelor, G. K. and Gill, A. E. [1962] Analysis of the Stability of Axisymmetric Jets, J. Fluid Mech. 14, 529.

Becker, H. A. and Massaro, T. A. [1968] Vortex Evolution in a Round Jet, J. Fluid Mech. 31, 435.

Bendat, J. S. and Piersol, A. G. [1971] Random Data: Analysis and Measurement Procedures, Wiley-Interscience, New York, N.Y.

Bevilaqua, P. M. [1973] Intermittency, the Entrainment Problem. Ph.D. thesis, Purdue University.

Binder, G. and Favre-Marinet, M. [1972] Flapping Jets, Proceedings of the Symposium on Flow Induced Structural Vibrations, Karlsruhe, Germany.

Bradbury, L. J. S. [1965] The Structure of a Self-preserving Turbulent Plane Jet, J. Fluid Mech., 23, 31.

Bradshaw, P. [1970] Experimental Fluid Mechanics, 2nd Edition, Pergamon Press, Elmsford, N.Y.

Bradshaw, P., Ferriss, D. H. and Johnson, R. F. [1963] Turbulence in the Noise-Producing Region of a Circular Jet, NPL Aero Report 1054.

Brown, G. and Roshko, A. [1971] On Density Effects and Large Structure in Turbulent Mixing Layers, J. Fluid Mech., 64, 775.

Bruun, H. H. and Yule, A. J. [1974] Hot-wire Eduction Measurements in a Round Jet, lecture given at the Colloquium on Coherent Structures in Turbulence held at the University of Southampton, England 26-29 March, 1974.

Chan, Y. Y. [1974] Spatial waves in Turbulent Jets, The Physics of Fluids, 17, 1, 46.

Chanaud, R. C. and Powell, A. [1962] Experiments Concerning the Sound-Sensitive Jet, J. Acoust. Soc. Am., 34, 7, 907.

Corcos, G. M. [1964] The Structure of the Turbulent Pressure Field in Boundary-Layer Flows, J. Fluid Mech., 18, 353.

Corrsin, S. and Kistler, A. L. [1954] Free-Stream Boundaries of Turbulent Flows, NACA TN 3133.

Crow, S. C. and Champagne, F. H. [1971] Orderly Structure in Jet Turbulence, J. Fluid Mech., 48, 547.

Davies, P. O. A. L. and Yule, A. J. [1975] Coherent Structures in Turbulence, J. Fluid Mech., 69, 513.

Favre, A. J. [1965] Review of Space-Time Correlations in Turbulent Fluids, J. App. Mech., 32, Ser E, 2, 241.

Favre, A. J., Gaviglio, J. J., and Dumas, R. J. [1958] Further Space-Time Correlations of Velocity in a Turbulent Boundary Layer, J. Fluid Mech., 3, 344

Fiedler, H. E. [1974] On Turbulence Structure and Mixing Mechanism in Free Turbulent Shear Flows, Project SQUID Workshop on Turbulent Mixing in Nonreactive and Reactive Flows, Purdue University, Plenum Press, New York, N.Y.

Fisher, J. J. and Davies, P. O. A. L. [1963] Correlation Measurements in a Non-Frozen Pattern of Turbulence, J. Fluid Mech., 18, 97.

Flora Jr., J. J. and Goldschmidt, V. W. [1969] Virtual Origins of a Free Plane Turbulent Jet, AIAA J., 7, 12, 2344.

Freymuth, P. [1966] On Transition in a Separated Laminar Boundary Layer, J. Fluid Mech., 25, 683.

Fuchs, H. V. [1972] Space Correlations on the Fluctuating Pressure in Subsonic Turbulent Jets., J. Sound and Vibr., 23, 1, 77.

Gaster, M. [1965] The Role of Spatially Growing Waves in the Theory of Hydrodynamic Stability, Progress in Aeronautical Sciences, 6, 251.

Glass, D. R. [1968] Effects of Acoustic Feedback on the Spread and Decay of Supersonic Jets, AIAA Journal, 6, 10, 1890.

Goertler, H. [1942] Berechnung von Aufgaben der freien Turbulent duf Grund emes neven Näherungsansatzes, ZAMM 22, 244.

Goldschmidt, V. W. and Bradshaw P. [1973] Flapping of a Plane Jet, The Physics of Fluids, 16, 354.

Goldschmidt, V. W. and Kaiser, K. F. [1971] Interaction of an Acoustic Field and a Turbulent Plane Jet: Mean Flow Measurements, Chem. Engr. Progress Symp. Series, 67, 109, 91

Grant, H. L. [1958] The large Eddies of Turbulent Motion, J. Fluid Mech., 4, 149.

Gutmark, E. and Wygnanski, I. [1976] The Planar Turbulent Jet., J. Fluid Mech., 73, 465.

Heskestad, G. [1965] Hot-Wire Measurements in a Plane Turbulent Jet, J. App. Mech., 32, 4, 721.

Hinze, J. O. [1959] Turbulence, An Introduction to its Mechanism and Theory, McGraw-Hill Book Company, New York, N.Y.

Hussain, A. K. M. F. and Reynolds, W. C. [1970] The Mechanics of an Organized Wave in Turbulent Shear Flow, J. Fluid Mech., 41, 241.

_____. [1972] The Mechanics of an Organized Wave in Turbulent Shear Flow. Part 2. Experimental results, J. Fluid Mech., 54, 241.

Hussain, A. K. M. F. and Zaman, K. B. M. Q. [1975] Effect of Acoustic Excitation on the Turbulent Structure of a Circular Jet, Proceedings of the Third Interagency Symposium on University Research in Transportation Noise, Univ. of Utah, S. Lake City, Utah.

Jenkins, G. M. and Watts, D. G. [1968] Spectral Analysis and its Applications, Holden-Day, San Francisco, Calif.

Jenkins, P. E. [1974] A Study of the Intermittent Region of a Heated Two-Dimensional Plane Jet, Ph.D. Thesis, Purdue University.

Kaiser, K. F. [1971] An Experimental Investigation of the Interaction of an Acoustic Field and a Plane Turbulent Jet, MSME Thesis, Purdue University.

Kelly, R. D., Enochson, L. D. and Rondinelli, L. A. [1967] Techniques and Errors in Measuring Cross-Correlations and Cross-Spectral Density Functions., NASA CR-74505.

Ko, N. W. M. and Davies, P. O. A. L. [1971] The Near Field Within the Potential Core of Subsonic Cold Jets, J. Fluid Mech., 50, 49.

Landahl, M. T. [1967] A Wave-Guide Model for Turbulent Shear Flow, J. Fluid Mech., 29, 441.

Lange, H. B. H. [1966] Correlation Techniques, D. Van Nostrand Company, Princeton, N.J.

Lathi, B. P. [1968] An Introduction to Random Signals and Communication Theory, International Textbook Company, Scranton, Penn.

Lau, J. C. and Fisher, M. J. [1975] The Vortex Street Structure of 'Turbulent' Jets. Part 1, J. Fluid Mech., 67, 299.

Lau, J. C., Fisher, M. J. and Fuchs, H. V. [1972] The Intrinsic Structure of Turbulent Jets, J. Sound and Vibr. 22, 279.

Leconte, J. [1858] On the Influence of Musical Sounds on the Flame of a Jet of Coal-Gas, Phil. Mag., 15, 235.

Liu, J. T. C. [1974] Developing Large-Scale Wavelike Eddies and the Near Jet Noise Field, J. Fluid Mech., 62, 437.

Mattingly, G. E. and Criminale, Jr., W. O. [1971] Disturbance Characteristics in a Plane Jet, The Physics of Fluids, 14, 11, 2258.

Merkine, L. and Liu, J. T. C. [1975] On the development of Noise-Producing Large-Scale Wavelike Eddies in a Plane Turbulent Jet, J. Fluid Mech., 70, 353.

Michalke, A. [1970] The Instability of Free Shear Layers: A Survey of the State of the Art. Dsch. Luft-and Raunfahrt Mitt. 70-04.

_____. [1972] An Expansion Scheme for the Noise from Circular Jets., Z. Flügwiss, 20, 229.

Mih, C. and Hoopes, J. A. [1972] Mean and Turbulent Velocities for Plane Jet, J. Hydr. Div, ASCE, HY7, 1277.

Miskad, R. [1972] Experiments on the Nonlinear Stages of Free-Shear-Layer Transition, J. Fluid Mech., 72, 695.

Mollo-Christensen, E. [1967] Jet Noise and Shear Flow Instability Seen from an Experimenter's Viewpoint, J. App. Mech., 89, 1.

Morkovin, M. V. [1964] Flow Around Circular Cylinder--A Kaleidoscope of Challenging Fluid Phemonena, ASME Symp. on Fully Separated Flows, Philadelphia, Pa., May 1964.

Mulej, D. J. [1975] Velocity and Foldover of the Turbulent Non-Turbulent Interface in a Plane Jet, M.S.M.E. Thesis, Purdue University.

Ott, E. S. [1972] Convective Velocities in a Turbulent Plane Jet, M.S.M.E. Thesis, Purdue University.

Papailiou, D. D. and Lykoudis, P. S. [1974] Turbulent Vortex Streets and the Entrainment Mechanism of the Turbulent Wake, J. Fluid Mech., 62, 11.

Phillips, O. M. [1966] The Dynamics of the Upper Ocean, Cambridge Univ. Press.

Planchon, Jr., H. P. [1974] The Fluctuating Static Pressure Field in a Round Jet Turbulent Mixing Region, Ph.D. thesis, University of Illinois at Urbana-Champaign.

Reichardt, H. [1951] Gesetzmäßigkeiten der freien Turbulenz, VDI-Forschmgscheft 414, Zudedition.

Reynolds, W. C. and Hussain A. K. M. F. [1972] The Mechanics of an Organized Wave in Turbulent Shear Flow. Part 3. Theoretical Models and Comparisons with Experiments, J. Fluid Mech., 54, 263.

Rockwell, D. O. [1971] The Macroscopic Nature of Jet Flows Subjected to Small Amplitude Periodic Disturbances, Chem. Engr. Progress Symp. Series, 67, 109, 99.

_____. [1972] External Excitation of Planar Jets, J. App. Mech., ASME, 39, 4, 883.

Rockwell, D. O. and Niccolls, W. O. [1972] Natural Breakdown of Planar Jets, J. Bas. Engr., ASME, 94, 4, 720.

Roshko, A. [1975] Progress and Problems in Understanding Turbulent Shear Flows, Turbulent Mixing in Nonreactive and Reactive Flows, a Project SQUID Workshop. Plenum Press, New York, N. Y.

Sato, H. [1960] The Instability and Transition of a Two-Dimensional Jet, J. Fluid Mech., 7, 53.

Schlichting, H. [1968] Boundary-Layer Theory, 6th ed., McGraw-Hill Book Company, New York, N.Y.

Siddon, T. E. [1969] On the response of Pressure Measuring Instrumentation in Unsteady Flow, Univ. of Toronto, UTIAS report No. 136.

Simcox, C. D. and Hoglund, R. F. [1971] Acoustic Interactions with Turbulent Jets, ASME J. of Basic Engr., 93, 1, 42.

Spencer, B. W. [1970] Statistical Investigation of Turbulent Velocity and Pressure Fields in a Two-Stream Mixing Layer, Ph.D. thesis, University of Illinois at Urbana-Champaign.

Spencer, B. W. and Jones, B. G. [1971] Statistical Investigation of Pressure and Velocity Fields in the Turbulent Two-Stream Mixing Layer, AIAA paper 71-613.

Stiffler, A. K. [1971] Sinusoidal Excitation of a Free Turbulent Jet, Ph.D. thesis, The Penn. State. Univ.

Taylor, G. I. [1935] Statistical Theory of Turbulence, Proc. Roy. Soc. London, 151A, 421.

Tennekes, H. and Lumley, J. L. [1972] A First Course in Turbulence, The MIT Press, Cambridge, Mass.

Tollmien, W. [1926] Berechnung turbulenter Auvbreitingsvorgänge, ZAMM 6, 468

Townsend, A. A. [1956] The Structure of Turbulent Shear Flow, Cambridge Univ. Press, Cambridge, Gr. Br.

Van Der Hegge Zijnen, B. G. [1958] Measurements of the Velocity Distribution in a Plane Turbulent Jet of Air, App. Sci. Res., Sec. A, 7, 256.

Winant, C. D. and Browand, F. K. [1974] Vortex Pairing: The Mechanism of Turbulent Mixing-Layer Growth at Moderate Reynolds Number, J. Fluid Mech., 63, 237.

Wooldridge, C. E., Wooten, D. C. and Amaro, A. J. [1972] The Structure of Jet Turbulence Producing Jet Noise, AIAA pap. 72-158.

Wygnanski, I. and Gutmark, E. [1971] Lateral Motion of the Two-Dimensional Jet Boundaries, The Physics of Fluids, 14, 7, 1309.

Young, M. F. [1973] A Turbulence Study: Convective Velocities, Energy Spectra, and Turbulent Scales in a Plane Air Jet, M.S.M.E. thesis, Purdue Univ.

Yule, A. J., Brown, H. H., Baxter, D. R. J. and Davies, P. O. A. L. [1974] Structure of Turbulent Jets, ISVR Memo 506, Univ. of Southampton.

General References

Ajagu, C. O. [1976] Fold-Over, Imtermittency and Crossing Frequency of a Plane Jet Interface With and Without an Acoustic Disturbance, M.S.M.E. Thesis, Purdue University.

Betchov, R. and Criminale Jr., W. O. [1967] Stability of Parallel Flows, Academic Press Inc., New York, N.Y.

Birkhoff, G. and Zarantonello, E. H. [1957] Jets, Wakes and Cavities, Academic Press Inc., New York, N.Y.

Brodkey, R. S. [1967] The Phenomena of Fluid Motions, Addison-Wesley Publishing Co., Reading, Mass.

Laufer, J. [1975] New Trends in Experimental Turbulence Research, Ann. Rev. Fluid Mech., 7, 307.

Lin, C. C. [1965] The Theory of Hydrodynamic Stability, Cambridge Univ. Press., Cambridge, Gr. Br.

Miller, D. R. and Comings, E. W. [1957] Static Pressure Distribution in the Free Turbulent Jet, J. Fluid Mech. 3, 1

Sandborn, V. A. [1972] Resistance Temperature Transducers. Metrology Press, Ft. Collins, Colorado.

Thompson, C. [1975] Organized Motions in a Plane Turbulent Jet Under Controlled Excitation, Ph. D. Thesis, University of Houston.

Wooldridge, C. E. and Wooten, D. C. [1971] A Study of the Large-Scale Eddies of Jet Turbulence Producing Jet Noise, AIAA pap 71-154.

APPENDICES

Appendix A

Self-Preservation Characteristics of the Plane Turbulent Jet

Mean velocity traverses were performed at several x/d stations, as described in Chapter 3. The resulting profiles are presented in Figure A.1, where the local mean velocity and the lateral y-coordinate have been nondimensionalized by the centerline mean velocity U_m and the jet half-width b respectively, corresponding to each x/d station. Also presented in Figure A.1 are Reichardt's [1951] experimental results. Self-preservation of the turbulent jet is then attained for the range of x/d reported in this investigation.

The similarity and self-preservation principles, already well-documented both theoretically and experimentally in the existing literature (see for instance, Abramovich [1963], Schlichting [1968]), allow one to write the following expressions:

$$\frac{b}{d} = K_1 \left(\frac{x}{d} - C_1\right) \tag{A.1}$$

$$\left(\frac{U_m}{U_o}\right)^{-2} = K_2 \left(\frac{x}{d} - C_2\right) \tag{A.2}$$

In these relationships, K_1, K_2, C_1, C_2 are empirical constants the first two measuring the widening rate of the flow and the last two indicating the geometric and kinematic

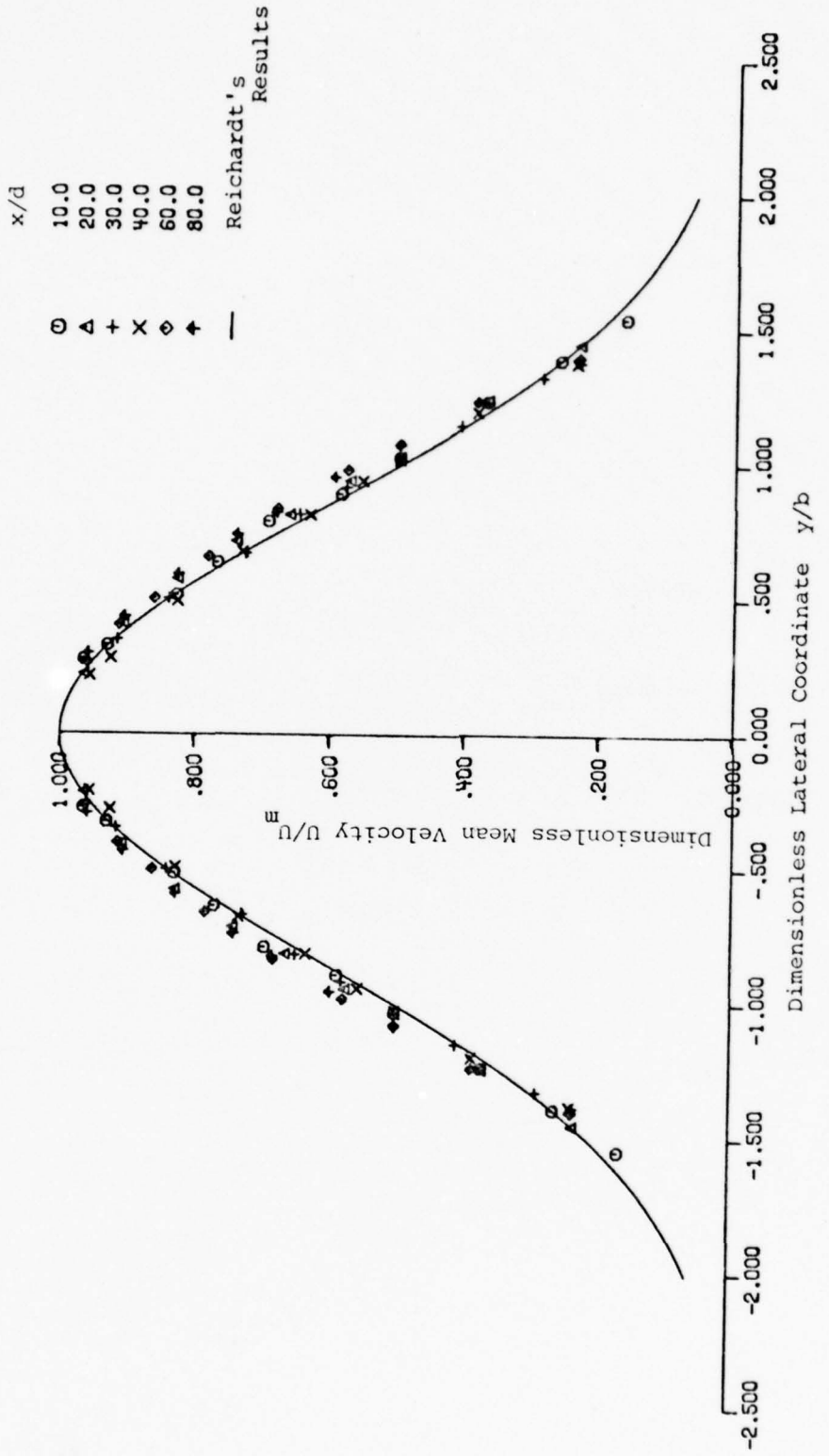

Figure A.1 Mean Velocity Profiles

virtual origins of the jet, respectively. There is no reason to expect coincidence of these origins as reported by Flora and Goldschmidt [1969]. Being their determination the result of graphical extrapolation and therefore not sufficiently accurate, their values are different from one experimental setup to another as noted in Table A.1, where these parameters obtained by various authors are compared.

The results obtained in the present investigation corresponding to expressions (A.1) and (A.2) respectively, are as follows:

$$\frac{b}{d} = 0.083 \left(\frac{x}{d} + 6.62\right) \qquad (A.3)$$

$$\left(\frac{U_m}{U_o}\right)^{-2} = 0.24 \left(\frac{x}{d} - 4.53\right) \qquad (A.4)$$

They are also presented graphically in Figures A.2 and A.3, respectively.

Table A.1 Spreading Parameters of Plane Jets.

INVESTIGATOR	Re	K_1	K_2	C_1	C_2
Van der Hegge Zijnen [1958]	1.33×10^4	0.1	0.205	0.0	-1.7
Heskestad [1965]	2.5×10^4	0.11	0.364	5.3	5.3
Flora and Goldschmidt [1969]	1.7×10^4-2.9×10^4	0.108-0.113	0.158-0.164	0.0	2.5
Kaiser [1971]	1×10^4-4×10^4	0.101	0.208	-2.6	0.0
Ott [1972]	1×10^4	0.0968	0.228	-3.0	7.0
Young [1973]	1×10^4	0.0875	0.15	-8.75	-1.25
Jenkins [1974]	1.45×10^4	0.091	0.16	-3.0	4.0
Mulej [1975]	1.6×10^4	0.095	0.185	-0.789	13.2
Present Work	1×10^4	0.0831	0.243	-6.62	4.53

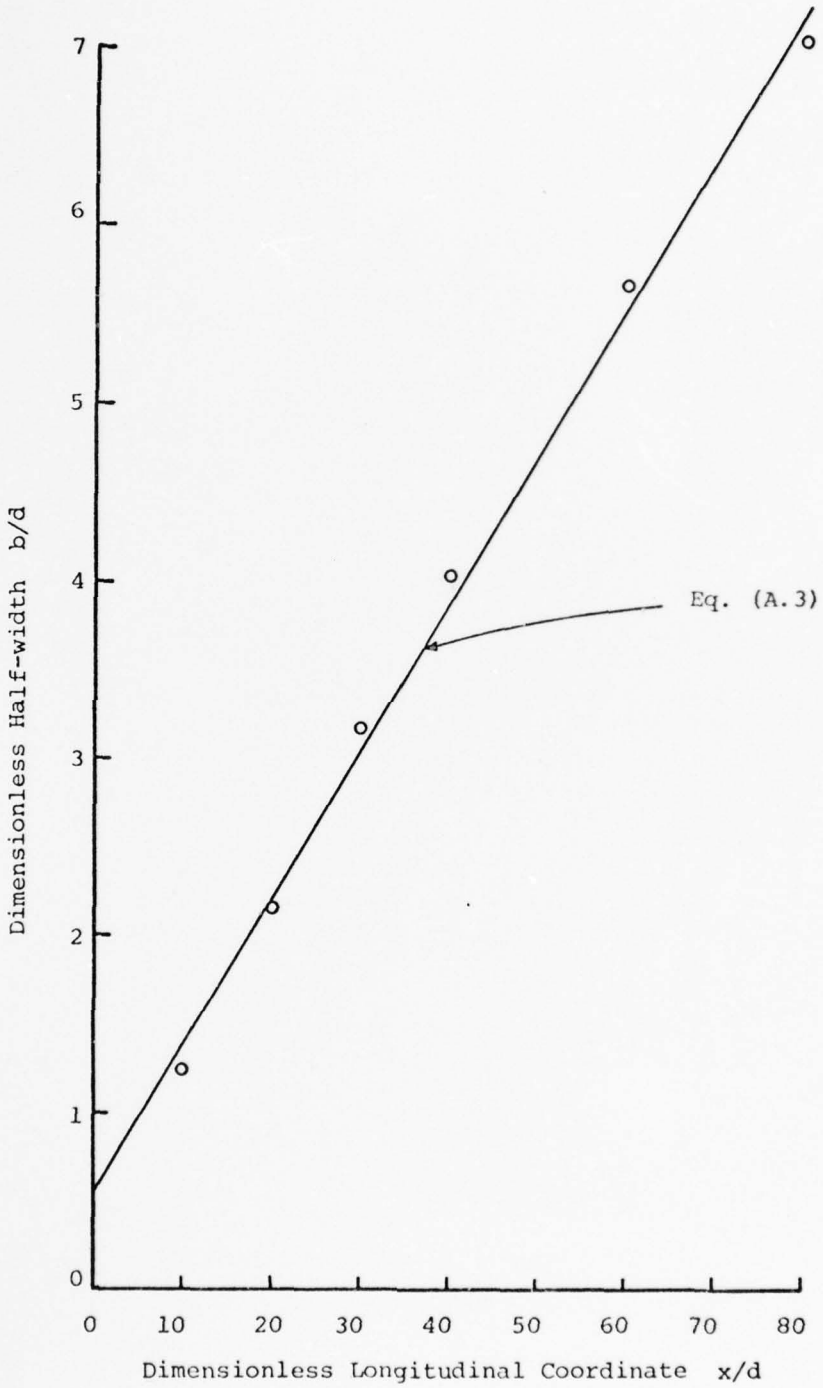

Figure A.2 Jet Half-width b/d vs. x/d

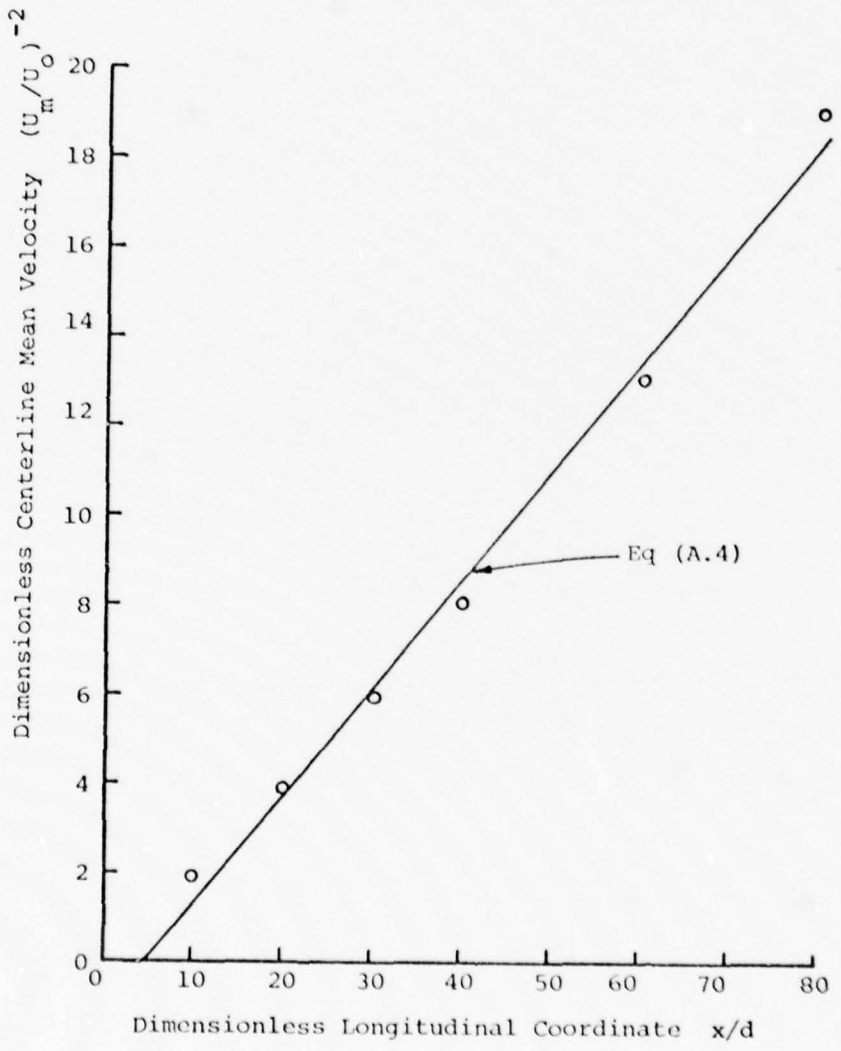

Figure A.3 Centerline Mean Velocity vs. x/d

Appendix B

Application of the HP Fourier Analyzer

The Hewlett-Packard 5452A-2114B Fourier Analyzer System is able to compute the crosscorrelation function between any two given analog voltage signals. Both signals representing any two physical quantities, are first low-pass filtered (according to the sampling rate used in converting the signals to digital form) in order to avoid aliasing. Once digitized and stored in the memory, the crosscorrelation between the signals is computed via the Fast Fourier Transform algorithm, as the flow diagram in Figure B.1 indicates.

The analyzer can do this operation in a repetitive way for any number of samples and compute an average of them, if properly programmed. The block diagram and listing of a program used to estimate an average of crosscorrelation functions from 250 samples, are presented in Figure B.2 and Table B.1, respectively.

In order to estimate the autocorrelation function of the v-component of the velocity at the centerline, a different and somehow more complicated program was used. In fact, it was necessary to compute actually four different correlation functions for this case, as equation (B.1) states:

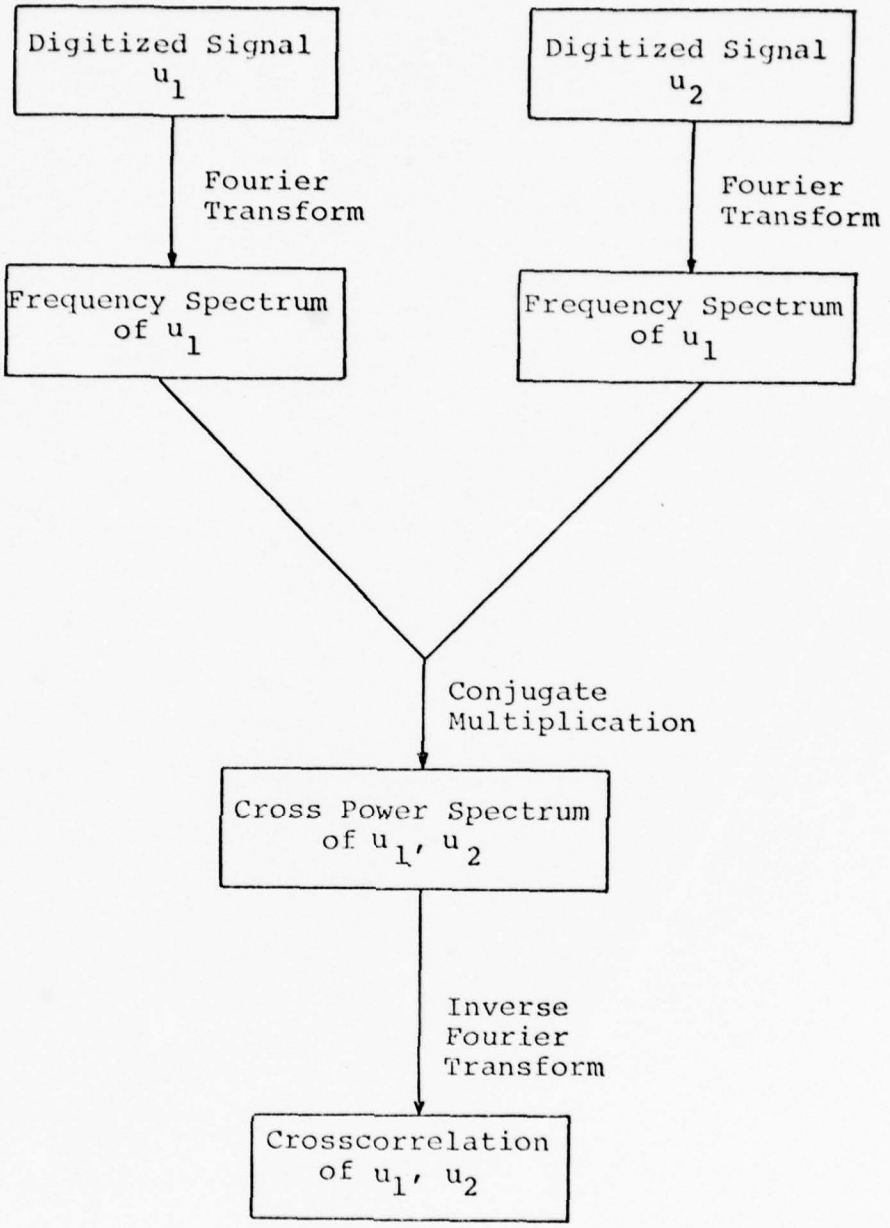

Figure B.1

Block Diagram of Crosscorrelation Computation

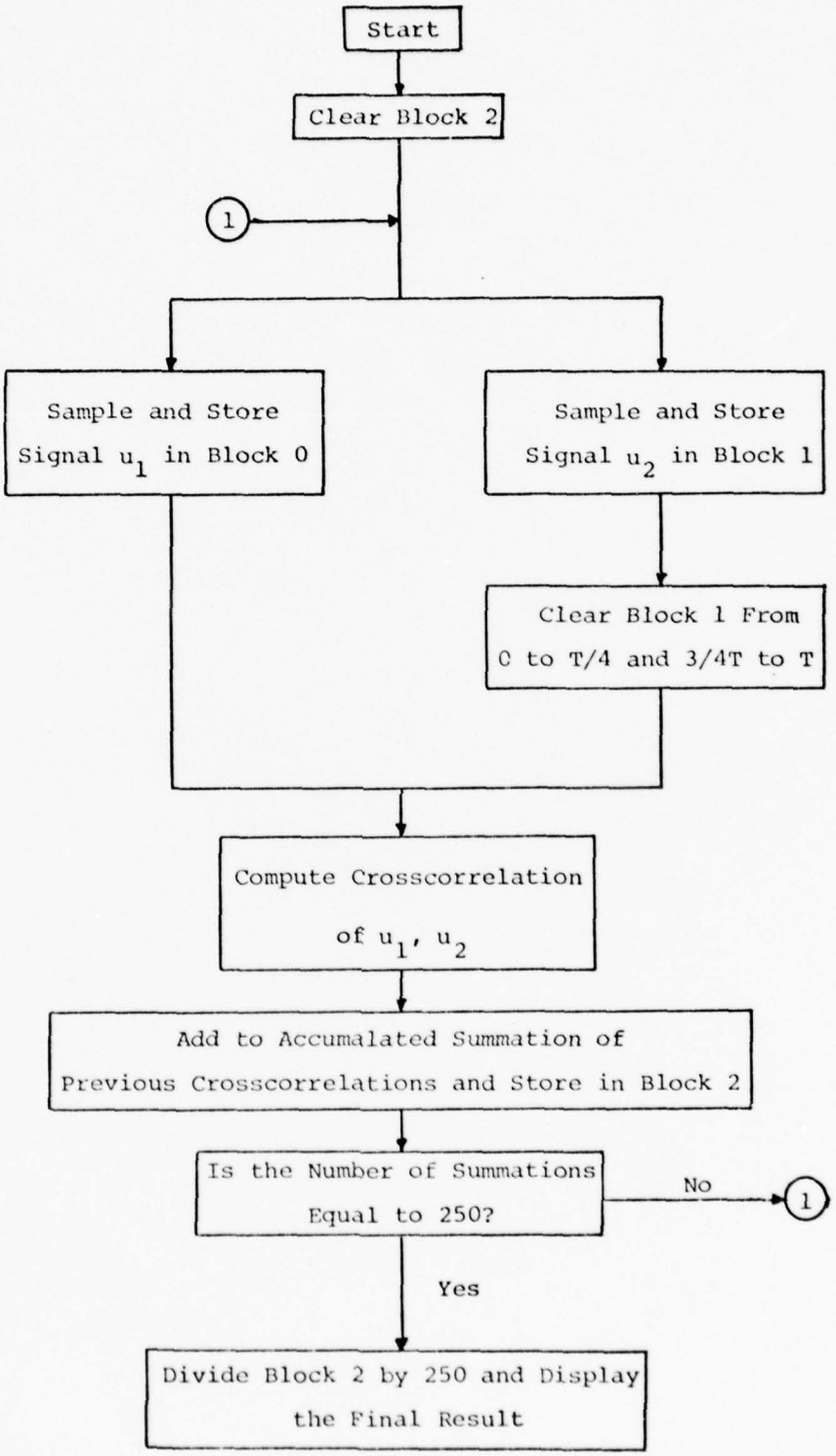

Figure B.2

Flow Diagram of the Program Used by the Fourier Analyzer in Computing Crosscorrelation Averages

Table B.1 Program Used by the Fourier Analyzer in Computing Crosscorrelation Averages.

```
LABEL 0 ENTER
CLEAR 2 ENTER
LABEL 1 ENTER
ANALOG 0 SPACE 1 SPACE 2 ENTER
CLEAR 1 SPACE 0 SPACE 128 ENTER
CLEAR 1 SPACE 384 SPACE 512 ENTER
CORR 1 ENTER
+ 2 ENTER
STORE 2 ENTER
COUNT 1 SPACE 250 ENTER
÷ 0 SPACE 250 ENTER
END ENTER
```

$$R_v(\tau) = \overline{v(t)v(t+\tau)} = \frac{1}{4S_v^2}\left[\overline{e_1(t)e_1(t+\tau)} + \overline{e_2(t)e_2(t+\tau)} - \overline{e_1(t)e_2(t+\tau)} - \overline{e_2(t)e_1(t+\tau)}\right] \quad \text{(B.1)}$$

where e_1 and e_2 are the voltage signals from the two sensing elements of the x-wire, respectively, and S_v is the v-component sensitivity of the wires. (S_v is approximately the same for both wires if they are properly matched). Equation (B.1) can be obtained easily with some algebraic manipulations, from the standard relationships defining the voltages of an x-wire:

$$e_1(t) = S_u\, u(t) + S_v\, v(t)$$

$$e_2(t) = S_u\, u(t) - S_v\, v(t) \quad \text{(B.2)}$$

A listing of the program used for the autocorrelation computation is given in Table B.2.

In estimating any function which involves time shifting operations (like correlations or convolutions), the analyzer computes integrations between the limits 0 and T (that is, the size of the sampled data). The analyzer further assumes that the sampled data is periodic with

Table B.2 Program Used by the Fourier Analyzer in Computing Autocorrelation Averages.

```
LABEL 0 ENTER
CLEAR 3 ENTER
LABEL 1 ENTER
ANALOG 4 SPACE 5 SPACE 3 ENTER
LOAD 4 ENTER
STORE 1 ENTER
SUBJUMP 2 ENTER
STORE 2 ENTER
LOAD 5 ENTER
CORR 1 ENTER
INTERCHNG 2 ENTER
- 2 ENTER
STORE 2 ENTER
LOAD 5 ENTER
STORE 1 ENTER
SUBJUMP 2 ENTER
+ 2 ENTER
STORE 2 ENTER
LOAD 4 ENTER
CORR 1 ENTER
INTERCHNG 2 ENTER
- 2 ENTER
+ 3 ENTER
STORE 3 ENTER
```

Table B.2 (continued)

COUNT 1 SPACE n ENTER
÷ 0 SPACE n ENTER
SUBROUTINE
CLEAR 1 SPACE 0 SPACE 128 ENTER
CLEAR 1 SPACE 384 SPACE 512 ENTER
CORR 1 ENTER
SUBRTRN ENTER

period T. The estimated function therefore results in error (the so called wrap-around error). In order to effectively avoid this (at least partially), one of the data records is cleared to zero from 0 to T/4 and from 3/4T to T, before the data is processed. In this way, the resulting cross-correlation function is valid from 0 to T/4 and from 3/4T to T (corresponding to the interval $-T/4 \leq \tau \leq T/4$). The remaining parts of the estimated function are still in error (HP Fourier Analyzer Training Manual).

Appendix C

Some Aspects of Stability Theory

Considerable interest has developed in modeling the large-scale structure of turbulent shear flows through stability analyses. This parallel approach has been mainly motivated by the jet-noise generation problem.

The objective of any theory of hydrodynamic stability is to predict the future behavior of a disturbance, once it is introduced into the flow being analyzed. In the classical linear theory of parallel flows, small perturbations are considered in the equations of motion and these in turn are linearized.

Assuming that any disturbance is composed of travelling waves with an exponential time factor, the equations of motion for the case of a two-dimensional flow with two-dimensional disturbances, reduce to a fourth-order differential equation (the so-called Orr-Sommerfeld equation). This equation together with appropriate boundary conditions, constitutes an eigenvalue problem, the solution of which, determines the oscillatory modes with their characteristic wave-number, propagation speed and amplification factor. If solutions are found that decay in time, the flow is considered as stable; if they increase with time, the flow is said to be unstable (Schlichting [1968]).

The theory has been applied with considerable success to some simple laminar flows in the verge of becoming

turbulent, and the similarity between the turbulent coherent structures and the events leading to transition in laminar flows, have motivated some investigators to study the former through stability theory.

Hydrodynamic stability theory, as applied to laminar and transitional regimes of mixing layers and jets, constitutes a subject by itself. Among the notable works in this area are the ones by Michalke [1970] (for instance), Mattingly and Criminale [1971], Batchelor and Gill [1962], and Gaster [1965] covering the theoretical aspects, and the ones by Sato [1960], Phillips [1966], Freymuth [1966] and Miskad [1972] dealing with physical experiments.

The work by Landahl [1967] is an example of this postulated relationship between the turbulent structure and the events related to transition. In attempting to relate the statistical properties of the wall pressure in a turbulent boundary layer to the characteristics of the mean flow, Landahl [1967] formulated a wave-guide model (i.e., the admission of wave propagation modes) for the turbulent velocity fluctuations. An approximate solution was obtained from a non-homogeneous Orr-Sommerfeld equation, where the non-linear turbulent stresses were considered as the forcing elements. Considerable agreement with the experimental results reported by Corcos [1964] was obtained for the streamwise decay of the fluctuations. However, the agreement was not found for the measured and predicted convective velocities.

One method of getting an insight into shear flow structure and experimentally testing wave-guide models is to introduce a periodic disturbance of known frequency and amplitude into the flow and to determine the response of the flow to it. Such a procedure was followed by Crow and Champagne [1971] for a circular jet. They introduced a periodic surging upstream of the plenum chamber and measured the response along the centerline in terms of several axial component quantities like mean velocity, root-mean-square fluctuations, etc. After trying various frequencies and amplitudes, they obtained as a preferred mode, the one corresponding to the average frequency of vortex-puffs formation in the transitional region of the jet, previously measured by themselves through visualization experiments (it corresponded to a Strouhal number fd/U_o of 0.3). According to their results, the preferred wave attained its maximum amplitude through the combined effects of linear amplification and non-linear saturation at a certain axial position and then gradually decayed downstream.

Following the same pattern, Chan [1974] performed pressure measurements in a disturbed circular jet. Through an appropriate triggering scheme using the narrow-band filtered signal from a traversing microphone, he obtained oscilloscope traces representing the spatial variation of the pressure signal at a fixed time. The results obtained along the centerline agreed with the ones by Crow and

Champagne and Ko and Davies [1971]. Furthermore, his measurements for the mixing layer and the near field seemed to confirm a stability model previously developed by Michalke [1972], as referred to by Chan [1974].

In getting appropriate data for the development of the wave-guide approach of shear flow turbulence, Hussain and Reynolds [1970, 1972] performed experiments on a channel flow with artificially introduced wave disturbances. Using a phase averaging technique with selective sampling through the cyclic position of the wave-maker, they surveyed downstream of the initial disturbance and extracted the organized wave motion from a hot-wire signal. Realizing that the experimental results suggested that more than one wave mode was excited by the initial disturbance, they performed an approximate single-mode linear analysis of the propagation characteristics. The dynamical equations were further derived for the small amplitude wave disturbances and closure schemes were proposed.

More recently, Hussain and Zaman [1975] reported preliminary results in extending the previous experiments by Crow and Champagne [1971] to a wider range of excitation Strouhal numbers.

The instability waves developing in compressible flows were mathematically studied by Liu [1974] for a mixing layer and by Merkine and Liu [1975] for a plane jet. They considered the kinetic energy aspects of the organized wave,

once it has been separated from the mean and fine-scale components of the flow. A remark was made on the role of the symmetric or varicose and asymmetric or sinuous modes.

The wave-guide representation of turbulent shear flows has some inherent difficulties. For instance, the case of interest in a physical problem is included in spatial stability theory. However, this formulation predicts an exponential amplification of the wave in the downstream direction and the original small amplitude assumption becomes inconsistent, unless some kind of limitation is imposed on that amplification.

In any case, a realistic wave-guide model should account for a spatially growing wave, which attains a maximum growth through some kind of saturation effect after nonlinear interactions. Thereafter it might begin to decay, as the experiments of Crow and Champagne [1971] suggested for the circular jet.

One way of studying turbulent shear flows through a wave-guide representation, is by separating the flow field into three components: the mean flow, the instability wave and the small-scale turbulent fluctuations. Once the fluctuating quantities have been decomposed in the above three terms, they are then introduced into the basic equations. An ordinary time average is taken first, followed by a phase averaging. This leads to dynamical equations for each one of the components. The phase averaging is defined as the

average over a large number of periods of the wave at a given position (Liu [1974]) and is physically realizable for instance, by considering an ensemble of points having the same phase with respect to a reference oscillator, when a disturbance is artificially introduced (Hussain and Reynolds [1970]).

Reynolds and Hussain [1972] pointed out a serious closure problem in the equations for the organized wave as the result of the outlined averaging procedures. They further considered the necessity to take into account the interaction of the organized waves and the small scale fluctuations, perhaps through the use of an eddy viscosity model, as Landahl [1967] had previously speculated.

Following the same approach of separating the flow field into three components, Liu [1974] formulated a model for a compressible mixing layer and later extended it to a two-dimensional jet (Merkine and Liu [1975]). In what follows, a summary of such procedure is given.

Any flow quantity which is a function of time and spatial coordinates is split into three components:

$$q = \bar{q} + q' + q'' \qquad (C.1)$$

where $\bar{q}$ denotes the time-averaged component, q' the instantaneous periodic component and q'' the small-scale turbulent component. The organized wave part q' is given by:

$$q' = \langle q \rangle - \bar{q} \tag{C.2}$$

where $\langle\ \rangle$ indicates phase averaging.

Introducing these quantities into the Navier-Stokes equations, performing the described averaging procedures and making use of boundary layer type of approximation, a two-dimensional von Kármán integral equation can be obtained for the kinetic energy of the instability wave, which for an incompressible flow, reads:

$$\frac{1}{2}\frac{d}{dx}\int_{-\infty}^{\infty}\bar{u}\,\overline{(u'^2+v'^2)}\,dy \approx -\int_{-\infty}^{\infty}\overline{u'v'}\,\frac{\partial\bar{u}}{\partial y}\,dy$$
$$-\int_{-\infty}^{\infty}\Bigg[-(\langle u''^2\rangle-\overline{u''^2})\frac{\partial u'}{\partial x}-(\langle u''v''\rangle-\overline{u''v''})\left(\frac{\partial u'}{\partial y}+\frac{\partial v'}{\partial x}\right)$$
$$-(\langle v''^2\rangle-\overline{v''^2})\,\frac{\partial v'}{\partial y}\Bigg]\,dy \tag{C.3}$$

The left-hand side of equation (C.3) represents the net rate of increase of the kinetic energy of the wave and the terms on the right-hand side are the mechanisms governing this change: energy conversion from the mean flow (or production) and kinetic energy exchange between the wave and the fine-scale turbulence (molecular viscosity effects have been neglected).

If it is further assumed a linear relationship between the wave induced stresses and the instability wave rate of strain of the type:

$$-(\langle u''^2\rangle - \overline{u''^2}) = 2\varepsilon\frac{\partial u'}{\partial x} \tag{C.4}$$

then equation (C.3) reduces to:

$$\frac{1}{2}\frac{d}{dx}\int_{-\infty}^{\infty}\bar{u}\overline{(u'^2+v'^2)}\,dy = -\int_{-\infty}^{\infty}\overline{u'v'}\,\frac{\partial\bar{u}}{\partial y}\,dy$$

$$-\int_{-\infty}^{\infty}2\varepsilon\left[\overline{\left(\frac{\partial u'}{\partial x}\right)^2}+\overline{\left(\frac{\partial v'}{\partial y}\right)^2}+\frac{1}{2}\overline{\left(\frac{\partial u'}{\partial y}+\frac{\partial v'}{\partial x}\right)^2}\right]dy \tag{C.5}$$

where ε is an eddy viscosity.

Once the basic equation has been established, closure is attempted (and here is the essence of Liu's model) by assuming the wave as the product of an amplitude function (to be determined from the kinetic energy equation), and a shape function (to be determined from the linear eigenvalue problem corresponding to the local mean flow).

In effect, any fluctuating quantity q' pertaining to the organized wave is assumed to be given by:

$$q'(\xi,\eta) = A(\xi)Q(\eta;\xi)\exp(-i\beta t) + c.c. \tag{C.6}$$

where Q is the eigenfunction obtained from the local spatial stability theory, A is the modifying amplitude function, and $\xi = x/d$, $\eta = y/b$, β = local dimensionless frequency, t = dimensionless time, and c.c. stands for complex conjugate.

The eigenvalue problem to determine the shape function Q is solved with appropriate boundary conditions. Among them, the possibility to have varicose or symmetric and sinuous or asymmetric (the one connected to the flapping behavior) modes are considered.

As discussed by Merkine and Liu [1975] the amplification and decay of the organized wave comes primarily from the amplitude function A rather than from the amplification rates of the stability theory. The eigenfunctions of the type Q and their associated amplification rates, play only a subsidiary role.

The amplitude function may be determined by substituting the equations of the type (C.6) into the energy relation (C.5). An expression for the amplitude function is obtained involving the various energy integrals; these can be evaluated numerically after assuming an initial condition through the energy density of the initial disturbance.

Although the computational results obtained by Merkine and Liu are not directly applicable to the present investigation (as they refer to a high-speed compressible jet flow), some of their findings may be qualitatively

described.

The various energy exchange mechanisms in equation (C.5) determine the development of the amplitude of the organized wave. In the first stages, the amplitude increases rapidly as the result of larger production as compared with dissipation. As the development continues, the dissipation term dominates over the production one, causing the amplitude of the wave to attain its maximum value and then to decay.

The above described process is retarded for the low frequency components; in other words, the lower the frequency of the wave, the further downstream its maximum amplitude is attained.

Finally, the role of the varicose and simuous modes (although not much differentiated at the early stages) is such that the sinuous waves have larger amplification rates (as predicted by local stability theory and suggested by earlier workers (Rockwell and Niccolls [1972], Mattingly and Criminale [1971])) and show more delayed saturation values in the downstream direction.

The formulation of a wave-guide theory for turbulent shear flows is a very promising one, but is still in a developing stage with many difficulties to be overcome.

VITA

VITA

Jaime Cervantes de Gortari was born on December 13, 1946, to Constantino Cervantes Panza and Carlota de Gortari de Cervantes, in Mexico City, Mexico. He attended public school in Mexico City until graduation from Escuela Nacional Preparatoria in 1963. He received the degree of Ingeniero Mecánico Electricista in 1970 and the degree of Maestro en Ingeniería Mecánica in 1972, both from Universidad Nacional Autónoma de México. In 1970, he joined the Faculty of the same university as a part time Assistant Professor. On leave of absence, he continued his graduate education in 1972 at Purdue University. Mr. Cervantes is married to the former Armandina Cervera Flores and they have a daughter.